

Functional renormalisation group for turbulence

Léonie Canet^{1,2†}

¹Université Grenoble Alpes, CNRS, LPMMC, 38000 Grenoble, France.

²Institut Universitaire de France, 1 rue Descartes, 75005 Paris, France

Turbulence is a complex nonlinear and multi-scale phenomenon. Although the fundamental underlying equations, the Navier-Stokes equations, have been known for two centuries, it remains extremely challenging to extract from them the statistical properties of turbulence. Therefore, for practical purpose, a sustained effort has been devoted to obtaining some effective description of turbulence, that we may call turbulence modelling, or statistical theory of turbulence. In this respect, the Renormalisation Group (RG) appears as a tool of choice, since it is precisely designed to provide effective theories from fundamental equations by performing in a systematic way the average over fluctuations. However, for Navier-Stokes turbulence, a suitable framework for the RG, allowing in particular for non-perturbative approximations, have been missing, which has thwarted for long RG applications. This framework is provided by the modern formulation of the RG called functional renormalisation group. The use of the FRG has rooted important progress in the theoretical understanding of homogeneous and isotropic turbulence. The major one is the rigorous derivation, from the Navier-Stokes equations, of an analytical expression for any Eulerian multi-point multi-time correlation function, which is exact in the limit of large wavenumbers. We propose in this *JFM Perspectives* a survey of the FRG method for turbulence. We provide a basic introduction to the FRG and emphasise how the field-theoretical framework allows one to systematically and profoundly exploit the symmetries. We stress that the FRG enables one to describe fully developed turbulence forced at large scales, which was not accessible by perturbative means. We show that it yields the energy spectrum and second-order structure function with accurate estimates of the related constants, and also the behaviour of the spectrum in the near-dissipative range. Finally, we expound the derivation of the spatio-temporal behaviour of n -point correlation functions, and largely illustrate these results through the analysis of data from experiments and direct numerical simulations.

CONTENTS

1. Introduction	2
2. Scale invariance and the Renormalisation Group	4
2.1. Renormalisation Group and turbulence	4
2.2. Hydrodynamical equations	6
3. Field theoretical formalism for turbulence	7
3.1. Path integral representation of a stochastic dynamical equation	7
3.2. Action for the hydrodynamical equations	10
3.3. Symmetries and extended symmetries	11

† Email address for correspondence: leonie.canet@grenoble.cnrs.fr

3.4. Kármán-Howarth and Yaglom relations from symmetries	15
4. The functional renormalisation group	17
4.1. Progressive integration of fluctuations	17
4.2. Exact flow equation for the effective average action	18
4.3. Non-perturbative approximation schemes	19
5. A warm-up example: Burgers-KPZ equation	20
5.1. FRG for the Burgers-KPZ equation	21
5.2. Scaling dimensions	23
5.3. Results in $d = 1$	24
5.4. Results in $d > 1$	26
6. Fixed-point for Navier-Stokes turbulence	27
6.1. Ansatz for the effective average action	28
6.2. Stationarity	29
6.3. Fixed-point renormalisation functions	30
6.4. Kinetic energy spectrum	32
6.5. Second and third order structure functions	33
7. Space-time correlations from FRG	35
7.1. Overview of space-time correlations in turbulence	36
7.2. Closure in the large wavenumber limit of the FRG flow equations	37
7.3. General expression of the time-dependence of n -point correlation functions	40
7.4. Intuitive physical interpretation	44
8. Comparison with Direct Numerical Simulations	45
8.1. Small time regime and sweeping	45
8.2. Three-point correlation function	46
8.3. Large time regime	49
8.4. Kinetic energy spectrum in the near-dissipation range	49
9. Time-dependence of correlation functions in passive scalar turbulence	51
9.1. FRG results for the correlation functions of passive scalars	52
9.2. Passive scalars in Navier-Stokes flow	53
9.3. Passive scalars in the Kraichnan model	54
9.4. Passive scalars in a time-correlated synthetic flow	56
10. Conclusion and Perspectives	57
Appendix A	60
Appendix B	61
Appendix C	63

1. Introduction

This *JFM Perspectives* proposes a guided tour through the recent achievements and open prospects of the Functional Renormalisation Group (FRG) formalism applied to the problem of turbulence. Why the Renormalisation Group (RG) should be useful at all to study turbulence ? The very essence of the RG is to eliminate degrees of freedom in a systematic way, by averaging over fluctuations at all scales, starting from the fundamental description of a system. It thereby provides an effective model “from first principles”. This is precisely what is needed, and often lacking, in many turbulence problems. Indeed, the fundamental equations for fluid dynamics are the Navier-Stokes (NS) equations, but the number of degrees of freedom necessary to describe turbulence grows as $\text{Re}^{9/4}$. Conceiving an appropriate modelling, e.g. devising some reliable effective equations to simplify the problem, is a major goal in many applications. This is of course a very difficult task in general, and the RG

certainly offers a valuable tool, at least for idealised situations. The program of applying RG to turbulence started in the early eighties, but it was bound to rely on the tools at disposal at that time, which were based on perturbative expansions. However, there is no small parameter for turbulence, and this program was largely thwarted. The only way out was to introduce in the theoretical description a forcing of the turbulence with a power-law spectrum, *i.e.* acting at all scales, which is unphysical (Eyink (1994)). Results for a physical large-scale forcing are then extrapolated from a certain limit which cannot be justified. This is explained in more details in Sec. 2.

In the meantime, functional and non-perturbative ways of realising the RG procedure were developed (Wetterich (1993); Morris (1994)). They allow one in particular to incorporate from the onset a physical large-scale forcing, and thereby to completely circumvent the inextricable issues posed by perturbative expansions. Indeed, the FRG offers a very powerful way to implement non-perturbative – yet controlled – approximation schemes, *i.e.* approximations not requiring the existence of a small parameter. The main scheme consists in the use of an ansatz for a central object in field theory which is called effective action (see Sec. 3). The construction of this ansatz relies on the fundamental symmetries of the problem. This approach has yielded many results, allowing one to obtain very accurate – although approximate – estimates for various quantities, including whole functions, not only numbers. We present as examples in Sec. 5 the results for the scaling functions for Burgers equation, and in Sec. 6 the results for the energy spectrum, the second and third order structure functions for NS equations, including an accurate estimate of the Kolmogorov constant. More strikingly, the FRG can also be used to obtain exact results, which are not based on an ansatz. In turbulence, these results are explicit expressions for n -point Eulerian spatio-temporal correlation functions. They are obtained as an exact limit at large wavenumbers. Given the very few exact results available for 3D turbulence, this result is particularly remarkable and is the main topic of this *Perspectives*.

Let us emphasise that all the results obtained so far with FRG concern stationary, homogeneous and isotropic turbulence. This *Perspectives* is thus focused on this idealised situation. However, the scope of application of FRG is not restricted to this situation. It certainly cannot tackle arbitrarily complicated situations and would be of no use to determine the precise flow configuration around such particular airfoils or in some specific meteorological conditions. However, it could be used, and be efficient, for small-scale modelling, as it is designed to provide an effective description, *e.g.* the form of the coarse-grained effective equations, at any given scale, in particular at the grid scale of large-scale numerical simulations for instance. This direction of research is still in its infancy, and will not be further developed in this contribution, although it definitely maps out a promising program for the future.

Let us also point out that there can be different level of reading of this *Perspectives*. Some parts (*e.g.* Sec. 3, Sec. 4, Sec. 7.2 and Sec. 7.3) are rather technical, with the objective of providing a comprehensive introduction on the basic settings of the FRG for turbulence, and more importantly on the essential ingredients, in particular symmetries, that enter approximation schemes in this framework. Therefore, the underlying hypotheses are clearly stated to highlight the range of validity of the different results presented. Other parts (*e.g.* Sec. 5.3, Sec. 5.4, Sec. 6.4, Sec. 8 and Sec. 9) are devoted to illustrating the physical implications of these results, by comparing them with actual data and observations from experiments and Direct Numerical Simulations (DNS). Therefore one may first wish to focus on the concrete outcomes of FRG, deferring the technical aspects.

In details, this *JFM Perspectives* is organised as follows. We start in Sec. 2 by stressing the interest of RG as a mean to study turbulence and its different implementations. We explain in Sec. 3.1 how one can represent stochastic fluctuations as a path integral, to arrive

at the field theory for turbulence in Sec. 3.2. A key advantage of this formulation is that it provides a framework to deeply exploit the symmetries. We show in Sec. 3.3 how one can derive exact identities relating different correlation functions from symmetries (and extended symmetries) of the field theory. These identities include well-known relations such as the Kármán-Howarth or Yaglom relations (Sec. 3.4), but are far more general. The FRG formalism is introduced in Sec. 4 with the standard approximation schemes used within this framework. To illustrate the application of this method, we start in Sec. 5 with the Burgers equation as a warm-up example. We then present in Sec. 6 a first important result for NS turbulence ensuing from FRG, which is the existence of a fixed-point corresponding to the stationary turbulence forced at large scales, and the determination of the associated statistical properties. The main achievement following from FRG method, addressed in Sec. 7, is the derivation of the formal general expression of n -point spatio-temporal correlation functions at large wavenumbers. The rest of this *Perspectives* is dedicated to illustrating these results, for NS turbulence in Sec. 8, and for passive scalar turbulence in Sec. 9. Another result, concerning the form of the kinetic energy spectrum in the near-dissipation range of scale is briefly mentioned in Sec. 8.4. Finally, the conclusion and perspectives are gathered in Sec. 10.

2. Scale invariance and the Renormalisation Group

2.1. Renormalisation Group and turbulence

Let us explain why RG should be useful to study turbulence from the point of view of statistical physics. The aim of statistical physics is to determine from a fundamental theory at the microscopic scale the effective behaviour at the macroscopic scale of the system, comprising a large number $\sim N_A$ of particles (in a broad sense). This requires to average over stochastic fluctuations (thermal, quantum, *etc.* . .). When the fluctuations are Gaussian, and elementary constituents are non-interacting, central limit theorem applies and allows one to perform the averaging (which is how one obtains e.g. the equation of states of the perfect gas). However, when the system becomes strongly correlated, this procedure fails since the constituents are no longer statistically independent. This problem appeared particularly thorny for critical phenomena, and have impeded for long progress in their theoretical understanding. Indeed, at a second order phase transition, the correlation length of the system diverges, which means that all the degrees of freedom are correlated and fluctuations develop at all scales. The divergence of the correlation length leads to the quintessential property of scale invariance, characterised by universal scaling laws, with anomalous exponents, *i.e.* exponents not complying with dimensional analysis.

The major breakthrough to understand the physical origin of this anomalous behaviour, and primarily to compute it, was achieved with the RG. Although the RG had already been used under other forms in high-energy physics, it acquired its plain physical meaning from the work of K. Wilson (Wilson & Kogut (1974)). The RG provides the tool to perform the average over fluctuations, whatever their nature, *i.e.* eliminate degrees of freedom, even in the presence of strong correlations, and thereby to build the effective theory at large scale from the microscopic one. One of the key feature of the RG is that all the useful information is encoded in the RG *flow*, *i.e.* in the differential equation describing the change of the system under a change of scale. In particular, a critical point, associated with scale invariance, corresponds by essence to a fixed-point of the RG flow. Let us notice that the notion of large scale is relative to the microscopic one, and it depends on the context. For turbulence, the microscopic scale, denoted Λ^{-1} , refers to the scale at which the continuum description of a fluid, in terms of NS equation, is valid, say the order of the mean-free-path in the fluid (much

smaller than the Kolmogorov scale η). The “large” scale of the RG then refers to typical scales at which the behaviour of the fluid is observed, *i.e.* inertial or dissipation ranges, thus including the usual “small” scales of turbulence.

The analogy between critical phenomena and turbulence is obvious, and was early pointed out in (Nelkin (1974)), and later refined in *e.g.* (Eyink & Goldenfeld (1994)). Indeed, when turbulence is fully developed, one observes in the inertial range universal behaviours, described by scaling laws with anomalous critical exponents, akin at an equilibrium second-order phase transition. As the RG had been so successful in the latter case, it early arose as the choice candidate to tackle the former. Concomitantly, the RG was extended to study not only the equilibrium but also the dynamics of systems (Martin *et al.* (1973); Janssen (1976); de Dominicis (1976)), and the first implementations of the “dynamical RG” to study turbulence date back to the early eighties (Forster *et al.* (1977); DeDominicis & Martin (1979); Fournier & Frisch (1983); Yakhot & Orszag (1986)). However, the formulation of the RG has remained for long intimately linked with perturbative expansions, relying on the existence of a small parameter. This small parameter is generically chosen as the distance $\varepsilon = d_c - d$ to an upper critical dimension d_c , which is the dimension where the fixed-point associated with the phase transition under study becomes Gaussian, and the interaction coupling vanishes. In the paradigmatic example of the ϕ^4 theory which describes the second-order phase transition in the Ising universality class, the interaction coupling g has a scaling dimension L^{4-d} . Thus it vanishes in the $L \rightarrow \infty$ limit for $d \geq d_c = 4$, which means that fluctuations become negligible and the mean-field approximation suffices to provide a reliable description. The Wilson-Fisher fixed-point describing the transition below d_c can then be captured by a perturbative expansion in $\varepsilon = d_c - d$ and the coupling g .

In contrast, in turbulence, the “interaction” is the non-linear advection term, whose “coupling” is unity, *i.e.* it is not small, and does not vanish in any dimension. Thus, one lacks a small parameter to control perturbative expansion. The usual strategy has been to introduce an artificial parameter ε through a forcing with power-law correlations behaving in wavenumber space as $p^{4-d-\varepsilon}$, *i.e.* applying a forcing on all scales, which is unphysical (Eyink (1994)) [†]. Fully developed turbulence in $d = 3$ should then correspond to an infrared (IR) dominated spectrum of the stirring force, as it occurs for $\varepsilon \geq 2$, hence for large values for which the extrapolation of the perturbative expansions is fragile. Moreover, one finds an ε -dependent fixed-point, with an energy spectrum $E(p) \propto p^{1-2\varepsilon/3}$. The K41 value is recovered for $\varepsilon = 4$, but this value should somehow freeze for ε larger than 4, and such a freezing mechanism can only be invoked within the perturbative analysis (Fournier & Frisch (1983)). In fact, the situation is even worse since it was recently shown that the turbulence generated by a power-law forcing or by a large-scale forcing is simply different (it corresponds to two distinct fixed-points of the RG, in particular the latter is intermittent whereas the former is not for any value of ε including $\varepsilon = 4$) (Fontaine *et al.* (2022)). Therefore, NS turbulence with a large-scale forcing simply cannot be extrapolated from the setting with power-law forcing. Not only recovering the K41 spectrum turns out to be difficult within this framework, but the first RG analyses also failed to capture the sweeping effect (Yakhot *et al.* (1989); Chen & Kraichnan (1989); Nelkin & Tabor (1990)), and led to the conclusion that one should go to a quasi-Lagrangian framework to obtain a reliable description (L’vov & Procaccia (1995); L’vov *et al.* (1997)). However, the difficulties encountered were severe enough to thwart progress in this direction. We refer to (Smith & Woodruff (1998); Adzhemyan *et al.* (1999); Zhou (2010)) for reviews of these developments.

In the meantime, a novel formulation of the RG has emerged, which allows for non-

[†] Note that the letter p is used to denote a wavenumber throughout this *Perspectives*. The pressure is denoted with a letter π to avoid any confusion.

perturbative approximation schemes, and thereby bypasses the need of a small parameter. The FRG is a modern implementation of Wilson’s original conception of the RG (Wilson & Kogut (1974)). It was formulated in the early nineties (Wetterich (1993); Morris (1994); Ellwanger (1994)), and widely developed since then (Berges *et al.* (2002); Kopietz *et al.* (2010); Delamotte (2012); Dupuis *et al.* (2021)). One of the noticeable features of this formalism is its versatility, as testified by its wide range of applications, from high-energy physics (QCD and quantum gravity) to condensed matter (fermionic and bosonic quantum systems) and classical statistical physics, including non-equilibrium classical and quantum systems or disordered ones. We refer the interested reader to (Dupuis *et al.* (2021)) for a recent review. This has led to fertile methodological transfers, borrowing from an area to the other. The FRG was moreover promoted to a high-precision method, since it was shown to yield for the archetypical three-dimensional Ising model results for the critical exponents competing with the best available estimates in the literature (Balog *et al.* (2019)), and to the most precise ones for the $O(N)$ models in general (De Polsi *et al.* (2020, 2021)).

The FRG has been applied to study turbulence in several works (Tomassini (1997); Mejía-Monasterio & Muratore-Ginanneschi (2012); Barbi & Münster (2013); Canet *et al.* (2016, 2017); Tarpin *et al.* (2018, 2019); Pagani & Canet (2021)), including a study of decaying turbulence within a perturbative implementation of the FRG (Fedorenko *et al.* (2013)). This method has turned out to be fruitful in this context, which is the motivation of this *Perspectives*.

2.2. Hydrodynamical equations

The starting point of field-theoretical methods is a “microscopic model”. For fluids, this model is the fundamental hydrodynamical description provided by NS equation

$$\partial_t \mathbf{v}_\alpha + \mathbf{v}_\beta \partial_\beta \mathbf{v}_\alpha = -\frac{1}{\rho} \partial_\alpha \pi + \nu \nabla^2 \mathbf{v}_\alpha + \mathbf{f}_\alpha \quad (2.1)$$

where the velocity field \mathbf{v} , the pressure field π , and the external force \mathbf{f} depend on the space-time coordinates (t, \mathbf{x}) , and with ν the kinematic viscosity and ρ the density of the fluid. We focus in this review on incompressible flows, satisfying

$$\partial_\alpha \mathbf{v}_\alpha = 0. \quad (2.2)$$

The external stirring force is introduced to maintain a stationary turbulent state. Since the small-scale (*i.e.* $\ell \ll L$, that is inertial and dissipative) properties are expected to be universal with respect to the large-scale forcing, it can be chosen as a stochastic force, with a Gaussian distribution, of zero average and covariance

$$\langle f_\alpha(t, \mathbf{x}) f_\beta(t', \mathbf{x}') \rangle = 2\delta(t - t') N_{\alpha\beta} \left(\frac{|\mathbf{x} - \mathbf{x}'|}{L} \right), \quad (2.3)$$

where N is concentrated around the integral scale L , such that it models the most common physical situation, where the energy is injected at large scales. This is one of the great advantages of the FRG approach compared to perturbative RG: it can incorporate any functional form for the forcing, and not necessarily a power-law. Hence, one can consider a large-scale forcing, and therefore completely bypass the difficulties encountered in perturbative approaches which arise from trying to access the physical situation as an ill-defined limit from a power-law forcing.

We are also interested in a passive scalar field $\theta(t, \mathbf{x})$ advected by a turbulent flow. The dynamics of the scalar is governed by the advection-diffusion equation

$$\partial_t \theta + \mathbf{v}_\beta \partial_\beta \theta - \kappa_\theta \nabla^2 \theta = f_\theta, \quad (2.4)$$

where κ_θ is the molecular diffusivity of the scalar, and f_θ is an external stirring force acting on the scalar, which can also be chosen Gaussian distributed with zero mean and covariance

$$\langle f_\theta(t, \mathbf{x}) f_\theta(t', \mathbf{x}') \rangle = 2\delta(t - t') M \left(\frac{|\mathbf{x} - \mathbf{x}'|}{L_\theta} \right), \quad (2.5)$$

with L_θ the integral scale of the scalar.

Finally, we consider a simplified model of turbulence, introduced by Burgers (Burgers (1948)), which describes the dynamics of a 1D compressible randomly stirred fluid. The Burgers equation reads

$$\partial_t v + v \partial_x v = \nu \partial_x^2 v + f, \quad (2.6)$$

and can be interpreted as a model for fully compressible hydrodynamics, or pressureless Navier-Stokes equation (see Bec & Khanin (2007) for a review). f is again a random Gaussian force with covariance

$$\langle f(t, x) f(t', x') \rangle = 2\delta(t - t') D(x - x'). \quad (2.7)$$

It corresponds to model C of (Forster *et al.* (1977)). In fact, there exists an exact mapping between the Burgers equation and the Kardar-Parisi-Zhang equation which describes the kinetic roughening of a stochastically growing interface (Kardar *et al.* (1986)). The KPZ equation gives the time evolution of the height field $h(t, \mathbf{x})$ of a $(d - 1)$ -dimensional interface growing in a d -dimensional space as

$$\partial_t h = \nu \nabla^2 h + \frac{\lambda}{2} (\nabla h)^2 + \eta, \quad (2.8)$$

and has become a fundamental model in statistical physics for non-equilibrium scaling phenomena and phase transitions, akin the Ising model at equilibrium (Halpin-Healy & Zhang (1995); Krug (1997); Takeuchi (2018)). For the standard KPZ equation, η is interpreted as a microscopic (small-scale) noise which is delta-correlated also in space

$$\langle \eta(t, \mathbf{x}) \eta(t', \mathbf{x}') \rangle = 2D\delta(t - t') \delta^d(\mathbf{x} - \mathbf{x}'), \quad (2.9)$$

but it can be generalised to include a long-range noise $D(|\mathbf{x} - \mathbf{x}'|)$. Defining the velocity field $\mathbf{v} = -\lambda \nabla h$, one obtains from (2.8) the d -dimensional generalisation of the Burgers equation (2.6) for a potential flow, with forcing $\mathbf{f} = -\lambda \nabla \eta$.

The equations (2.1), (2.4) and (2.6) all yield for some parameters a turbulent regime, where the velocity, pressure, or scalar fields undergo rapid and random variations in space and time. One must account for these fluctuations to build a statistical theory of turbulence. A natural way to achieve this is via a path integral, which includes all possible trajectories weighted by their respective probability. How to write such a path integral is explained in Sec. 3.1.

3. Field theoretical formalism for turbulence

3.1. Path integral representation of a stochastic dynamical equation

The random forcing in the stochastic partial differential equations (2.1), (2.4) and (2.6) acts as a noise source, and thus these stochastic equations are formally equivalent to a Langevin equation. The fundamental difference is that, in usual Langevin description, the origin of the noise lies at the microscopic scale, it is introduced to model some microscopic collision processes, and one is usually interested in the statistical properties of the system at large scales. In the stochastic NS equation, the randomness is introduced at the integral scale, and one is interested in the statistical properties of the system at small scales (but large with respect to the microscopic scale Λ).

Despite this conceptual difference, in both cases, the dynamical fields are fluctuating ones, and there exists a well-known procedure to encompass all the stochastic trajectories within a path integral, which is the Martin–Siggia–Rose–Janssen–de Dominicis (MSRJD) formalism, (Martin *et al.* (1973); Janssen (1976); de Dominicis (1976)). The idea is simple, and since it is the starting point of all the subsequent analysis, it is useful to describe the procedure in the simplest case of a scalar field $\varphi(t, \mathbf{x})$, following the generic Langevin equation

$$\partial_t \varphi(t, \mathbf{x}) = -\mathcal{F}[\varphi(t, \mathbf{x})] + \eta(t, \mathbf{x}), \quad (3.1)$$

where \mathcal{F} represents the deterministic forces and η the stochastic noise. \mathcal{F} is a functional of the fields and their spatial derivatives. The noise has a Gaussian distribution with zero average and a correlator of the form

$$\langle \eta(t, \mathbf{x}) \eta(t', \mathbf{x}') \rangle = 2\delta(t - t') D(|\mathbf{x} - \mathbf{x}'|). \quad (3.2)$$

The probability distribution of the noise is thus given by

$$\mathcal{P}[\eta] = \mathcal{N} \exp\left(-\frac{1}{4} \int_{t, \mathbf{x}, \mathbf{x}'} \eta(t, \mathbf{x}) D^{-1}(|\mathbf{x} - \mathbf{x}'|) \eta(t, \mathbf{x}')\right), \quad (3.3)$$

with \mathcal{N} a normalisation constant. Note that the derivation we present can be generalised to include temporal correlations, or a field dependence into the noise correlations (3.2). The path integral representation of the stochastic equation is obtained in the following way. The probability distribution of the trajectories of the field follows from an average over the noise as

$$\mathcal{P}[\varphi] = \int \mathcal{D}\eta \mathcal{P}[\eta] \delta(\varphi - \varphi_\eta), \quad (3.4)$$

where φ_η is a solution of (3.1) for a given realisation of η . A change of variable allows one to replace the constraint $\varphi - \varphi_\eta = 0$ by the explicit equation of motion

$$\mathcal{G}[\varphi(t, \mathbf{x})] = 0 = \partial_t \varphi(t, \mathbf{x}) + \mathcal{F}[\varphi(t, \mathbf{x})] - \eta(t, \mathbf{x}), \quad (3.5)$$

which introduces the functional Jacobian $\mathcal{J}[\varphi] = \left| \frac{\delta \mathcal{G}}{\delta \varphi} \right|^\dagger$, and leads to

$$\mathcal{P}[\varphi] = \int \mathcal{D}\eta \mathcal{P}[\eta] \mathcal{J}[\varphi] \delta(\mathcal{G}[\varphi]). \quad (3.6)$$

One can then use the Fourier representation of the functional Dirac deltas in Eq. (3.6), e.g. $\delta(\psi) = \int \mathcal{D}\psi e^{-i \int \bar{\varphi} \psi}$, where the conjugate Fourier variable is now a field, denoted with an

[†] Two remarks are in order here. First, the existence and uniqueness of the solution of (3.1) has been implicitly assumed. Actually, only a solution in a weak sense is required. For the NS equation, even the existence and uniqueness of weak solutions is a subtle issue from a mathematical viewpoint, and uniqueness may not hold in some cases (Buckmaster & Vicol (2019)). However, uniqueness is not strictly required in this derivation, in the sense that for a typical set of initial conditions, there may exist a set of non-unique velocity configurations, provided they are of zero measure. Second, the expression of the Jacobian $\mathcal{J}[\varphi]$ depends on the discretisation of the Langevin equation (3.1). In the Ito's scheme, \mathcal{J} is independent of the fields and can be absorbed in the normalisation of $\mathcal{P}[\varphi]$, while in the Stratonovich's convention, it depends on the fields, and it can be expressed introducing two Grassmann anti-commuting fields ψ and $\bar{\psi}$ as $\mathcal{J}[\varphi] = \left| \det \frac{\delta \mathcal{G}(t, \mathbf{x})}{\delta \varphi(t', \mathbf{x}')} \right| = \int \mathcal{D}\psi \mathcal{D}\bar{\psi} e^{\int_{t, \mathbf{x}, \mathbf{x}'} \bar{\psi} \frac{\delta \mathcal{G}}{\delta \varphi} \psi}$. This representation just follows from Gaussian integration of Grassmann variables, which yields the determinant of the operator in the quadratic form (here $\frac{\delta \mathcal{G}}{\delta \varphi}$) rather than its inverse, as for standard (non-Grassmann) variables (Zinn-Justin (2002)). For an additive noise, which means that the noise part in Eq. (3.1) and its covariance (3.2) do not depend on the field φ , the statistical properties of the system are not sensitive to the choice of the discretisation scheme, and both Ito and Stratonovich conventions yield the same results. We shall here mostly use the Ito's discretisation for convenience and omit the Jacobian contribution henceforth.

overbar, and called auxiliary field, or response field. Thus, introducing the auxiliary field $\bar{\varphi}$ in Eq. (3.6) yields

$$\mathcal{P}[\varphi] = \int \mathcal{D}\eta \mathcal{P}[\eta] \mathcal{D}\bar{\varphi} e^{-i \int_{t,x} \bar{\varphi} \mathcal{G}[\varphi]} = \int \mathcal{D}\bar{\varphi} e^{-S[\varphi, \bar{\varphi}]} . \quad (3.7)$$

The second equality stems from the integration over the Gaussian noise η , resulting in the action

$$S[\varphi, \bar{\varphi}] = i \int_{t,x} \left\{ \bar{\varphi} (\partial_t \varphi + \mathcal{F}[\varphi]) \right\} + \int_{t,x,x'} \bar{\varphi}(t, \mathbf{x}) D(|\mathbf{x} - \mathbf{x}'|) \bar{\varphi}(t, \mathbf{x}') . \quad (3.8)$$

One usually absorbs the complex i into a redefinition of the auxiliary field $\bar{\varphi} \rightarrow -i\bar{\varphi}$. The action resulting from the MSRJD procedure exhibits a simple structure. The response field appears linearly as Lagrange multiplier for the equation of motion, while the characteristics of the noise, namely its correlator, are encoded in the quadratic term in $\bar{\varphi}$.

The path integral formulation offers a simple way to compute all the correlation and response functions of the model. Their generating functional is defined by

$$\mathcal{Z}[J, \bar{J}] = \left\langle e^{\int_{t,x} \{J \varphi + \bar{J} \bar{\varphi}\}} \right\rangle = \int \mathcal{D}\varphi \mathcal{P}[\varphi] e^{\int_{t,x} \{J \varphi + \bar{J} \bar{\varphi}\}} = \int \mathcal{D}\varphi \mathcal{D}\bar{\varphi} e^{-S[\varphi, \bar{\varphi}] + \int_{t,x} \{J \varphi + \bar{J} \bar{\varphi}\}} , \quad (3.9)$$

where J, \bar{J} are the sources for the fields $\varphi, \bar{\varphi}$ respectively. Correlation functions are obtained by taking functional derivatives of \mathcal{Z} with respect to the corresponding sources, e.g.

$$\langle \varphi(t, \mathbf{x}) \rangle = \frac{\delta \mathcal{Z}}{\delta J(t, \mathbf{x})} , \quad (3.10)$$

and functional derivatives with respect to response sources generate response functions (*i.e.* response to an external drive), hence the name “response fields”. We shall henceforth use “correlations” in a generalised sense including both correlation and response functions. In equilibrium statistical mechanics, \mathcal{Z} embodies the partition function of the system, while in probability theory, it is called the characteristic function, which is the generating function of moments.

One usually also considers the functional $\mathcal{W} = \ln \mathcal{Z}$, which is the analogue of a Helmholtz free energy in the context of equilibrium statistical mechanics. In probability theory, it is the generating function of cumulants. The generalisation of cumulants for fields rather than variables are called connected correlation functions, and hence \mathcal{W} is the generating functional of connected correlation functions, for instance,

$$\langle \varphi(t, \mathbf{x}) \varphi(t', \mathbf{x}') \rangle_c \equiv \langle \varphi(t, \mathbf{x}) \varphi(t', \mathbf{x}') \rangle - \langle \varphi(t, \mathbf{x}) \rangle \langle \varphi(t', \mathbf{x}') \rangle = \frac{\delta^2 \mathcal{W}}{\delta J(t, \mathbf{x}) \delta J(t', \mathbf{x}')} . \quad (3.11)$$

More generally, one can obtain a n -point generalised connected correlation function $\mathcal{W}^{(n)}$ by taking n functional derivatives with respect to either J or \bar{J} evaluated at n different space-time points (t_i, \mathbf{x}_i) as

$$\mathcal{W}^{(n)}(t_1, \mathbf{x}_1, \dots, t_n, \mathbf{x}_n) = \frac{\delta^n \mathcal{W}}{\delta \mathcal{J}_{i_1}(t_1, \mathbf{x}_1) \cdots \delta \mathcal{J}_{i_n}(t_n, \mathbf{x}_n)} . \quad (3.12)$$

where $\mathcal{J} = (J, \bar{J})$ and hence $i_k \in \{1, 2\}$. It is also useful to introduce another notation $\mathcal{W}^{(\ell, m)}$, which specifies that the ℓ first derivatives are with respect to J and the m last to \bar{J} ,

that is

$$\mathcal{W}^{(\ell,m)}(t_1, \mathbf{x}_1, \dots, t_{\ell+m}, \mathbf{x}_{\ell+m}) = \frac{\delta^{\ell+m} \mathcal{W}}{\delta J(t_1, \mathbf{x}_1) \cdots \delta J(t_\ell, \mathbf{x}_\ell) \delta \bar{J}(t_{\ell+1}, \mathbf{x}_{\ell+1}) \cdots \delta \bar{J}(t_{\ell+m}, \mathbf{x}_{\ell+m})}. \quad (3.13)$$

A last generating functional which plays a central role in field theory and in the FRG framework is the Legendre transform of \mathcal{W} , *i.e.* the analogue of the Gibbs free energy in equilibrium statistical mechanics, defined as

$$\Gamma[\langle \varphi \rangle, \langle \bar{\varphi} \rangle] = \sup_{\{J, \bar{J}\}} \left[\int_{t, \mathbf{x}} \left\{ J \langle \varphi \rangle + \bar{J} \langle \bar{\varphi} \rangle \right\} - \mathcal{W}[J, \bar{J}] \right]. \quad (3.14)$$

Γ is called the effective action, it is a functional of the average fields, defined with the usual Legendre conjugate relations

$$\langle \varphi(t, \mathbf{x}) \rangle = \frac{\delta \mathcal{W}}{\delta J(t, \mathbf{x})}, \quad J(t, \mathbf{x}) = \frac{\delta \Gamma}{\delta \langle \varphi(t, \mathbf{x}) \rangle}, \quad (3.15)$$

and similarly for the response fields. From a field-theoretical viewpoint, Γ is the generating functional of one-particle-irreducible correlation functions, which are obtained by taking functional derivatives of Γ with respect to average fields

$$\Gamma^{(n)}(t_1, \mathbf{x}_1, \dots, t_n, \mathbf{x}_n) = \frac{\delta^n \Gamma}{\delta \Psi_{i_1}(t_1, \mathbf{x}_1) \cdots \delta \Psi_{i_n}(t_n, \mathbf{x}_n)}. \quad (3.16)$$

where $\Psi = (\langle \varphi \rangle, \langle \bar{\varphi} \rangle)$ and $i_k \in \{1, 2\}$. They are also denoted $\Gamma^{(\ell,m)}$ conforming to the definition (3.13). The one-particle-irreducible correlation functions are also simply called vertices, because in diagrammatic representations *à la* Feynman they precisely correspond to the vertices of the diagrams, as for instance in Fig. 1. An important point to be highlighted is that both sets of correlation functions $\Gamma^{(n)}$ and $\mathcal{W}^{(n)}$ contain the exact same information on the statistical properties of the model. Each set can be simply reconstructed from the other *via* a sum of tree diagrams.

To conclude these general definitions, we also consider the Fourier transforms in space and time of all these correlation functions. The Fourier convention, used throughout this *Perspectives*, is

$$f(\omega, \mathbf{q}) = \int_{t, \mathbf{x}} f(t, \mathbf{x}) e^{-i\mathbf{q} \cdot \mathbf{x} + i\omega t}, \quad f(t, \mathbf{x}) = \int_{\omega, \mathbf{q}} f(\omega, \mathbf{q}) e^{i\mathbf{q} \cdot \mathbf{x} - i\omega t}, \quad (3.17)$$

where $\int_{t, \mathbf{x}} \equiv \int dt d^d \mathbf{x}$ and $\int_{\omega, \mathbf{q}} \equiv \int \frac{d^d \mathbf{q}}{(2\pi)^d} \frac{d\omega}{2\pi}$. Because of translational invariance in space and time, the Fourier transform of a n -point correlation function, *e.g.* $\Gamma^{(n)}$, takes the form

$$\Gamma^{(n)}(\omega_1, \mathbf{p}_1, \dots, \omega_n, \mathbf{p}_n) = (2\pi)^{d+1} \delta \left(\sum_i \omega_i \right) \delta^d \left(\sum_i \mathbf{p}_i \right) \bar{\Gamma}^{(n)}(\omega_1, \mathbf{p}_1, \dots, \omega_{n-1}, \mathbf{p}_{n-1}), \quad (3.18)$$

that is, the total wavevector and total frequency are conserved, and the last frequency-wavevector arguments ω_n, \mathbf{p}_n can be omitted since they are fixed as minus the sum of the others.

3.2. Action for the hydrodynamical equations

The MSRJD procedure can be straightforwardly applied to the (d -dimensional) Burgers equation where the field φ is replaced by the velocity field \mathbf{v} . Introducing the response field

$\bar{\mathbf{v}}$, it yields the action

$$S_B = \int_{t,x} \bar{v}_\alpha \left[\partial_t v_\alpha + v_\beta \partial_\beta v_\alpha - \nu \nabla^2 v_\alpha \right] - \int_{t,x,x'} \bar{v}_\alpha D_{\alpha\beta}(\mathbf{x} - \mathbf{x}') \bar{v}_\beta. \quad (3.19)$$

For the NS equation, one has to also include the incompressibility constraint (2.2). This can be simply achieved by including the factor $\delta(\partial_\beta v_\beta)$ in (3.4). This functional delta can then be exponentiated along with the equation of motion through the introduction of an additional response field $\bar{\pi}$. This yields the following path integral representation

$$\mathcal{Z}[\mathbf{J}, \bar{\mathbf{J}}, K, \bar{K}] = \int \mathcal{D}\mathbf{v} \mathcal{D}\bar{\mathbf{v}} \mathcal{D}\pi \mathcal{D}\bar{\pi} e^{-S_{NS}[\mathbf{v}, \bar{\mathbf{v}}, \pi, \bar{\pi}] + \int_{t,x} \left\{ \mathbf{J} \cdot \mathbf{v} + \bar{\mathbf{J}} \cdot \bar{\mathbf{v}} + K \pi + \bar{K} \bar{\pi} \right\}}, \quad (3.20)$$

for the fluctuating velocity and pressure fields and their associated response fields, with the NS action

$$\begin{aligned} S_{NS}[\mathbf{v}, \bar{\mathbf{v}}, \pi, \bar{\pi}] = & \int_{t,x} \left\{ \bar{\pi} \partial_\alpha v_\alpha + \bar{v}_\alpha \left[\partial_t v_\alpha - \nu \nabla^2 v_\alpha + v_\beta \partial_\beta v_\alpha + \frac{1}{\rho} \partial_\alpha \pi \right] \right\} \\ & - \int_{t,x,x'} \bar{v}_\alpha(t, \mathbf{x}) N_{\alpha\beta} \left(\frac{|\mathbf{x} - \mathbf{x}'|}{L} \right) \bar{v}_\beta(t, \mathbf{x}'). \end{aligned} \quad (3.21)$$

In this formulation, we have kept the pressure field and introduced a response field $\bar{\pi}$ to enforce the incompressibility constraint. Alternatively, the pressure field can be integrated out using the Poisson equation, such that one obtains a path integral in terms of two fields \mathbf{v} and $\bar{\mathbf{v}}$ instead of four, at the price of a resulting action which is non-local (Barbi & Münster (2013)). We here choose to keep the pressure fields since the whole pressure sector turns out to be very simple to handle, as is shown in Appendix A.

We now consider a passive scalar field θ transported by a turbulent NS velocity flow according to the advection-diffusion equation (2.4). The associated field theory is simply obtained by adding the two fields $\theta, \bar{\theta}$ and the two corresponding sources j, \bar{j} to the field multiplet $\Phi = (\mathbf{v}, \bar{\mathbf{v}}, \pi, \bar{\pi}, \theta, \bar{\theta})$ and source multiplet $\mathcal{J} = (\mathbf{J}, \bar{\mathbf{J}}, K, \bar{K}, j, \bar{j})$ respectively. The generating functional then reads

$$\mathcal{Z}[\mathcal{J}] = \int \mathcal{D}\Phi e^{-S_{NS}[\mathbf{v}, \bar{\mathbf{v}}, \pi, \bar{\pi}] - S_\theta[\theta, \bar{\theta}, \mathbf{v}] + \int_{t,x} \mathcal{J}_\ell \Phi_\ell}, \quad (3.22)$$

with the passive scalar action given by

$$S_\theta[\theta, \bar{\theta}, \mathbf{v}] = \int_{t,x} \bar{\theta} \left[\partial_t \theta + v_\beta \partial_\beta \theta - \kappa_\theta \nabla^2 \theta \right] - \int_{t,x,x'} \bar{\theta}(t, \mathbf{x}) M \left(\frac{\mathbf{x} - \mathbf{x}'}{L_\theta} \right) \bar{\theta}(t, \mathbf{x}'). \quad (3.23)$$

The two actions (3.21) and (3.23) possess fundamental symmetries, some of which have only been recently identified. They can be used to derive a set of exact identities relating among each other different correlation functions of the system. These identities, which include as particular cases the Kármán-Howarth and Yaglom relations, contain fundamental information on the system. We provide in the next Sec. 3.3 a detailed analysis of these symmetries, and show how the set of exact identities can be inferred from Ward identities.

3.3. Symmetries and extended symmetries

We are interested in the stationary state of fully developed homogeneous and isotropic turbulence. We hence assume translational invariance in space and time, as well as rotational invariance. Beside these symmetries, the NS equation possesses other well-known symmetries, such as the Galilean invariance. In the field-theoretical formulation, these symmetries are obviously carried over, but they are moreover endowed with a systematic framework to

be fully exploited. Indeed, the path integral formulation provides the natural tool to express the consequences of the symmetries on the correlation functions of the theory, under the form of exact identities which are called Ward identities.

In fact, the field-theoretical formulation is even more far-reaching, in the sense that the very notion of symmetry can be extended. A symmetry means an invariance of the model (equation of motion or action) under a given transformation of the fields and space-time coordinates. Identifying the symmetries of a model is very useful because it allows for simplification, and also to uncover invariants, as according to Noether's theorem, continuous symmetries are associated with conserved quantities. In general, the symmetries considered are global symmetries, *i.e.* their parameters are constants (e.g. angle of a global rotation, vector of a global translation). However, if one can identify local symmetries, *i.e.* whose parameters are space and/or time dependent, this will lead to local conservation laws, which are much richer, much more constraining. In general, the global symmetries of the model cannot be simply promoted to local symmetries by letting their parameters depend on space and/or time. However, this can be achieved in certain cases at the price of extending the notion of symmetry. More precisely, it is useful to also consider transformations that do not leave the model strictly invariant, but “almost”, in the sense that they lead to a variation which is at most linear in the fields. We refer to them as extended symmetries. The key is that one can deduce from them exact local identities, which are thus endowed with a stronger content than the original global identities associated with global symmetries, *i.e.* they provide additional constraints.

One may wonder why one focuses on linear variations specifically and what is special about them. In fact, in principle, one can consider any transformation of the fields and coordinates and just write down the corresponding variation of the action. Once inserted in the path integral (3.9), this leads to a relation for the average value of this variation. The reason is that only when it is linear in the fields can this relation be turned into an identity for the generating functionals themselves. In this case, it becomes extremely powerful because it allows one to obtain an infinite set of exact relations between correlation functions by taking functional derivatives. The mechanism is very simple, and is exemplified in the simplest case of the symmetries of the pressure sector in Appendix A.0.1. In the following, we detail two specific extended symmetries, since they play a fundamental role in Sec. 7, and refer to Appendix A for additional ones. Indeed, these two symmetries yield the identities (3.30) and (3.35), which allow for an exact closure at large wavenumbers of the FRG equations.

3.3.1. Time-dependent Galilean symmetry

A fundamental symmetry of the NS equation is the Galilean invariance, which is the invariance under the global transformation $\mathbf{x} \rightarrow \mathbf{x}' = \mathbf{x} + \mathbf{v}_0 t$, $\mathbf{v}(t, \mathbf{x}) \rightarrow \mathbf{v}(t, \mathbf{x}') - \mathbf{v}_0$. In fact, it was early recognised in the field-theoretical context that a time-dependent, (also called time-gauged), version of this transformation leads to an extended symmetry of the NS action and useful Ward identities ((Adzhemyan *et al.* 1994, 1999; Antonov *et al.* 1996)). Considering an infinitesimal arbitrary time-dependent vector $\boldsymbol{\varepsilon}(t)$, this transformation reads

$$\begin{aligned}\delta v_\alpha(t, \mathbf{x}) &= -\dot{\varepsilon}_\alpha(t) + \varepsilon_\beta(t) \partial_\beta v_\alpha(t, \mathbf{x}) \\ \delta \Phi_k(t, \mathbf{x}) &= \varepsilon_\beta(t) \partial_\beta \Phi_k(t, \mathbf{x})\end{aligned}\tag{3.24}$$

where $\dot{\varepsilon}_\alpha = \frac{d\varepsilon_\alpha}{dt}$, and Φ_k denotes any other fields $\bar{\mathbf{v}}, \pi, \bar{\pi}, \dots$. The variation $\varepsilon_\beta(t) \partial_\beta(\cdot)$ just originates from the change of coordinates. The global Galilean transformation is recovered for a constant velocity $\dot{\boldsymbol{\varepsilon}}(t) = \mathbf{v}_0$.

The overall variation of the NS action under the transformation (3.24) is

$$\delta S_{\text{NS}} = - \int_{t,\mathbf{x}} \varepsilon_\alpha(t) \partial_t^2 \bar{v}_\alpha(t, \mathbf{x}). \quad (3.25)$$

Since the field transformation (3.24) is a mere affine change of variable in the functional integral \mathcal{Z} , it must leave it unaltered. Performing this change of variable in (3.20) and expanding the exponential to first order in ε , one obtains:

$$\langle \delta S_{\text{NS}} \rangle = \left\langle \delta \int_{t,\mathbf{x}} \mathcal{J}_\ell \Phi_\ell \right\rangle = \int_{t,\mathbf{x}} \left\{ -\dot{\varepsilon}_\alpha(t) J_\alpha(t, \mathbf{x}) + \varepsilon_\beta(t) \mathcal{J}_\ell(t, \mathbf{x}) \partial_\beta \Psi_\ell(t, \mathbf{x}) \right\}. \quad (3.26)$$

Since this identity is valid for arbitrary $\varepsilon(t)$, one deduces

$$\int_{\mathbf{x}} \left\{ \partial_t J_\alpha(t, \mathbf{x}) + \mathcal{J}_\ell(t, \mathbf{x}) \partial_\alpha \Psi_\ell(t, \mathbf{x}) \right\} = - \int_{\mathbf{x}} \partial_t^2 \bar{u}_\alpha(t, \mathbf{x}). \quad (3.27)$$

We use throughout this paper the notation $\mathbf{u} \equiv \langle \mathbf{v} \rangle$ and $\bar{\mathbf{u}} \equiv \langle \bar{\mathbf{v}} \rangle$ for the average fields, and generically for the field multiplet $\Psi \equiv \langle \Phi \rangle$. The identity (3.27) is integrated over space, but local in time. In contrast, the identity stemming from the usual Galilean invariance with a constant \mathbf{v}_0 is integrated over time as well, and the r.h.s. is replaced by zero since the action is invariant under global Galilean transformation.

One can express the sources in term of derivatives of Γ using (3.15) and rewrite the exact identity (3.27) as the following Ward identity for the functional Γ

$$\int_{\mathbf{x}} \left\{ \partial_t \frac{\delta \Gamma}{\delta u_\alpha} + \partial_\alpha \Psi_\ell \frac{\delta \Gamma}{\delta \Psi_\ell} \right\} = - \int_{\mathbf{x}} \partial_t^2 \bar{u}_\alpha. \quad (3.28)$$

Note that replacing instead the average values of the fields using (3.15), the identity (3.27) can be equivalently written for the functional \mathcal{W} as

$$\int_{\mathbf{x}} \left\{ \partial_t J_\alpha + \mathcal{J}_\ell \partial_\alpha \frac{\delta \mathcal{W}}{\delta \mathcal{J}_\ell} \right\} = - \int_{\mathbf{x}} \partial_t^2 \frac{\delta \mathcal{W}}{\delta \bar{J}_\alpha}. \quad (3.29)$$

The identities (3.28) and (3.29) are functional in the fields. One can deduce from them, by functional differentiation, an infinite set of exact identities amongst the correlation functions $\Gamma^{(n)}$ or $\mathcal{W}^{(n)}$. Let us express them for the vertices. They are obtained by taking functional derivatives of the identity (3.28) with respect to ℓ velocity and m response velocity fields, and setting the fields to zero, which yields in Fourier space:

$$\begin{aligned} \Gamma_{\alpha\alpha_1 \dots \alpha_{\ell+m}}^{(\ell+1,m)}(\omega, \mathbf{p} = \mathbf{0}, \omega_1, \mathbf{p}_1, \dots, \omega_{\ell+m}, \mathbf{p}_{\ell+m}) \\ = - \sum_{k=1}^{\ell+m} \frac{p_k^\alpha}{\omega} \Gamma_{\alpha_1 \dots \alpha_{\ell+m}}^{(\ell,m)}(\omega_1, \mathbf{p}_1, \dots, \omega_k + \omega, \mathbf{p}_k, \dots, \omega_{\ell+m}, \mathbf{p}_{\ell+m}) \\ \equiv \mathcal{D}_\alpha(\omega) \Gamma_{\alpha_1 \dots \alpha_{\ell+m}}^{(\ell,m)}(\omega_1, \mathbf{p}_1, \dots, \omega_{\ell+m}, \mathbf{p}_{\ell+m}), \end{aligned} \quad (3.30)$$

where the α_i are the space indices of the vector fields. We refer to (Tarpin *et al.* (2018)) for details on the derivation. The operator $\mathcal{D}_\alpha(\omega)$ hence successively shifts by ω all the frequencies of the function on which it acts. The identities (3.30) exactly relate an arbitrary $(\ell + m + 1)$ -point vertex function with one vanishing wavevector carried by a velocity field u_α to a lowered-by-one order $(\ell + m)$ -point vertex function. It is clear that this type of identity can constitute a key asset to address the closure problem of turbulence, since the latter precisely requires to express higher-order statistical moments in terms of lower-order ones. Of course, this relation only fixes $\Gamma^{(\ell+m+1)}$ in a specific configuration, namely with

one vanishing wavevector, so it does not allow one to completely eliminate this vertex, and it is not obvious *a priori* how it can be exploited. In fact, we will show that, within the FRG framework, this type of configurations play a dominant role at small scales, and the exact identities (3.30) (together with (3.34)) in turn yields the closure of the FRG equations in the corresponding limit.

3.3.2. Shift of the response fields

It was also early noticed in the field-theoretical framework that the NS action is invariant under a constant shift of the velocity response fields (as by integration by parts in (3.21) this constant can be eliminated). However, it was not identified until recently that this symmetry could also be promoted to a time-dependent one (Canet *et al.* (2015)). The latter corresponds to the following infinitesimal coupled transformation of the response fields

$$\begin{aligned}\delta \bar{v}_\alpha(t, \mathbf{x}) &= \bar{e}_\alpha(t) \\ \delta \bar{p}(t, \mathbf{x}) &= v_\beta(t, \mathbf{x}) \bar{e}_\beta(t).\end{aligned}\quad (3.31)$$

This transformation indeed induces a variation of the NS action which is only linear in the fields

$$\delta S_{\text{NS}} = \int_{t, \mathbf{x}} \bar{e}_\beta(t) \partial_t v_\beta(t, \mathbf{x}) + 2 \int_{t, \mathbf{x}, \mathbf{x}'} \bar{e}_\alpha(t) N_{\alpha\beta} \left(\frac{|\mathbf{x} - \mathbf{x}'|}{L} \right) \bar{v}_\beta(t, \mathbf{x}'). \quad (3.32)$$

Hence, interpreted as a change of variable in (3.20), this yields the identity $\langle \delta S_{\text{NS}} \rangle = \langle \delta \int_{t, \mathbf{x}} \mathcal{J}_\ell \Phi_\ell \rangle$, which can be written as the following Ward identity for the functional Γ

$$\int_{\mathbf{x}} \left\{ \frac{\delta \Gamma}{\delta \bar{u}_\alpha(t, \mathbf{x})} + u_\alpha(t, \mathbf{x}) \frac{\delta \Gamma}{\delta \bar{p}(t, \mathbf{x})} \right\} = \int_{\mathbf{x}} \partial_t u_\alpha(t, \mathbf{x}) + 2 \int_{\mathbf{x}, \mathbf{x}'} N_{\alpha\beta} \left(\frac{|\mathbf{x} - \mathbf{x}'|}{L} \right) \bar{u}_\beta(t, \mathbf{x}'). \quad (3.33)$$

Note that this identity is again local in time. Taking functional derivatives with respect to velocity and response velocity fields and evaluating at zero fields, one can deduce again exact identities for vertex functions (Canet *et al.* (2016)). They give the expression of any $\Gamma^{(\ell, m)}$ with one vanishing wavevector carried by a response velocity, which simply reads in Fourier space

$$\Gamma_{\alpha_1 \dots \alpha_{\ell+m}}^{(\ell, m)}(\omega_1, \mathbf{p}_1, \dots, \omega_\ell, \mathbf{p}_\ell, \omega_{\ell+1}, \mathbf{p}_{\ell+1} = \mathbf{0}, \dots) = 0, \quad (3.34)$$

for all (ℓ, m) except for the two lower-order ones which keep their original form given by $S_{\text{NS}, \alpha\beta}^{(1,1)}$ and $S_{\text{NS}, \alpha\beta\gamma}^{(2,1)}$ respectively, *i.e.* :

$$\begin{aligned}\Gamma_{\alpha\beta}^{(1,1)}(\omega_1, \mathbf{p}_1, \omega_2, \mathbf{p}_2 = \mathbf{0}) &= i\omega_1 \delta_{\alpha\beta} (2\pi)^{d+1} \delta(\omega_1 + \omega_2) \delta^d(\mathbf{p}_1 + \mathbf{p}_2), \\ \Gamma_{\alpha\beta\gamma}^{(2,1)}(\omega_1, \mathbf{p}_1, \omega_2, \mathbf{p}_2, \omega_3, \mathbf{p}_3 = \mathbf{0}) &= -i \left(p_2^\alpha \delta_{\beta\gamma} + i p_1^\beta \delta_{\alpha\gamma} \right) \\ &\quad \times (2\pi)^{d+1} \delta(\omega_1 + \omega_2 + \omega_3) \delta^d(\mathbf{p}_1 + \mathbf{p}_2 + \mathbf{p}_3). \quad (3.35)\end{aligned}$$

Let us emphasise that the analysis of extended symmetries can still be completed. First, for 2D turbulence, additional extended symmetries have recently been unveiled, which are reported in Appendix C. One of them is also realised in 3D turbulence but has not been exploited yet in the FRG formalism. Second, another important symmetry of the Euler or NS equation is the scaling or dilatation symmetry, which amounts to the transformation $\mathbf{v}(t, \mathbf{x}) \rightarrow b^h \mathbf{v}(b^z t, b\mathbf{x})$ (Frisch (1995); Dubrulle (2019)). One can also derive from this symmetry, possibly extended, functional Ward identities. This route has not been explored either. Both could lead to future fruitful developments.

3.4. Kármán-Howarth and Yaglom relations from symmetries

The path integral formulation conveys an interesting viewpoint on well-known exact identities such as the Kármán-Howarth relation (von Kármán & Howarth (1938)) or the equivalent Yaglom relation for passive scalars (Yaglom (1949)). The Kármán-Howarth relation stems from the energy budget equation associated with the NS equation, upon imposing stationarity, homogeneity and isotropy. From this relation, one can derive the exact four-fifths Kolmogorov law for the third order structure function $S^{(3)}$ (see e.g. Frisch (1995)). It turns out that the Kármán-Howarth relation also emerges as the Ward identity associated with a *spacetime-dependent* shift of the response fields (which is a generalisation of the *time-dependent* shift discussed in Sec. 3.3.2), and can thus be obtained in the path integral formulation as a consequence of symmetries (Canet *et al.* (2015)).

To show this, let us consider the NS action (3.21) with an additional source $L_{\alpha\beta}$ in (3.20) coupled to the local quadratic term $v_\alpha(t, \mathbf{x})v_\beta(t, \mathbf{x})$ (which is a composite operator in the field-theoretical language), *i.e.* the term $\int_{t,\mathbf{x}} v_\alpha L_{\alpha\beta} v_\beta$ is added to the source terms. This implies that a local, *i.e.* at coinciding space-time points, quadratic average of the velocities, can then be simply obtained by taking a functional derivative of \mathcal{W} with respect to this new source

$$\langle v_\alpha(t, \mathbf{x})v_\beta(t, \mathbf{x}) \rangle = \frac{\delta \mathcal{W}}{\delta L_{\alpha\beta}(t, \mathbf{x})} = -\frac{\delta \Gamma}{\delta L_{\alpha\beta}(t, \mathbf{x})}, \quad (3.36)$$

where the last equality stems from the Legendre transform relation (3.14). [†]

The introduction of the source for the composite operator $v_\alpha v_\beta$ allows one to consider a further extended symmetry of the NS action, namely the time *and* space dependent version of the field transformation (3.31), which amounts to $\bar{\varepsilon}_\alpha(t) \rightarrow \bar{\varepsilon}_\alpha(t, \mathbf{x})$. The variation of the NS action under this transformation writes

$$\langle \delta \mathcal{S}_{\text{NS}} \rangle = \left\langle \partial_t v_\alpha + \frac{1}{\rho} \partial_\alpha \pi - \nu \nabla^2 v_\alpha + \partial_\beta (v_\alpha v_\beta) - 2 \int_{\mathbf{x}'} \left(N_{\alpha\beta} \left(\frac{|\mathbf{x} - \mathbf{x}'|}{L} \right) \bar{v}_\beta(t, \mathbf{x}') \right) \right\rangle, \quad (3.37)$$

which is linear in the fields, but for the local quadratic term. However, this term can be expressed as a derivative with respect to $L_{\alpha\beta}$ using (3.36). The resulting Ward identity can be written equivalently in terms of Γ or \mathcal{W} . We here write it for \mathcal{W} since it renders more direct the connection with the Kármán-Howarth relation

$$-\partial_t \frac{\delta \mathcal{W}}{\delta J_\alpha} - \frac{1}{\rho} \partial_\alpha \frac{\delta \mathcal{W}}{\delta K} + \nu \nabla^2 \frac{\delta \mathcal{W}}{\delta J_\alpha} + \bar{J}_\alpha + \bar{K} \frac{\delta \mathcal{W}}{\delta J_\alpha} - \partial_\beta \frac{\delta \mathcal{W}}{\delta L_{\alpha\beta}} + 2 \int_{\mathbf{x}'} N_{\alpha\beta} \left(\frac{|\mathbf{x} - \mathbf{x}'|}{L} \right) \frac{\delta \mathcal{W}}{\delta \bar{J}_\beta(t, \mathbf{x}')} = 0. \quad (3.38)$$

We emphasise that, compared to (3.33), this identity is now *fully local*, in space as well as in time, *i.e.* it is no longer integrated over space. It is also an exact identity for the generating functional \mathcal{W} itself, which means that it entails an infinite set of exact identities amongst correlation functions. The Kármán-Howarth relation embodies the lowest order one, which is obtained by differentiating (3.38) with respect to $J_\gamma(t_y, \mathbf{y})$, and evaluating the resulting identity at zero external sources. Note that in the MSRJD formalism, the term proportional to $N_{\alpha\beta}$ is simply equal to a force-velocity correlation $\langle f_\alpha(t, \mathbf{x})v_\gamma(t_y, \mathbf{y}) \rangle$ (Canet *et al.* (2015)).

[†] Note that to define Γ , the Legendre transform is not taken with respect to the source $L_{\alpha\beta}$, *i.e.* both functional \mathcal{W} and Γ depend on $L_{\alpha\beta}$, hence the relation (3.36).

Summing over $\gamma = \alpha$ and specialising to equal time $t_y = t$, one deduces

$$\begin{aligned} & -\partial_t \langle v_\alpha(t, \mathbf{x}) v_\alpha(t, \mathbf{y}) \rangle + v(\Delta_x + \Delta_y) \langle v_\alpha(t, \mathbf{x}) v_\alpha(t, \mathbf{y}) \rangle \\ & -\partial_\beta^x \langle v_\alpha(t, \mathbf{x}) v_\beta(t, \mathbf{x}) v_\alpha(t, \mathbf{y}) \rangle - \partial_\beta^y \langle v_\alpha(t, \mathbf{y}) v_\beta(t, \mathbf{y}) v_\alpha(t, \mathbf{x}) \rangle \\ & + \langle f_\alpha(t, \mathbf{x}) v_\alpha(t, \mathbf{y}) \rangle + \langle f_\alpha(t, \mathbf{y}) v_\alpha(t, \mathbf{x}) \rangle = 0, \end{aligned} \quad (3.39)$$

which is the Kármán-Howarth relation. This fundamental relation is usually expressed in terms of the longitudinal velocity increments $\delta v_\parallel(\ell) = (\mathbf{v}(\mathbf{r} + \ell) - \mathbf{v}(\ell)) \cdot \ell / \ell$ by choosing the two space points as $\mathbf{y} = \mathbf{x} + \ell$ and $\mathbf{x} = \mathbf{r}$. Using homogeneity and isotropy, (3.39) can be equivalently expressed as

$$\begin{aligned} \epsilon(\ell) & \equiv -\frac{1}{4} \nabla_\ell \cdot \langle |\delta \mathbf{v}(\ell)|^2 \delta \mathbf{v}(\ell) \rangle \\ & = -\frac{1}{2} \partial_t \langle \mathbf{v}(\mathbf{r}) \mathbf{v}(\mathbf{r} + \ell) \rangle + \langle \mathbf{v}(\mathbf{r}) \cdot \frac{\mathbf{f}(\mathbf{r} + \ell) + \mathbf{f}(\mathbf{r} - \ell)}{2} \rangle + v \nabla_\ell^2 \langle \mathbf{v}(\mathbf{r}) \cdot \mathbf{v}(\mathbf{r} + \ell) \rangle. \end{aligned}$$

Once again, taking other functional derivatives with respect to arbitrary sources yields infinitely many exact relations. To give another example, by differentiating twice Eq. (3.38) with respect to $L_{\mu\nu}(t_y, \mathbf{y})$ and $J_\gamma(t_z, \mathbf{z})$, one obtains the exact relation for a pressure-velocity correlation (Canet *et al.* (2015))

$$\begin{aligned} & v \langle v_\alpha(t, \mathbf{x}) \Delta_x v_\alpha(t, \mathbf{x}) v^2(t, \mathbf{y}) \rangle - \frac{1}{\rho} \partial_\alpha^x \langle v^2(t, \mathbf{y}) v_\alpha(t, \mathbf{x}) \pi(t, \mathbf{x}) \rangle \\ & + \langle f_\alpha(t, \mathbf{x}) v_\alpha(t, \mathbf{x}) v^2(t, \mathbf{y}) \rangle - \frac{1}{2} \partial_\alpha^x \langle v_\alpha(t, \mathbf{x}) v^2(t, \mathbf{x}) v^2(t, \mathbf{y}) \rangle = 0, \end{aligned} \quad (3.40)$$

which was first derived in (Falkovich *et al.* (2010)). Taking additional functional derivatives with respect to \mathbf{J} or \mathbf{L} (or of the any other sources) generates new exact relations between higher-order correlation functions, involving in the averages one more \mathbf{v} or \mathbf{v}^2 (or any of the other fields) respectively with each derivative compared to (3.39). Although exact, relations for high-order correlation functions may not be of direct practical use since they are increasingly difficult to measure, but they are important at the theoretical level.

Shortly after Kolmogorov's derivation of the exact relation for the third-order structure function, Yaglom established the analogous formula for scalar turbulence (Yaglom (1949)). It was shown in (Pagani & Canet (2021)) that this relation can also be simply inferred from symmetries of the passive scalar action (3.23). More precisely, it ensues from the spacetime-dependent shift of the response fields

$$\bar{\theta}(t, \mathbf{x}) \rightarrow \bar{\theta}(t, \mathbf{x}) + \bar{\varepsilon}(t, \mathbf{x}), \quad \bar{\pi}(t, \mathbf{x}) \rightarrow \bar{\pi}(t, \mathbf{x}) + \bar{\varepsilon}(t, \mathbf{x}) \theta(t, \mathbf{x}) \quad (3.41)$$

in the path integral (3.22), in the presence of the additional source term $\int_{t, \mathbf{x}} L_\alpha v_\alpha \theta$ where L_α is the source coupled to the composite operator $v_\alpha \theta$. Following the same reasoning, one deduces an exact functional Ward identity for the passive scalar, which writes in term of \mathcal{W}

$$\left(\partial_t - \kappa_\theta \nabla^2 \right) \frac{\delta W}{\delta j(t, \mathbf{x})} + \partial_\beta \frac{\delta W}{\delta L_\beta(t, \mathbf{x})} - \int_{\mathbf{y}} M \left(\frac{|\mathbf{x} - \mathbf{y}|}{L_\theta} \right) \frac{\delta W}{\delta \bar{j}(t, \mathbf{y})} = 0. \quad (3.42)$$

The lowest order relation stemming from it is the Yaglom relation

$$-\frac{1}{2} \frac{\partial}{\partial(x-y)_\alpha} \left\langle |\theta(t, \mathbf{x}) - \theta(t, \mathbf{y})|^2 (v_\alpha(t, \mathbf{x}) - v_\alpha(t, \mathbf{y})) \right\rangle = 2\epsilon_\theta, \quad (3.43)$$

where ϵ_θ is the mean dissipation rate of the scalar. As for the Kármán-Howarth relation, it

can be re-expressed using homogeneity and isotropy in the more usual form

$$\left\langle \left| \theta(t, \mathbf{r}) - \theta(t, \mathbf{r} + \boldsymbol{\ell}) \right|^2 \delta_{\mathbf{V}_{\parallel}}(t, \boldsymbol{\ell}) \right\rangle = -\frac{4}{3} \epsilon_{\theta} \ell, \quad (3.44)$$

This relation hence also follows from symmetries in the path integral formulation. Again, an infinite set of higher-order exact relations between scalar and velocity correlation functions can be obtained by further differentiating (3.42) with respect to sources \mathbf{L} or j .

4. The functional renormalisation group

As mentioned in Sec. 2, the idea underlying the FRG is Wilson's original idea of progressive averaging of fluctuations in order to build up the effective description of a system from its microscopic model. This progressive averaging is organised scale by scale, in general in wavenumber space, and thus leads to a sequence of scale-dependent models, embodied in Wilson's formulation in a scale-dependent Hamiltonian or action (Wilson & Kogut (1974)). In the FRG formalism, one rather considers a scale-dependent effective action Γ_{κ} , called effective average action, where κ denotes the RG scale. It is a wavenumber scale, which runs from the microscopic ultraviolet (UV) scale Λ to a macroscopic IR scale (e.g. the inverse integral scale L^{-1}). The interest of the RG procedure is that the information about the properties of the system can be captured by the *flow* of these scale-dependent models, *i.e.* their evolution with the RG scale, without requiring to explicitly carry out the integration of the fluctuations in the path integral. The RG flow is governed by an exact very general equation, which can take different forms depending on the precise RG used (Wilson (Wilson & Kogut (1974)) or Polchinski flow equation (Polchinski (1984)), Callan-Symanzik flow equation (Callan (1970); Symanzik (1970)), ...). The one at the basis of the FRG formalism is usually called the Wetterich equation (Wetterich (1993)). We briefly introduce it in the next sections on the example of the generic scalar field theory of Sec. 3.1, denoting generically $\Phi(t, \mathbf{x})$ the field multiplet, e.g. $\Phi = (\varphi, \bar{\varphi})$, $\Psi = \langle \Phi \rangle$ the multiplet of average fields, and \mathcal{J} the multiplet of corresponding sources.

4.1. Progressive integration of fluctuations

The core of the RG procedure is to turn the global integration over fluctuations in the path integral (3.9) into a progressive integration, organised by wavenumber shells. To achieve this, one introduces in the path integral a scale-dependent weight $e^{-\Delta S_{\kappa}}$ whose role is to suppress fluctuations below the RG scale κ , giving rise to a new, scale-dependent generating functional

$$\mathcal{Z}_{\kappa}[\mathcal{J}] = \int \mathcal{D}\Phi e^{-S[\Phi] - \Delta S_{\kappa}[\Phi] + \int_{t,\mathbf{x}} \mathcal{J}_{\ell} \Phi_{\ell}}. \quad (4.1)$$

The new term ΔS_{κ} is chosen quadratic in the fields

$$\Delta S_{\kappa}[\Phi] = \frac{1}{2} \int_{t,\mathbf{x},\mathbf{x}'} \Phi_m(t, \mathbf{x}) \mathcal{R}_{\kappa,mm'}(|\mathbf{x} - \mathbf{x}'|) \Phi_{m'}(t, \mathbf{x}'), \quad (4.2)$$

where \mathcal{R}_{κ} is called the regulator, or cut-off, matrix. Note that it has been chosen here proportional to $\delta(t - t')$, or equivalently independent of frequencies. This means that the selection of fluctuations is operated in space, and not in time, as in equilibrium. [†]

[†] The selection can in principle be operated also in time, although it poses some technical difficulties, not to violate causality (Canet *et al.* (2011a)) and symmetries involving time – typically the Galilean invariance. A spacetime cutoff was implemented only in (Duclut & Delamotte (2017)) for Model A, which is a simple, purely dissipative, dynamical extension of the Ising model. In the following, we restrict ourselves to frequency-independent regulators.

The precise form of the elements $[\mathcal{R}]_{\kappa,ij}$ of the cutoff matrix is not important, provided they satisfy the following requirements:

$$\begin{aligned} R_\kappa(\mathbf{p}) &\sim \kappa^2 & \text{for } |\mathbf{p}| \lesssim \kappa \\ R_\kappa(\mathbf{p}) &\longrightarrow 0 & \text{for } |\mathbf{p}| \gtrsim \kappa, \end{aligned} \quad (4.3)$$

where R_κ denotes a generic non-vanishing element of the matrix \mathcal{R}_κ . The first constraint endows the low wavenumber modes with a large “mass” κ^2 , such that these modes are damped, or filtered out, for their contribution in the functional integral to be suppressed. The second one ensures that the cutoff vanishes for large wavenumber modes, which are thus unaffected. Hence, only these modes are integrated over, thus achieving the progressive averaging. Moreover, $R_{\kappa=\Lambda}$ is required to be very large such that all fluctuations are frozen at the microscopic (UV) scale, and $R_{\kappa=0}$ to vanish such that all fluctuations are averaged over in this (IR) limit.

It follows that the free energy functional $\mathcal{W}_\kappa = \ln \mathcal{Z}_\kappa$ also becomes scale-dependent. One defines the scale-dependent effective average action through the modified Legendre transform

$$\Gamma_\kappa[\Psi] + \Delta\mathcal{S}_\kappa[\Psi] = \sup_{\mathcal{J}} \left[\int_{t,x} \mathcal{J}_\ell \Psi_\ell - \mathcal{W}_\kappa[\mathcal{J}] \right]. \quad (4.4)$$

The regulator term is added in the relation in order to enforce that, at the scale $\kappa = \Lambda$, the effective average action coincides with the microscopic action $\Gamma_{\kappa=\Lambda} = \mathcal{S}$. For fluid dynamics, the scale Λ^{-1} represents a very small scale, typically a few mean-free-paths, where the description in term of a continuous equation becomes valid, and the “microscopic” action is the Navier-Stokes action \mathcal{S}_{NS} . This scale is thus much smaller than the Kolmogorov scale η , and the effect of fluctuations (the renormalisation) is already important at scales $\ell \simeq \eta$, *i.e.* the statistical properties of the turbulence in the dissipative range are non-trivial. In the opposite limit $\kappa \rightarrow 0$ (or equivalently $\kappa \ll L^{-1}$) the standard effective action Γ , encompassing all the fluctuations, is recovered since the regulator is removed in this limit $\Delta\mathcal{S}_{\kappa=0} = 0$. Thus, the sequence of Γ_κ provides an interpolation between the microscopic action [the NS action] and the full effective action [the statistical properties of the fluid].

4.2. Exact flow equation for the effective average action

The evolution of the generating functionals \mathcal{W}_κ and Γ_κ with the RG scale κ obeys an exact differential equation, which can be simply inferred from (4.1) and (4.4) since the dependence on κ only comes from the regulator term $\Delta\mathcal{S}_\kappa$. The derivation is very general and can be found in standard references, *e.g.* Sec. 2.3.3. of (Delamotte (2012)). One finds the following exact flow equation for \mathcal{W}_κ

$$\partial_s \mathcal{W}_\kappa[\mathcal{J}] = -\frac{1}{2} \text{Tr} \left[\partial_s \mathcal{R}_{\kappa,mn} \left(\frac{\delta^2 \mathcal{W}_\kappa[\mathcal{J}]}{\delta \mathcal{J}_m \delta \mathcal{J}_n} + \frac{\delta \mathcal{W}_\kappa[\mathcal{J}]}{\delta \mathcal{J}_m} \frac{\delta \mathcal{W}_\kappa[\mathcal{J}]}{\delta \mathcal{J}_n} \right) \right], \quad (4.5)$$

where $s \equiv \log(\kappa/\Lambda)$. This equation is very similar to Polchinski equation (Polchinski (1984)). Some simple algebra then leads to the Wetterich equation for Γ_κ

$$\partial_s \Gamma_\kappa[\Psi] = \frac{1}{2} \text{Tr} [\partial_s \mathcal{R}_{\kappa,mn} G_{\kappa,mn}] \equiv \frac{1}{2} \text{Tr} \left[\partial_s \mathcal{R}_{\kappa,mn} \left(\Gamma_\kappa^{(2)}[\Psi] + \mathcal{R}_\kappa \right)_{mn}^{-1} \right], \quad (4.6)$$

where $G_\kappa \equiv \mathcal{W}_\kappa^{(2)}$ is the propagator, and is the inverse of $(\Gamma_\kappa^{(2)} + \mathcal{R}_\kappa)$ from the Legendre relation. To alleviate notations, the indices m, n refer to the field indices within the multiplet, as well as other possible indices (*e.g.* vector component) and space-time coordinates. Accordingly, the trace includes the summation over all internal indices as well as the

integration over all spacial and temporal coordinates (conforming to deWitt notation, integrals are implicit).

While Eq. (4.6) or (4.5) are exact, they are functional partial differential equations which cannot be solved exactly in general. Their functional nature implies that they encompass an infinite set of flow equations for the associated correlation functions or vertices. For instance, taking one functional derivative of (4.6) with respect to a given field and evaluating the resulting expression at a fixed background field configuration (say $\Psi(t, \mathbf{x}) = 0$) yields the flow equation for the one-point vertex $\Gamma_\kappa^{(1)}$. This equation depends on the three-point vertex $\Gamma_\kappa^{(3)}$. More generally, the flow equation for the n -point vertex $\Gamma_\kappa^{(n)}$ involves the vertices $\Gamma_\kappa^{(n+1)}$ and $\Gamma_\kappa^{(n+2)}$, such that one has to consider an infinite hierarchy of flow equations. This pertains to the very common closure problem of non-linear systems. It means that one has to devise some approximations.

4.3. Non-perturbative approximation schemes

This part may appear very technical for readers not familiar with RG methods. Its objective is to explain the rationale underlying the approximation schemes used in the study of turbulence, which are detailed in the rest of the *Perspectives*.

In the FRG context, several approximation schemes have been developed and are commonly used (Dupuis *et al.* (2021)). Of course one can implement a perturbative expansion, in any available small parameter, such as a small coupling or an infinitesimal distance to a critical dimension $\varepsilon = d - d_c$. One then retrieves results obtained from standard perturbative RG techniques. However, the key advantage of the FRG formalism is that it is suited to the implementation of non-perturbative approximation schemes. The most commonly used is the derivative expansion, which consists in expanding the effective average action Γ_κ in powers of gradients and time derivatives (thus yielding an ansatz for Γ_κ). This is equivalent to an expansion around zero external wavenumbers $|\mathbf{p}_i| = 0$ and frequencies $\omega_i = 0$ and is thus adapted to describe the long-distance long-time properties of a system. One can in particular obtain universal properties of a system at criticality (e.g. critical exponents), but also non-universal properties, such as phase diagrams. Even though it is non-perturbative in the sense that it does not rely on an explicit small parameter, it is nonetheless controlled. It can be systematically improved, order by order (adding higher-order derivatives), and an error can be estimated at each order, using properties of the cutoff (De Polsi *et al.* (2022)). The convergence and accuracy of the derivative expansion have been studied in depth for archetypal models, namely the Ising model and $O(N)$ models (Dupuis *et al.* (2021)). The outcome is that the convergence is fast, and most importantly that the results obtained for instance for the critical exponents are very precise. For the 3D Ising model, the derivative expansion has been pushed up to the sixth order $O(\partial^6)$ and the results for the critical exponents compete in accuracy with the best available estimates in the literature (stemming from conformal bootstrap methods) (Balog *et al.* (2019)). For the $O(N)$ models, the FRG results are the most accurate ones available (De Polsi *et al.* (2020, 2021)).

The derivative expansion is by construction restricted to describe the zero wavenumber and frequency sector, it does not allow one to access the full space-time dependence of generic correlation functions. To overcome this limitation, one can resort to another approximation scheme, which consists in a vertex expansion. The most useful form of this approximation is called the Blaizot–Mendez–Wschebor (BMW) scheme (Blaizot *et al.* (2006, 2007); Benitez *et al.* (2008)). It lies at the basis of all the FRG studies dedicated to turbulence. The BMW scheme essentially exploits an intrinsic property of the Wetterich flow equation conveyed by the presence of the regulator. The Wetterich equation has a one-loop structure. To avoid any confusion, let us emphasise that this does not mean that it is

equivalent to a one-loop perturbative expansion: the propagator entering Eq. (4.6) is the full (functional) renormalised propagator of the theory, not the bare one. This simply means that the flow equation involves only one internal, or loop, (*i.e.* integrated over) wavevector \mathbf{q} and frequency ω . This holds true for the flow equation of any vertex $\Gamma_\kappa^{(n)}$, which depends on the n external wavevectors \mathbf{p}_i and frequencies ϖ_i , but always involves only one internal (loop) wavevector and frequency (ω, \mathbf{q}) .

The key feature of the Wetterich equation is that the internal wavevector \mathbf{q} is controlled by the scale-derivative of the regulator. Because of the requirement (4.3), $\partial_s \mathcal{R}_\kappa(\mathbf{q})$ is exponentially vanishing for $q \equiv |\mathbf{q}| \gtrsim \kappa$, which implies that the loop integral is effectively cut to $q \simeq \kappa$, with κ the RG scale. This points to a specific limit where this property can be exploited efficiently, namely the large wavenumber limit. Indeed, if one considers large external wavenumbers $p_i \equiv |\mathbf{p}_i| \gg \kappa$, then $|\mathbf{q}| \ll |\mathbf{p}_i|$ is automatically satisfied, or otherwise stated $|\mathbf{q}|/|\mathbf{p}_i| \rightarrow 0$. Hence the limit of $|\mathbf{p}_i| \rightarrow \infty$ is formally equivalent to the limit $|\mathbf{q}| \rightarrow 0$ (because the \mathbf{p}_i and \mathbf{q} always come as sum or product in the propagator and vertices). Moreover, the presence of the regulator ensures that all the vertices are analytical functions of their arguments at any finite κ , and can thus be Taylor expanded (Berges *et al.* (2002)). The BMW approximation precisely consists in expanding the vertices entering the flow equation around $\mathbf{q} \simeq 0$, which can be interpreted as an expansion at large p_i . This expansion becomes formally exact in the limit where all $p_i \rightarrow \infty$. Besides, one has that a generic $\Gamma_\kappa^{(n)}$ vertex with one zero wavevector can be expressed as a derivative with respect to a constant field of the corresponding vertex $\Gamma_\kappa^{(n-1)}$ stripped of the field with zero wavevector. This allows one in the original BMW approximation scheme to close the flow equation at a given order (say for the two-point function), at the price of keeping a dependence in a background constant field Ψ_0 , *i.e.* $\bar{\Gamma}_\kappa^{(2)}(\varpi, \mathbf{p}; \Psi_0)$, which can be cumbersome. This approximation can also in principle be improved order by order, by achieving the \mathbf{q} expansion in the flow equation for the next order $(n+1)$ vertex instead of the n th one, although it becomes increasingly difficult.

In the context of non-equilibrium statistical physics, the BMW approximation scheme was implemented successfully to study the Burgers or equivalently Kardar-Parisi-Zhang equation (2.8), which is detailed in Sec. 5. For the NS equation, the BMW approximation scheme turns out to be remarkably efficient in two respects which will become clear in the following: technically, the symmetries and extended symmetries allow one to get rid of the background field dependence, and thus to achieve the closure exactly. Moreover, physically, the large wavenumber limit is not trivial for turbulence, which is unusual. In critical phenomena exhibiting standard scale invariance, the large wavenumbers simply decouple from the IR properties and this limit carries no independent information (see Sec. 5).

5. A warm-up example: Burgers-KPZ equation

The Burgers equation is often considered as a toy model for classical hydrodynamics. In the inviscid limit, its solution develops shocks after a finite time even for smooth initial conditions (Bec & Khanin (2007)). Most studies consider potential flows, for which case the (irrotational d -dimensional) Burgers equation exactly maps to the KPZ equation (2.8). The forcing is assumed to be a power-law $D(\mathbf{p}) \sim p^\beta$, which mainly injects energy at small scales (UV modes) for $\beta > 0$, while it acts on large scales (IR modes) for $\beta < 0$.

One is generally interested in the space-time correlations of the velocity

$$C^{(n)}(\tau, \ell) = \left\langle \left[\mathbf{v}(t + \tau, \mathbf{x} + \ell) - \mathbf{v}(t, \mathbf{x}) \right]^n \right\rangle. \quad (5.1)$$

The structure functions, which correspond to the equal-time correlations, behave as power-law in the inertial range $S_n(\ell) \sim \ell^{\zeta_n}$. Besides, the two-point correlation function is expected

to endow a scaling form

$$C^{(2)}(\tau, \ell) \equiv C(\tau, \ell) = \ell^{2(\chi-1)} F(\tau/\ell^z), \quad (5.2)$$

where χ and z are universal critical exponents called the roughness and dynamical exponent in the context of interface growth, and F is a universal scaling function. The roughness exponent is simply related to ζ_2 as $\zeta_2 = 2(\chi - 1)$. The dynamical and roughness exponents are related in all dimensions by the exact identity $z + \chi = 2$ stemming from Galilean invariance.

In one dimension $d = 1$, the critical exponents are known exactly. For $\beta > 0$, one has (Medina *et al.* (1989); Janssen *et al.* (1999); Kloss *et al.* (2014a))

$$\chi = \max\left(\frac{1}{2}, -\frac{\beta}{3} + 1\right). \quad (5.3)$$

Moreover, shocks are overwhelmed by the forcing and there is no intermittency, *i.e.* $\zeta_n = n\zeta_2/2 = n(\chi - 1)$ (Hayot & Jayaprakash (1996)). For $\beta < -3$, the stationary state contains a finite density of shocks and the scaling of the velocity increments in the regime where $|\ell|$ is much smaller than the average distance between shocks but larger than the shock size can be estimated by a simple argument, yielding (Bec & Khanin (2007))

$$\zeta_n = \min(1, n). \quad (5.4)$$

While the intermediate regime $-3 < \beta < 0$ is not well understood, a wealth of exact results are available for $\beta = 2$, which have been obtained in the context of the KPZ equation (Corwin (2012)). In particular, the analytical form of the scaling function F in (5.2) has been determined exactly (Prähofer & Spohn (2000)).

In higher dimensions $d > 1$, very few is known. The most studied case corresponds to the KPZ equation $\beta = 2$. In contrast with $d = 1$ where the interface always roughens, in dimensions $d > 2$, the KPZ equation exhibits a (non-equilibrium) continuous phase transition between a smooth phase and a rough phase, depending on the amplitude λ of the non-linearity in (2.8). For $\lambda < \lambda_c$, the interface remains smooth, it is then described by the Edwards-Wilkinson equation which is the linear, non-interacting, $\lambda = 0$, version of KPZ, and which has a simple diffusive behaviour with $z = 2$ and $\chi = (2 - d)/2$. For $\lambda > \lambda_c$, the non-linearity is dominant and the interface becomes rough, with $\chi > 0$. This is the KPZ phase. Contrarily to $d = 1$, no exact result has been obtained for $d \neq 1$, and the critical exponents are known only numerically (Pagnani & Parisi (2015)).

Since the early days of the KPZ equation, perturbative RG techniques (usually referred to as dynamical RG) have been applied to determine the critical exponents (Kardar *et al.* (1986); Medina *et al.* (1989); Janssen *et al.* (1999)). However, the KPZ equation constitutes a striking example where the perturbative RG flow equations are known to all orders in perturbation theory, but nonetheless fails in $d \geq 2$ to find the strong-coupling fixed-point expected to govern the KPZ rough phase (Wiese (1998)). In contrast, the FRG framework allows one to access this fixed point in all dimensions even at the lowest order of the derivative expansion (Canet (2005); Canet *et al.* (2010)). This fixed-point turns out to be genuinely non-perturbative, *i.e.* not connected to the Edwards-Wilkinson fixed-point (which is the point around which perturbative expansions are performed) in any dimension, hence explaining the failure of perturbation theory, to all orders. We now briefly review these results.

5.1. FRG for the Burgers-KPZ equation

The correlation function (5.2) can be computed from the two-point functions $\Gamma^{(2)}$. The general FRG flow equation for these functions is obtained by differentiating twice the exact

The more advanced approximation which has been implemented so far for the Burgers-KPZ equation consists in truncating the effective average action Γ_κ at second order (SO) in the response field, and thus neglecting higher-order terms in this field which could in principle be generated by the RG flow. This means that the noise probability distribution is kept to be Gaussian as in the original Langevin description, which sounds reasonable. The

most general ansatz at this SO order compatible with the symmetries of the Burgers equation, *i.e.* using the previous construction, reads

$$\Gamma_\kappa[\mathbf{u}, \bar{\mathbf{u}}] = \int_{t,x} \left\{ \bar{u}_\alpha f_\kappa^\rho(D_t, \nabla) D_t u_\alpha - \bar{u}_\alpha f_\kappa^\nu(D_t, \nabla) \nabla^2 u_\alpha - \bar{u}_\alpha f_\kappa^D(D_t, \nabla) \bar{u}_\alpha \right\}. \quad (5.6)$$

It is parametrised by three scale-dependent renormalisation functions f_κ^ν , f_κ^D and f_κ^ρ , which are arbitrary functions of the covariant operators ∇ and D_t , beside depending on the RG scale κ [†]. Their initial condition at $\kappa = \Lambda$ is $f_\Lambda^\nu = \nu$, $f_\Lambda^D = (D_{\alpha\beta})^\parallel$ (longitudinal part of $D_{\alpha\beta}$) and $f_\Lambda^\rho = 1$ for which the initial Burgers-KPZ action (3.19) is recovered. The ansatz (5.6) encompasses the most general dependence in wavenumbers and frequencies, and also in velocity fields, of the two-point functions compatible with Galilean invariance. Indeed, arbitrary powers of the velocity field \mathbf{u} are included through the operator D_t . Thus Γ_κ is truncated only in the response field, not in the field itself.

The choice of an ansatz allows one to compute explicitly all the vertices $\Gamma_\kappa^{(n)}$, their expression can be found in Canet *et al.* (2011b). For example, it yields for the two-point functions in Fourier space

$$\begin{aligned} \bar{\Gamma}_\kappa^{(1,1)}(\omega, \mathbf{p}) &= i\omega f_\kappa^\rho(\omega, \mathbf{p}) + \mathbf{p}^2 f_\kappa^\nu(\omega, \mathbf{p}) \\ \bar{\Gamma}_\kappa^{(0,2)}(\omega, \mathbf{p}) &= -2f_\kappa^D(\omega, \mathbf{p}). \end{aligned} \quad (5.7)$$

The flow equations for the three functions f_κ^ν , f_κ^D and f_κ^ρ can then be computed from the flow equations (5.5). More details on the calculation, in particular on the choice of the regulator, are provided in Sec. 6 for NS, and can be found for Burgers-KPZ in e.g. (Canet *et al.* (2011b)).

5.2. Scaling dimensions

With the aim of analyzing the fixed point structure, one defines dimensionless and renormalised quantities. First, one introduces scale-dependent coefficients $\nu_\kappa \equiv f_\kappa^\nu(0, 0)$ and $D_\kappa \equiv f_\kappa^D(0, 0)$ [‡], which identify at the microscopic scale $\kappa = \Lambda$ with the parameters ν and D of the action (3.19) [¶]. They are associated with scale-dependent anomalous dimensions as

$$\eta_\kappa^D = -\partial_s \ln D_\kappa, \quad \eta_\kappa^\nu = -\partial_s \ln \nu_\kappa, \quad (5.8)$$

where $s = \ln(\kappa/\Lambda)$ is the RG “time” and $\partial_s = \kappa \partial_\kappa$. Indeed, one expects that if a fixed point is reached, these coefficients behave as power laws $D_\kappa \sim \kappa^{-\eta_\kappa^D}$ and $\nu_\kappa \sim \kappa^{-\eta_\kappa^\nu}$ where the $*$ denotes fixed-point quantities. The physical critical exponents can then be deduced from η_κ^D and η_κ^ν . For this, let us determine the scaling dimensions of the fields from Eq. (5.6). The three functions f_κ^ν , f_κ^D and f_κ^ρ have respective scaling dimensions ν_κ , D_κ and $\rho_\kappa \equiv 1$ by definition of these coefficients. Since Γ_κ has no dimension, one deduces from the term $\propto \partial_t$ in Γ_κ that $[u_\alpha \bar{u}_\alpha] = \kappa^d$ and from the viscosity term that $[u_\alpha \bar{u}_\alpha] = \kappa^d \omega \kappa^{-2} \nu_\kappa^{-1}$. Equating the two terms, this implies that the scaling dimension of the frequency is $[\omega] = \nu_\kappa \kappa^2 \equiv \kappa^z$, which defines the dynamical critical exponent as $z = 2 - \eta_\kappa^\nu$. The scaling dimensions of the fields can then be deduced from the forcing term of Γ_κ as

$$[u_\alpha] = (\kappa^{d-2} D_\kappa \nu_\kappa^{-1})^{1/2}, \quad [\bar{u}_\alpha] = (\kappa^{d+2} \nu_\kappa D_\kappa^{-1})^{1/2}. \quad (5.9)$$

[†] Note that f_κ^ν , f_κ^D and f_κ^ρ are scalar functions because they correspond to the longitudinal parts of $f_{\kappa, \alpha\beta}^\nu$, $f_{\kappa, \alpha\beta}^D$ and $f_{\kappa, \alpha\beta}^\rho$. The transverse parts vanish since the flow is potential.

[‡] equivalently D_κ is defined from f_κ^D evaluated at a finite \mathbf{p} if f_κ^D is non-analytic at $p = 0$.

[¶] The scaling dimension of f_κ^ρ is fixed to 1 by the symmetries so there is no need to introduce a coefficient ρ_κ associated with this function.

This implies in particular that the roughness critical exponent χ is related to η_*^ν and η_*^D as $\chi = (2 - d - \eta_*^\nu + \eta_*^D)/2$.

To introduce dimensionless quantities, denoted with a hat symbol, wavevectors are measured in units of κ , e.g. $\mathbf{p} = \kappa \hat{\mathbf{p}}$ and frequencies in units of $\nu_\kappa \kappa^2$, e.g. $\omega = \nu_\kappa \kappa^2 \hat{\omega}$. Dimensionless fields are defined as $\hat{\mathbf{u}} = (\kappa^{d-2} D_\kappa \nu_\kappa^{-1})^{-1/2} \mathbf{u}$, $\hat{\bar{\mathbf{u}}} = (\kappa^{d+2} \nu_\kappa D_\kappa^{-1})^{-1/2} \bar{\mathbf{u}}$, and dimensionless functions as

$$\hat{f}_\kappa^\nu(\hat{\omega}, \hat{\mathbf{p}}) \equiv \frac{1}{\nu_\kappa} f_\kappa^\nu \left(\frac{\omega}{\nu_\kappa \kappa^2}, \frac{\mathbf{p}}{\kappa} \right), \quad \hat{f}_\kappa^D(\hat{\omega}, \hat{\mathbf{p}}) \equiv \frac{1}{D_\kappa} f_\kappa^D \left(\frac{\omega}{\nu_\kappa \kappa^2}, \frac{\mathbf{p}}{\kappa} \right), \quad \hat{f}_\kappa^\rho(\hat{\omega}, \hat{\mathbf{p}}) \equiv f_\kappa^\rho \left(\frac{\omega}{\nu_\kappa \kappa^2}, \frac{\mathbf{p}}{\kappa} \right). \quad (5.10)$$

The non-dimensionalisation of the fields introduces a scaling dimension in front of the advection term. We define the corresponding dimensionless coupling as $\hat{\lambda}_\kappa = (\kappa^{d-4} D_\kappa \nu_\kappa^{-3})^{1/2} \lambda$ (where λ is the KPZ parameter, $\lambda = 1$ for the Burgers equation). The Ward identity for Galilean symmetry yields that λ is not renormalised, *i.e.* it stays constant throughout the RG flow, or otherwise stated its flow is zero $\partial_s \lambda = 0$. One thus obtains for the flow of $\hat{\lambda}_\kappa$

$$\partial_s \hat{\lambda}_\kappa = \frac{\hat{\lambda}_\kappa}{2} (d - 4 + 3\eta_\kappa^\nu - \eta_\kappa^D). \quad (5.11)$$

One can deduce from this equation that if a non-trivial fixed-point exists ($\hat{\lambda}_* \neq 0$), then the fixed point values of the anomalous dimensions satisfy the exact relation

$$d - 4 + 3\eta_*^\nu - \eta_*^D = 0. \quad (5.12)$$

Using the definitions of the critical exponents, this relation writes $\chi + z = 2$ in all dimensions, which is the exact identity mentioned in the introduction of this section.

5.3. Results in $d = 1$

Let us focus on the case $\beta = 2$, *i.e.* $D_{\alpha\beta}(\mathbf{p}) \equiv D p_\alpha p_\beta$ in (3.19), which corresponds to the KPZ equation, because exact results are available for this case in one dimension. In $d = 1$, there exists an additional discrete time-reversal symmetry which greatly simplifies the problem. This is one of the reasons why exact results could be obtained in this dimension only. In particular, one can show that it implies a particular form of fluctuation-dissipation theorem which writes for the two-point functions (Frey & Täuber (1994); Canet *et al.* (2011b))

$$2\text{Re}\bar{\Gamma}_\kappa^{(1,1)}(\omega, \mathbf{p}) = -\frac{\nu}{D} p^2 \bar{\Gamma}_\kappa^{(0,2)}(\omega, \mathbf{p}), \quad (5.13)$$

and in turn entails that $D_\kappa = \nu_\kappa$, $f_\kappa^D = f_\kappa^\nu \equiv f_\kappa$, and $f_\kappa^\rho \equiv 1$ †. Thus there remains only one renormalisation function f_κ and one anomalous dimension $\eta_\kappa^\nu = \eta_\kappa^D \equiv \eta_\kappa$ to compute in $d = 1$. This implies that the fixed-point value of the latter is fixed exactly by (5.12) to $\eta_* = 1/2$, which yields the well-known values $\chi = 1/2$ and $z = 3/2$. The flow equation for the associated dimensionless function \hat{f}_κ reads:

$$\partial_s \hat{f}_\kappa(\hat{\omega}, \hat{\mathbf{p}}) = \left[\eta_\kappa + (2 - \eta_\kappa) \hat{\omega} \partial_{\hat{\omega}} + \hat{\mathbf{p}} \partial_{\hat{\mathbf{p}}} \right] \hat{f}_\kappa(\hat{\omega}, \hat{\mathbf{p}}) + \frac{1}{D_\kappa} \partial_s f_\kappa(\omega, \mathbf{p}), \quad (5.14)$$

where the first term in square bracket comes from the non-dimensionalisation (5.10) and the last term corresponds to the nonlinear loop term calculated from the flow equations (5.5).

This flow equation can be integrated numerically, from the initial condition $\hat{f}_\Lambda(\hat{\omega}, \hat{\mathbf{p}}) = 1$ at scale $\kappa = \Lambda$. This has been performed in (Canet *et al.* (2011b)) to which we refer for details. One obtains that the flow reaches a fixed-point, where all quantities stop evolving.

† Note that the viscosity term in (5.6) has to be symmetrised to exactly preserve the Ward identities ensuing from the time-reversal symmetry for all the n -point vertices, see (Canet *et al.* (2011b)).

The function \hat{f}_κ converges to a fixed form $\hat{f}_*(\hat{\omega}, \hat{\mathbf{p}})$, which behaves as a power-law at large \mathbf{p} and large ω as

$$\hat{f}_\kappa(\hat{\omega}, \hat{\mathbf{p}}) \stackrel{|\hat{\mathbf{p}}| \gg 1}{\sim} |\mathbf{p}|^{-\eta_*}, \quad \hat{f}_\kappa(\hat{\omega}, \hat{\mathbf{p}}) \stackrel{\omega \gg 1}{\sim} \omega^{-\eta_*/(2-\eta_*)}. \quad (5.15)$$

In fact, this is expected from a very important property of the flow equation called decoupling. Decoupling means that the loop contribution $\frac{\partial_s f_\kappa}{D_\kappa}$ in the flow equation (5.14) becomes negligible in the limit of large wavenumbers and/or frequencies compared to the linear terms. Intuitively, a large wavenumber is equivalent to a large mass, and degrees of freedom with a large mass are damped and do not contribute in the dynamics at large scales. This means that the IR (effective) properties are not affected by the UV (microscopic) details, and this pertains to the mechanism for universality. Moreover, one can prove that the decoupling property entails scale invariance. Indeed, if the loop contribution $\partial_s \hat{f}_\kappa$ is negligible compared to the linear terms, one can readily prove that the general solution of (5.14) takes the scaling form

$$\hat{f}^*(\hat{\omega}, \hat{\mathbf{p}}) = \frac{1}{|\mathbf{p}|^{\eta_*}} \hat{\zeta}\left(\frac{\hat{\omega}}{|\hat{\mathbf{p}}|^z}\right) \quad (5.16)$$

where $\hat{\zeta}$ is a universal scaling function, which can be determined by explicitly integrating the full flow equation (5.14). The physical correlation function (5.2) can be deduced from the ansatz as

$$C(\omega, \mathbf{p}) = -\frac{\Gamma^{(0,2)}(\omega, \mathbf{p})}{|\Gamma^{(1,1)}(\omega, \mathbf{p})|^2} = \frac{2f(\omega, \mathbf{p})}{\omega^2 + p^4 f(\omega, \mathbf{p})^2}. \quad (5.17)$$

Replacing the function f by its fixed-point form (5.16) and using the value $\eta_* = 1/2$, one obtains

$$\hat{C}(\hat{\omega}, \hat{\mathbf{p}}) = \frac{2}{\hat{p}^{7/2}} \frac{\hat{\zeta}\left(\frac{\hat{\omega}}{\hat{p}^{3/2}}\right)}{\hat{\omega}^2/\hat{p}^3 + \hat{\zeta}^2\left(\frac{\hat{\omega}}{\hat{p}^{3/2}}\right)} \equiv \frac{2}{\hat{p}^{7/2}} \hat{F}\left(\frac{\hat{\omega}}{\hat{p}^{3/2}}\right). \quad (5.18)$$

The physical (dimensional) correlation function $C(\omega, \mathbf{p})$ takes the exact same form up to normalisation constants which are fixed in terms of the KPZ parameters ν , D and λ and the fixed point value of the dimensionless coupling $\hat{\lambda}_*$.

In the context of the KPZ equation, it is a very important result. First, this proves the existence of generic scaling, *i.e.* that the KPZ interface always becomes critical (rough) in $d = 1$, and so that its correlations are indeed described by the universal scaling form (5.2). Second, the associated scaling function have been computed exactly in (Prähofer & Spohn (2000)), and can be compared to the FRG result. In particular, the exactly known function, denoted $f(y)$, and its Fourier transform, denoted $\tilde{f}(k)$, are related to the FRG function \hat{F} by the integral relations

$$\tilde{f}(k) = \int_0^\infty \frac{d\tau}{\pi} \cos(\tau k^{3/2}) \hat{F}(\tau), \quad f(y) = \int_0^\infty \frac{dk}{\pi} \cos(ky) \tilde{f}(k). \quad (5.19)$$

The functions $f(y)$ and $\tilde{f}(k)$ computed from the FRG approach are displayed in Fig. 2 together with the exact results. Let us emphasise that there are no fitting parameters. The FRG functions match with extreme accuracy the exact ones. Interestingly, the function $\tilde{f}(k)$ is studied in detail in (Prähofer & Spohn (2004)), which show that this function first monotonously decreases to vanish at $k_0 \simeq 4.4$, then exhibits a negative dip, after which it decays to zero with a stretched exponential tail, over which are superimposed tiny oscillations around zero, only apparent on a logarithmic scale (inset of Fig. 2). The FRG function reproduces all these features. Regarding the tiny magnitude over which they develop, this

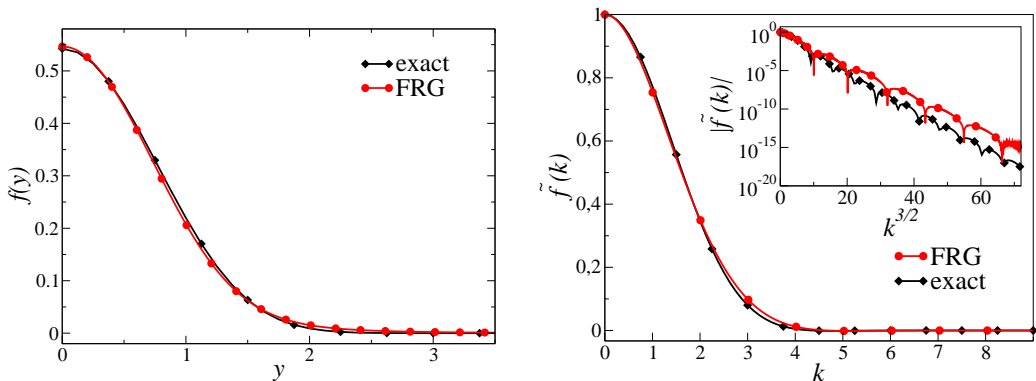


Figure 2: Scaling function $f(y)$ (left panel) and $\tilde{f}(k)$ (right panel) for the 1D Burgers-KPZ equation from FRG compared with the exact result from (Prähofer & Spohn (2000)).

agreement is remarkable. The Burgers equation with other values of $\beta > 0$ has been studied in (Kloss *et al.* (2014a)), which confirms the result (5.3).

5.4. Results in $d > 1$

In dimensions $d > 1$, the Burgers equation has also been studied only for $\beta > 0$, which is equivalent to the KPZ equation with long-range noise. As explained at the beginning of the section, for $\beta = 2$, the KPZ rough phase is controlled by a strong-coupling fixed-point, and perturbative RG fails to all orders to find it. Moreover, none of the mathematical methods used to derive exact results in $d = 1$ can be extended to non-integrable cases, which include $d \neq 1$. In contrast, the FRG can be straightforwardly applied to any dimension, and thereby offers the only controlled analytical approach to study this problem, and it has been used in several works (Kloss *et al.* (2012, 2014a,b); Squizzato & Canet (2019)). We will not review all these results here since they are mainly concern with KPZ. Perhaps the most noteworthy result is that the FRG provided the critical exponents and scaling functions in the physical dimensions $d = 2, 3$, as well as other universal quantities, such as universal amplitude ratios. The estimates for these amplitude ratios in $d = 2, 3$ were later confirmed in large-scale numerical simulations within less than 1% error in (Halpin-Healy (2013b,a)). The whole scaling function in $d = 2$ was computed in numerical simulations of the nonequilibrium Gross-Pitaevskii equation, which surprisingly falls in the KPZ universality class for certain parameters (Deligiannis *et al.* (2022)). The numerical result agrees very precisely with the FRG result, as shown in Fig. 3.

For other values of β , the results (5.3) were extended to $d > 1$, yielding

$$\chi = \max \left(\frac{1}{3}(4 - d - \beta_t(d)), -\frac{1}{3}(4 - d - \beta) + 1 \right), \quad (5.20)$$

where $\beta_t(1) = 3/2$ and monotonically decreases with d . The complete phase diagram of the problem has also been determined in (Kloss *et al.* (2014a)).

The values $\beta > 0$ correspond to a forcing mainly exerted at small scales, where it rather plays the role of a microscopic noise, which can be interpreted as a thermal noise for $\beta = 2$. This then describes a fluid at rest submitted to thermal fluctuations, as studied in (Forster *et al.* (1977)). The values $\beta < 0$ correspond to a large-scale forcing relevant for turbulence. This case has not been studied yet using FRG but it certainly deserves to be addressed in future

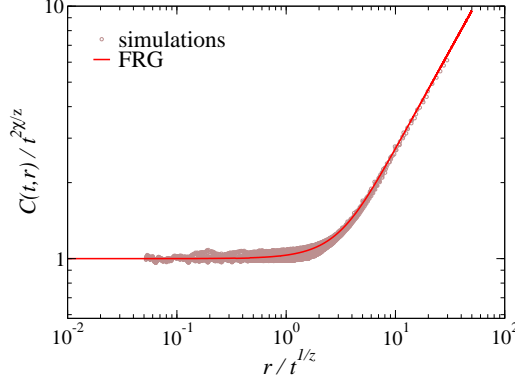


Figure 3: Scaling function for the 2D Burgers-KPZ equation from FRG compared with numerical simulations from (Deligiannis *et al.* (2022)).

works. In particular, it would be interesting to investigate whether the decoupling property breaks down for $\beta < 0$, as occurs for NS, which is presented in the next Section.

6. Fixed-point for Navier-Stokes turbulence

As mentioned in Sec. 2, perturbative RG approaches to turbulence have been hindered by the need to define a small parameter. The introduction of a forcing with power-law correlations $\propto p^{4-d-\varepsilon}$ leads to a fixed-point with an ε -dependent energy spectrum, which is not easily linked to the expected Kolmogorov one. In this respect, the first achievement of FRG was to find the fixed-point corresponding to fully developed turbulence generated by a physical forcing concentrated at the integral scale. As explained in Sec. 4.3, the crux is that one can devise in the FRG framework approximation schemes which are not based on a small parameter, thereby circumventing the difficulties encountered by perturbative RG. This fixed point was first obtained in a pioneering work by Tomassini (Tomassini (1997)), which has been largely overlooked at the time. He developed an approximation close in spirit to the BMW approximation, although it was not yet invented at the time. In the meantime, the FRG framework was successfully developed to study the Burgers-KPZ equation, as stressed in Sec. 5. Inspired by the KPZ example, the stochastic NS equation was revisited using similar FRG approximations in Refs. (Mejía-Monasterio & Muratore-Ginanneschi (2012); Canet *et al.* (2016)). We now present the resulting fixed-point describing fully developed turbulence.

To show the existence of the fixed point and characterise the associated energy spectrum, one can focus on the two-point correlation functions. We follow in this Section the same strategy as for the Burgers problem, that is we resort to an ansatz for the effective average action Γ_k to close the flow equations. It is clear that it is an approximation, and we establish the existence of the fixed-point within this approximation. However, as manifest in Sec. 5, it constitutes a very reliable approximation, built and constrained from the symmetries, which leads to extremely accurate results in the case of the Burgers equation. It is certainly reliable enough to prove the very existence of the fixed-point. Of course, the quantitative estimates associated with this fixed-point could be systematically improved by implementing successive orders of the approximation scheme.

6.1. Ansatz for the effective average action

One can first infer the general structure of Γ_κ for NS equations stemming from the symmetry constraints analysed in Sec. 3.3 and Appendix A. One can show that it endows the following form

$$\Gamma_\kappa[\mathbf{u}, \bar{\mathbf{u}}, p, \bar{p}] = \int_{t,x} \left[\bar{u}_\alpha \left(\partial_t u_\alpha + u_\beta \partial_\beta u_\alpha + \frac{\partial_\alpha \pi}{\rho} \right) + \bar{\pi} \partial_\alpha u_\alpha \right] + \tilde{\Gamma}_\kappa[\mathbf{u}, \bar{\mathbf{u}}], \quad (6.1)$$

where the explicit terms in square brackets are not renormalised, *i.e.* they remain unchanged throughout the RG flow, and are thus identical to the corresponding terms in the NS action. The functional $\tilde{\Gamma}_\kappa$ is renormalised, but it has to be invariant under all the extended symmetries of the NS action since they are preserved by the RG flow.

Let us now comment on the choice of the regulator. It should be quadratic in the fields, satisfy the general constraints (4.3), and preserve the symmetries. A suitable choice is

$$\Delta S_\kappa[\mathbf{u}, \bar{\mathbf{u}}] = - \int_{t,x,x'} \left\{ \bar{u}_\alpha(t, \mathbf{x}) N_{\kappa, \alpha\beta}(|\mathbf{x} - \mathbf{x}'|) \bar{u}_\beta(t, \mathbf{x}') + \bar{u}_\alpha(t, \mathbf{x}) R_{\kappa, \alpha\beta}(|\mathbf{x} - \mathbf{x}'|) u_\beta(t, \mathbf{x}') \right\}. \quad (6.2)$$

The first term is simply the original forcing term, promoted to a regulator by replacing the integral scale L by the RG scale κ^{-1} , since it naturally satisfy all the requirements. The forcing thus builds up with the RG flow, and the physical forcing scale is restored when $\kappa = L^{-1}$. The additional R_κ term can be interpreted as an Eckman friction term in the NS equation. Its presence is fundamental in $d = 2$ to damp the energy transfer towards the large scales. Within the FRG formalism, the energy pile-up at large scales manifests itself as an IR divergence in the flow equation when the R_κ term is absent, which is removed by its presence. This term is thus mandatory to properly regularise the RG flow in $d = 2$. Its effect is to introduce an effective energy dissipation at the boundary of the effective volume κ^{-d} . This form of dissipation is negligible in $d = 3$ compared to the dissipation at the Kolmogorov scale.

Introducing a scale-dependent forcing amplitude D_κ and a scale-dependent viscosity ν_κ , the two regulator terms can be parametrised as

$$N_{\kappa, \alpha\beta}(\mathbf{q}) = \delta_{\alpha\beta} D_\kappa \hat{n}(\mathbf{q}/\kappa), \quad R_{\kappa, \alpha\beta}(\mathbf{q}) = \delta_{\alpha\beta} \nu_\kappa \mathbf{q}^2 \hat{r}(\mathbf{q}/\kappa). \quad (6.3)$$

They are chosen diagonal in components without loss of generality since the propagators are transverse due to incompressibility, and thus the component $\propto q_\alpha q_\beta$ plays no role in the flow equations. The general structure of the propagator matrix \bar{G}_κ , *i.e.* the inverse of the Hessian of $\Gamma_\kappa + \Delta S_\kappa$ is determined in Appendix B. One can show in particular that the propagator in the velocity sector is purely transverse

$$\bar{G}_{\kappa, \alpha\beta}(\omega, \mathbf{q}) = P_{\alpha\beta}^\perp(\mathbf{q}) \bar{G}_{\kappa, \perp}(\omega, \mathbf{q}), \quad P_{\alpha\beta}^\perp(\mathbf{q}) = \delta_{\alpha\beta} - \frac{q_\alpha q_\beta}{q^2}. \quad (6.4)$$

So far we have just given in (6.1) the general structure of Γ_κ stemming from symmetry constraints. Now, one needs to make an approximation in order to solve the flow equations. For this, we devise an ansatz for $\tilde{\Gamma}$, which is very similar to the one considered for the Burgers problem. It is built to automatically preserve the Galilean symmetry. For NS, a lower order approximation than the SO one (5.6) was implemented. It is called LO (leading order) and was first introduced in the context of Burgers-KPZ in (Canet *et al.* (2010)). The LO approximation consists in keeping the most general wavevector, but not frequency, dependence for the two-point functions. The corresponding ansatz reads

$$\tilde{\Gamma}_\kappa[\mathbf{u}, \bar{\mathbf{u}}] = \int_{t,x,x'} \left\{ \bar{u}_\alpha(t, \mathbf{x}) f_{\kappa, \alpha\beta}^\nu(\mathbf{x} - \mathbf{x}') u_\beta(t, \mathbf{x}') - \bar{u}_\alpha(t, \mathbf{x}) f_{\kappa, \alpha\beta}^D(\mathbf{x} - \mathbf{x}') \bar{u}_\beta(t, \mathbf{x}') \right\}. \quad (6.5)$$

Compared to (5.6), the functions f_κ^ν and f_κ^D no longer depend on the covariant operator D_t , which amounts to neglecting the frequency dependence, but also the dependence in the field \mathbf{u} . For this reason, all higher-order vertices apart from the one present in the original NS action vanish. This means that the renormalisation of multi-point interactions is neglected in this ansatz, which is a rather simple approximation. However, it is sufficient for the Burgers-KPZ problem to find the fixed-point in all dimensions. At LO, the flow is projected onto the two renormalisation functions f_κ^ν and f_κ^D which can be interpreted as an effective viscosity and an effective forcing.

The initial condition of the flow at scale $\kappa = \Lambda$ corresponds to

$$f_{\Lambda, \alpha\beta}^D(\mathbf{x} - \mathbf{x}') = 0 \quad , \quad f_{\Lambda, \alpha\beta}^\nu(\mathbf{x} - \mathbf{x}') = -\nu \delta_{\alpha\beta} \nabla_x^2 \delta^{(d)}(\mathbf{x} - \mathbf{x}') \quad (6.6)$$

such that one recovers the original NS action (3.21) [†].

The calculation of the two-point functions from the LO ansatz is straightforward. At vanishing fields and in Fourier space, one obtains

$$\begin{aligned} \tilde{\Gamma}_{\kappa, \alpha\beta}^{(1,1)}(\omega, \mathbf{p}) &= f_{\kappa, \alpha\beta}^\nu(\mathbf{p}) \\ \tilde{\Gamma}_{\kappa, \alpha\beta}^{(0,2)}(\omega, \mathbf{p}) &= -2f_{\kappa, \alpha\beta}^D(\mathbf{p}). \end{aligned} \quad (6.7)$$

Within the LO approximation, the only non-zero vertex function is the one present in the NS action, which reads in Fourier space

$$\tilde{\Gamma}_{\kappa, \alpha\beta\gamma}^{(2,1)}(\omega_1, \mathbf{p}_1, \omega_2, \mathbf{p}_2) = -i(p_2^\alpha \delta_{\beta\gamma} + p_1^\beta \delta_{\alpha\gamma}). \quad (6.8)$$

One can then compute the flow equations for the two-point functions $\tilde{\Gamma}_{\kappa, \alpha\beta}^{(1,1)}$ and $\tilde{\Gamma}_{\kappa, \alpha\beta}^{(0,2)}$ from (5.5). They are purely transverse, and one can deduce from them the flow equations for $f_{\kappa, \perp}^\nu \equiv P_{\alpha\beta}^\perp f_{\kappa, \alpha\beta}^\nu$ and $f_{\kappa, \perp}^D \equiv P_{\alpha\beta}^\perp f_{\kappa, \alpha\beta}^D$, see Appendix B for details and their explicit expressions.

6.2. Stationarity

Since we are interested in the existence of a fixed point, it is convenient to non-dimensionalise all quantities by the RG scale as was done for the Burgers equation in Sec. 5.2. The two coefficients D_κ and ν_κ are associated with anomalous dimensions $\eta_\kappa^D = -\partial_s \ln D_\kappa$ and $\eta_\kappa^\nu = -\partial_s \ln \nu_\kappa$. As one expects a power-law behaviour for the coefficient ν_κ beyond a certain scale, e.g. the Kolmogorov scale η^{-1} , one can relate it to the physical viscosity $\nu \equiv \nu_\Lambda$ as

$$\nu_\kappa = \nu_{\eta^{-1}} (\kappa\eta)^{-\eta^\nu} \simeq \nu_\Lambda (\kappa\eta)^{-\eta^\nu}. \quad (6.9)$$

Because of Galilean invariance, the two anomalous dimensions η_κ^D and η_κ^ν are not independent as in the Burgers case and satisfy the same exact relation (5.12), which can be used to eliminate for instance η_κ^ν as

$$\eta_\kappa^\nu = (4 - d + \eta_\kappa^D)/3. \quad (6.10)$$

The running anomalous dimension η_κ^D should be determined by computing the flow equation for D_κ , which has to be integrated along with the flow equations for $f_{\kappa, \perp}^\nu(\mathbf{p})$ and $f_{\kappa, \perp}^D(\mathbf{p})$. In the case of fully developed turbulence, the value of η_κ^D can be inferred by requiring a stationary state, that is that the mean injection rate balances the mean dissipation rate all along the flow. The average injected power by unit mass at the scale κ can be expressed

[†] Note that the forcing has been incorporated in the regulator part ΔS_κ which is why the initial condition of $f_{\Lambda, \alpha\beta}^D$ is zero.

as (Canet *et al.* (2016))

$$\begin{aligned}
\bar{\epsilon} = \langle \epsilon_{\text{inj}} \rangle &= \langle f_\alpha(t, \mathbf{x}) v_\alpha(t, \mathbf{x}) \rangle = \lim_{\delta t \rightarrow 0^+} \int_{\mathbf{x}'} N_{\kappa, \alpha\beta}(|\mathbf{x} - \mathbf{x}'|) G_{\kappa, \alpha\beta}^{u\bar{u}}(t + \delta t, \mathbf{x}; t, \mathbf{x}') \\
&= D_\kappa \kappa^d \lim_{\delta t \rightarrow 0^+} \left[(d-1) \int_{\hat{\omega}, \hat{\mathbf{q}}} \hat{n}(\hat{\mathbf{q}}) e^{-i\hat{\omega}\delta t} \hat{G}_{\kappa, \perp}^{u\bar{u}}(\hat{\omega}, \hat{\mathbf{q}}) \right] \\
&\equiv D_\kappa \kappa^d \hat{\gamma},
\end{aligned} \tag{6.11}$$

where $\hat{\gamma}$ depends only on the forcing profile since the frequency integral of the response function is one because of causality. It is given by

$$\hat{\gamma} = (d-1) \int \frac{d^d \hat{\mathbf{q}}}{(2\pi)^d} \hat{n}(\hat{\mathbf{q}}) = (d-1) \frac{2\pi^{d/2}}{(2\pi)^d \Gamma(d/2)} \int_0^\infty d\hat{q} \hat{q}^{d-1} \hat{n}(\hat{q}), \tag{6.12}$$

where the last identity holds for an isotropic forcing.

The conditions for stationarity depend on the dimension, and in particular on the main form of energy dissipation, which differs in $d = 3$ and $d = 2$. Let us focus in the following on $d = 3$. One can show that in this dimension, the dissipation at the Kolmogorov scale prevails on the dissipation at the boundary mediated by the regulator R_κ , and that it does not depend on κ (it is given through an integral dominated by its UV bound $\propto \eta^{-1}$). One concludes that to obtain a steady state, the mean injection should balance the mean dissipation and thus it should not depend on κ either. This requires $D_\kappa \sim \kappa^{-d}$, that is $\eta_\kappa^D = d = 3$. The value of η^ν is then fixed by (6.10) to $\eta^\nu = 4/3$.

Thus, one may express the running coefficient ν_κ using (6.9) and the coefficient D_κ in term of the injection rate using (6.11) as

$$D_\kappa = \frac{\bar{\epsilon}}{\hat{\gamma}} \kappa^{-3}, \quad \nu_\kappa = \bar{\epsilon}^{1/3} \kappa^{-4/3}, \tag{6.13}$$

where we used the definition of the Kolmogorov scale as $\nu_\Lambda = \nu = \bar{\epsilon}^{1/3} \eta^{4/3}$.

Finally, the scaling dimension of any correlation or vertex function can be deduced from the scaling dimensions of the fields (as determined in Sec. 5.2). This yields for instance for the two-point correlation function

$$\bar{G}_{\kappa, \perp}^{uu}(\omega, \mathbf{p}) = \frac{\bar{\epsilon}^{1/3}}{\hat{\gamma} \kappa^{13/3}} \hat{G}_{\kappa, \perp}^{uu} \left(\hat{\omega} = \frac{\omega}{\bar{\epsilon}^{1/3} \kappa^{2/3}}, \hat{\mathbf{p}} = \frac{\mathbf{p}}{\kappa} \right). \tag{6.14}$$

6.3. Fixed-point renormalisation functions

Using the analysis of Sec. 6.2, we define the dimensionless functions \hat{h}_κ^ν and \hat{h}_κ^D as

$$f_{\kappa, \perp}^\nu(\mathbf{p}) = \nu_\kappa \kappa^2 \hat{p}^2 \hat{h}_\kappa^\nu(\hat{\mathbf{p}}) \quad \text{and} \quad f_{\kappa, \perp}^D(\mathbf{p}) = D_\kappa \hat{p}^2 \hat{h}_\kappa^D(\hat{\mathbf{p}}). \tag{6.15}$$

The flow equations of \hat{h}_κ^ν and \hat{h}_κ^D are given by

$$\begin{aligned}
\partial_s \hat{h}_\kappa^\nu(\hat{\mathbf{p}}) &= \eta_\kappa^\nu \hat{h}_\kappa^\nu(\hat{\mathbf{p}}) + \hat{\mathbf{p}} \partial_{\hat{\mathbf{p}}} \hat{h}_\kappa^\nu(\hat{\mathbf{p}}) + \frac{\partial_s f_{\kappa, \perp}^\nu(\mathbf{p})}{\nu_\kappa \kappa^2 \hat{p}^2} \\
\partial_s \hat{h}_\kappa^D(\hat{\mathbf{p}}) &= (\eta_\kappa^D + 2) \hat{h}_\kappa^D(\hat{\mathbf{p}}) + \hat{\mathbf{p}} \partial_{\hat{\mathbf{p}}} \hat{h}_\kappa^D(\hat{\mathbf{p}}) + \frac{\partial_s f_{\kappa, \perp}^D(\mathbf{p})}{D_\kappa \hat{p}^2}
\end{aligned} \tag{6.16}$$

with the substitutions for dimensionless quantities in the flow equations (B 8) and (B 9) for $\partial_s f_{\kappa, \perp}^\nu(\mathbf{p})$ and $\partial_s f_{\kappa, \perp}^D(\mathbf{p})$.

These flow equations are first-order differential equation in the RG scale κ , they can be

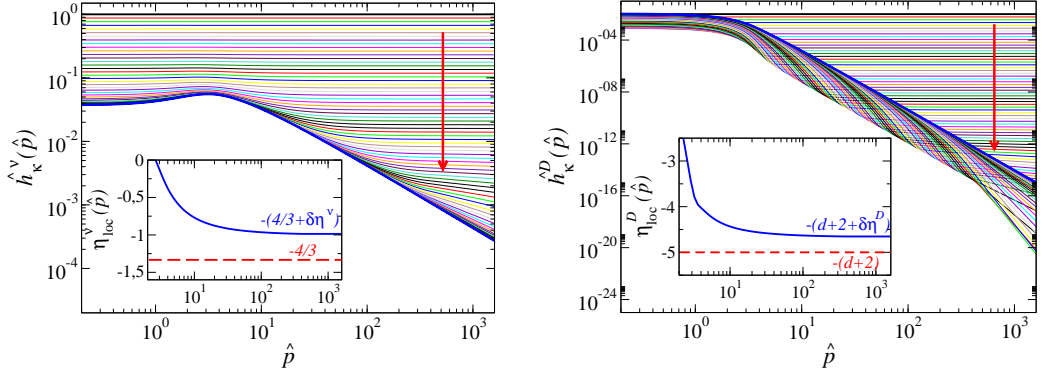


Figure 4: RG evolution of the renormalisation functions \hat{h}_κ^ν and \hat{h}_κ^D with the RG scale, from constant initial conditions (black horizontal lines) to their fixed-point shape (bold blue lines). The red arrows indicate the RG flow, decreasing the RG time from $s = 0$ to $s = -25$. *Insets*: local exponents, defined by (6.18), at the fixed-point, with the corresponding K41 values indicated as dashed lines.

integrated numerically from the initial condition (6.6), which corresponds to $\hat{h}_\kappa^\nu(\hat{p}) = 1$ and $\hat{h}_\kappa^D(\hat{p}) = 0$, down to $\kappa \rightarrow 0$. For this, the wavevectors are discretised on a (modulus, angle) grid. At each RG time step s , the derivatives are computed using 5-point finite differences, the integrals are computed using Gauss-Legendre quadrature, with both interpolation and extrapolation procedures to evaluate combinations $\mathbf{p} + \mathbf{q}$ outside of the mesh points. One observes that the functions \hat{h}_κ^ν and \hat{h}_κ^D smoothly deform from their constant initial condition to reach a fixed point where they stop evolving after a typical RG time $s \lesssim -10$. This is illustrated on Fig. 4, where the fixed-point functions recorded at $s = -25$ are highlighted with a thick line. This result shows that the fully developed turbulent state corresponds to a fixed point of the RG flow, which means that it is scale invariant. However, this fixed-point exhibits a very peculiar feature.

Indeed, the fixed point functions are found to behave as power laws at large wavenumbers as expected. However, the corresponding exponents differ from their K41 values. The fixed point functions can be described at large \hat{p} as

$$\hat{h}_*^\nu(\hat{p}) \sim \hat{p}^{-\eta^\nu + \delta\eta^\nu} \quad \text{and} \quad \hat{h}_*^D(\hat{p}) \sim \hat{p}^{-(\eta^D + 2) + \delta\eta^D} \quad (6.17)$$

where $\delta\eta^\nu$ and $\delta\eta^D$ are the deviations from K41 scaling. The insets of Fig. 4 show the actual local exponents η_{loc}^D and η_{loc}^ν at the fixed-point defined as

$$\eta_{\text{loc}}^D = \frac{d \ln \hat{h}_*^D(\hat{p})}{d \ln \hat{p}} \quad \eta_{\text{loc}}^\nu = \frac{d \ln \hat{h}_*^\nu(\hat{p})}{d \ln \hat{p}}. \quad (6.18)$$

When a function $f(x)$ behaves as a power law $f(x) \sim x^\alpha$ in some range, the local exponent defined by this logarithmic derivative identifies with α on this range. It is clear that η_{loc}^ν differs from its expected K41 value $\eta^\nu = 4/3$, and similarly for η_{loc}^D . The deviations are estimated numerically as $\delta\eta^\nu \simeq \delta\eta^D \simeq 0.33$.

Let us emphasize that it is a very unusual feature, which originates in the breaking of the decoupling property in the NS flow equations. Non-decoupling means that the loop contributions $\frac{\partial_s f_{\kappa,+}^D(\mathbf{p})}{D_\kappa \hat{p}^2}$ and $\frac{\partial_s f_{\kappa,+}^\nu(\mathbf{p})}{\nu_\kappa \kappa^2 \hat{p}^2}$ in the flow equations (6.16) do not become negligible in the limit of large wavenumbers compared to the linear terms. Intuitively, a large wavenumber is equivalent to a large mass, and degrees of freedom with a large mass are damped and do not contribute in the dynamics at large (non-microscopic) scale. This means that the IR

(effective) properties are not affected by the UV (microscopic) details, and this pertains to the mechanism for universality. For turbulence, this is not the case, and the consequences of this breaking, intimately related to sweeping, will be further expounded in Sec. 7. Within the simple LO approximation, the signature of this non-decoupling is that the exponent of the power-laws at large p are not fixed by the scaling dimensions η_κ^ν and η_κ^D , or in other words, the scaling behaviours in κ and in p are different. Indeed, the scaling in κ is fixed by (6.10), but η_κ^D and η_κ^ν do not control the scaling behaviour in p , given by (6.17) which exhibit explicit deviations $\delta\eta^\nu$ and $\delta\eta^D$. This is in sharp contrast with what was observed for the Burgers-KPZ case in Sec. 5, where decoupling was satisfied, and the behaviour in p and ω , e.g. in the scaling form (5.16) is indeed controlled by η_κ . However, it turns out that this peculiar feature plays no role for *equal-time* quantities. As we show in the next section, the LO approximation leads to Kolmogorov scaling for the energy spectrum and the structure functions. Hence the deviations $\delta\eta^\nu$ and $\delta\eta^D$ are a priori not directly observable.

6.4. Kinetic energy spectrum

Let us now compute from this fixed point physical observables, starting with the kinetic energy spectrum. The mean total energy per unit mass is given by

$$\frac{1}{2}\langle \mathbf{v}(t, \mathbf{x})^2 \rangle = \frac{1}{2}G_{\alpha\alpha}^{uu}(0, 0) = \frac{1}{2} \int \frac{d^d \mathbf{p}}{(2\pi)^d} \int \frac{d\omega}{2\pi} \bar{G}_{\alpha\alpha}^{uu}(\omega, \mathbf{p}). \quad (6.19)$$

The kinetic energy spectrum, defined as the energy density at wavenumber p , is hence given for an isotropic flow by

$$\mathcal{E}(p) = \frac{1}{2} \frac{2\pi^{d/2}}{(2\pi)^d \Gamma(d/2)} p^{d-1} (d-1) \int \frac{d\omega}{2\pi} \bar{G}_{\perp}^{uu}(\omega, p). \quad (6.20)$$

The statistical properties of the system are obtained once all fluctuations have been integrated over, *i.e.* in the limit $\kappa \rightarrow 0$. Since the RG flow reaches a fixed-point, the limit $\kappa \rightarrow 0$ simply amounts to evaluating at the fixed-point. Within the LO approximation, and in $d = 3$, one finds

$$\mathcal{E}(p) = \frac{\bar{\epsilon}^{2/3}}{\hat{\gamma} \kappa^{5/3}} \hat{E}(\hat{p}), \quad \text{with} \quad \hat{E}(\hat{p}) = \frac{1}{2\pi^2} \hat{p}^2 \frac{\hat{h}_*^D(\hat{p})}{\hat{h}_*^\nu(\hat{p})}. \quad (6.21)$$

The function $\hat{E}(\hat{p})$ is represented in Fig. 5, with in the inset the compensated spectrum $\hat{p}^{5/3} \hat{E}(\hat{p})$. At small \hat{p} , it behaves as \hat{p}^2 , which reflects equipartition of energy. At large \hat{p} , the two corrections $\delta\eta^\nu$ and $\delta\eta^D$ turn out to compensate in (6.21), such that one accurately recovers the Kolmogorov scaling $\hat{E}(\hat{p}) \simeq a \hat{p}^{-5/3}$, with $a \simeq 0.106$ a numerical factor, which can be read off from the plateau value of the compensated spectrum $\hat{p}^{5/3} \hat{E}(\hat{p})$ shown in the inset of Fig. 5. Thus one obtains for the spectrum

$$\mathcal{E}(p) = \frac{a}{\hat{\gamma}} \bar{\epsilon}^{2/3} p^{-5/3} \equiv C_K \bar{\epsilon}^{2/3} p^{-5/3}. \quad (6.22)$$

For the present choice of forcing profile, which is $\hat{n}(\hat{x}) = \hat{x}^2 e^{-\hat{x}^2}$, one obtains from (6.12) $\hat{\gamma} = \frac{3}{8}\pi^{-3/2}$, and thus $C_K \simeq 1.572$. This value is in precise agreement with typical experimental values, as compiled e.g. by (Sreenivasan (1995)), which yields $C_K \simeq 1.52 \pm 0.30$. Note that perturbative RG approaches yielded the estimate $C_K = 1.617$ (Yakhot & Orszag (1986); Dannevik *et al.* (1987)) although from an uncontrolled limit. Kraichnan had to resort to an improved DIA (Direct Interaction Approximation) scheme, called Lagrangean history DIA, to obtain the correct K41 spectrum and an estimate of this constant $C_K = 1.617$ (Kraichnan (1965)).

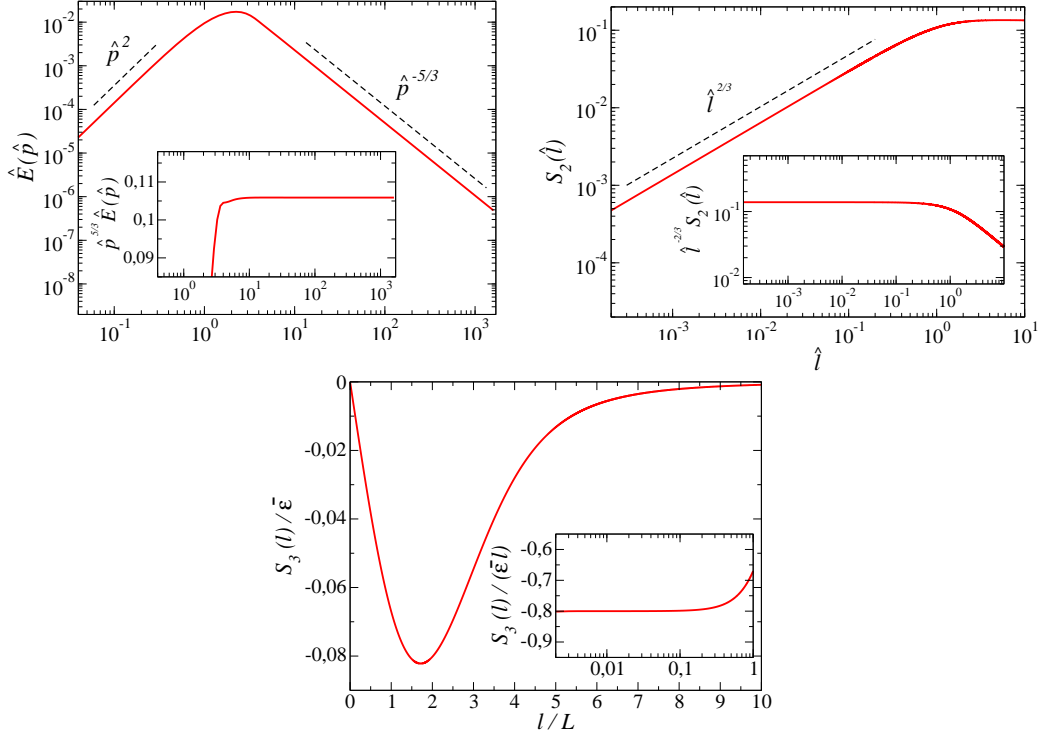


Figure 5: *Top left panel*: Kinetic energy spectrum (*main plot*) and compensated one (*inset*); *Top right panel*: Second order structure function (*main plot*) and compensated one (*inset*); *Bottom panel*: Third order structure function (*main plot*) and compensated one (*inset*). All functions are calculated from the FRG fixed-point obtained within the LO approximation in $d = 3$.

Let us emphasise that C_K explicitly depends on the forcing profile through $\hat{\gamma}$. It is thus a priori non-universal. However, it only depends on the integral of this profile, which is required to vanish at zero, be peaked around the integral scale and fastly decay after. Thus one can expect that this integral is not very sensitive to the precise shape of the forcing satisfying these constraints. Indeed, it was shown in (Tomassini (1997)) within an approximation similar to LO that the numerical value of C_K varies very mildly, in the range 1.2–1.8, upon changing the forcing profile.

6.5. Second and third order structure functions

The n th order structure function is defined as

$$S_n(\ell) = \left\langle \left[(\mathbf{v}(t, \mathbf{z} + \boldsymbol{\ell}) - \mathbf{v}(t, \mathbf{z})) \cdot \hat{\boldsymbol{\ell}} \right]^n \right\rangle. \quad (6.23)$$

The second order structure function can thus be calculated as

$$\begin{aligned} S_2(\ell) &= -2\hat{\ell}_\alpha \hat{\ell}_\beta \left\langle v_\beta(t, \mathbf{z} + \boldsymbol{\ell}) v_\alpha(t, \mathbf{z}) - v_\beta(t, \mathbf{z}) v_\alpha(t, \mathbf{z}) \right\rangle \\ &= -2 \int_{\omega, \mathbf{q}} \bar{G}_\perp^{uu}(\omega, \mathbf{q}) \left[e^{i\mathbf{q} \cdot \boldsymbol{\ell}} - 1 \right] \left[1 - \frac{(\hat{\boldsymbol{\ell}} \cdot \mathbf{q})^2}{q^2} \right]. \end{aligned} \quad (6.24)$$

Within the LO approximation and in $d = 3$, one obtains

$$S_2(\ell) = \frac{\bar{\epsilon}^{2/3}}{\hat{\gamma}} \kappa^{-2/3} \hat{S}_2(\hat{\ell}) \quad \text{with} \quad \hat{S}_2(\hat{\ell}) = -\frac{1}{2\pi^2} \int_0^\infty d\hat{q} \hat{q}^2 \frac{\hat{h}_*^D(\hat{q})}{\hat{h}_*^V(\hat{q})} I_2(\hat{q}\hat{\ell}), \quad (6.25)$$

and I_2 given by the integral

$$I_2(x) = \frac{4}{x^3} \left[\sin x - x \cos x - \frac{x^3}{3} \right]. \quad (6.26)$$

The function $\hat{S}_2(\hat{\ell})$ is plotted in Fig. 5. Again, for small $\hat{\ell}$, the corrections $\delta\eta^V$ and $\delta\eta^D$ precisely compensate such that the second order structure function behaves as the power law $\hat{S}_2(\hat{\ell}) = b\hat{\ell}^{2/3}$ with the Kolmogorov exponent 2/3 and $b \simeq 0.139$ (plateau value of the compensated S_2). Thus one obtains

$$S_2(\ell) = \bar{\epsilon}^{2/3} \frac{b}{\hat{\gamma}} \ell^{2/3} \equiv C_2 \bar{\epsilon}^{2/3} \ell^{2/3}, \quad (6.27)$$

with $C_2 \simeq 2.06$, well-within the error bars of the experimental values $C_2 \simeq 2.0 \pm 0.4$ (Sreenivasan (1995)).

Of course, the two constants C_2 and C_K are not independent. Using the expression $\frac{1}{2\pi^2} \hat{q}^2 \frac{\hat{h}_*^D(\hat{q})}{\hat{h}_*^V(\hat{q})} = \frac{a}{\hat{\gamma}} \hat{q}^{-5/3}$ deduced from (6.21) in (6.25), one obtains

$$C_2 = -\frac{a}{\hat{\gamma}} \int_0^\infty x^{-5/3} I_2(x) dx = \frac{27}{55} \Gamma(1/3) C_K, \quad (6.28)$$

where $a/\hat{\gamma} = C_K$ was used according to (6.22). One thus recovers the well-known relation between these two constants (Monin & Yaglom (2007)).

Finally, let us compute the third-order structure function. In fact, as we now show, this function is completely fixed in the inertial range by the spacetime-dependent shift symmetry of the response fields presented in Sec. 3.4 (or equivalently by the Kármán-Howarth relation) (Tarpin (2018)). Thus one recovers the exact result for S_3 for any approximation of the form (6.1) which automatically preserves the symmetries, and this is the case for the LO approximation.

The third-order structure function can be expressed, using translational invariance and incompressibility as (Tarpin (2018))

$$\begin{aligned} S_3(\ell) &= 6\hat{\ell}_\alpha \hat{\ell}_\beta \hat{\ell}_\gamma \langle v_\alpha(t, 0) v_\beta(t, 0) v_\gamma(t, \ell) \rangle \\ &= 6\hat{\ell}_\alpha \hat{\ell}_\beta \hat{\ell}_\gamma \int_{\omega, \mathbf{q}} \left[q^2 (\delta_{\beta\gamma} q_\alpha + \delta_{\alpha\gamma} q_\beta) - 2q_\alpha q_\beta q_\delta \right] \frac{\bar{K}(\omega, \mathbf{q})}{iq^4} e^{i(\mathbf{q} \cdot \hat{\ell})} \\ &= \frac{6}{(2\pi)^2} \int_0^\infty dq q I_3(q\ell) \int_{-\infty}^\infty \frac{d\omega}{2\pi} \bar{K}(\omega, \mathbf{q}), \end{aligned} \quad (6.29)$$

where I_3 is given by the integral

$$I_3(x) = -\frac{8}{x^4} \left[(x^3 - 3) \sin x + 3x \cos x \right]. \quad (6.30)$$

The function \bar{K} is related to the scalar part of the correlation function $\frac{\delta \mathcal{W}}{\delta L_{\alpha\beta}(t, 0) \delta J_\gamma(t, \ell)}$, which can be expressed in terms of the two-point functions. Indeed, taking one functional derivative of the Ward identity Eq. (3.38) with respect to J_γ , and evaluating at zero sources, one obtains in Fourier space

$$\bar{K}(\omega, \mathbf{q}) = (i\omega - \nu q^2) \bar{G}_\perp^{uu}(\omega, \mathbf{q}) + 2D_L \hat{n}(L\mathbf{q}) \bar{G}_\perp^{u\bar{u}}(-\omega, \mathbf{q}), \quad (6.31)$$

where D_L is the forcing amplitude at the integral scale, related to the mean energy injection as $\bar{\epsilon} = D_L L^{-3} \hat{\gamma}$ according to Eq. (6.11). The first contribution to S_3 , proportional to \bar{G}_{\perp}^{uu} , can be evaluated within the LO approximation. One obtains that it behaves at small ℓ as $(\ell/\eta)^{-1/3}$, which implies that it is negligible in the inertial range. In this range, S_3 is hence dominated by the second contribution, proportional to $\bar{G}_{\perp}^{u\bar{u}}$, which writes

$$S_3(\ell) = -\frac{6}{(2\pi)^2} \frac{\bar{\epsilon}}{\hat{\gamma}} L \int_0^\infty dy y I_3\left(y \frac{\ell}{L}\right) \hat{n}(y). \quad (6.32)$$

The result is represented in Fig. 5, for the choice $\hat{n}(x) = x^2 e^{-x^2}$. One observes that the 4/5th law is recovered for small scales in the inertial range. This result can also be demonstrated analytically from (6.32) since in the inertial range, I_3 is dominated by the small values of its argument, and $I_3(x) \sim \frac{8}{15}x$ for $x \rightarrow 0$. The remaining integral on y can then be identified with $\hat{\gamma}$ defined in Eq. (6.12), which yields

$$S_3(\ell) = -\frac{4}{5} \bar{\epsilon} \ell. \quad (6.33)$$

It is clear from this derivation that $C_3 = -4/5$ is a universal constant, contrarily to C_2 or C_K . It has no dependence left on $\hat{\gamma}$.

To conclude this section, the merits of this approach, based on the LO approximation, are to unambiguously establish the existence of the fixed-point with K41 scaling associated with fully developed turbulence generated by a realistic large-scale forcing. This has been out of reach of standard perturbative RG approaches. The approximation used here, in the form of the LO ansatz (6.5), is rather simple, since it completely neglects the frequency dependence of the two-point functions, as well as any renormalisation of the vertices. While it is sufficient to recover the exact result for S_3 , the K41 energy spectrum with a reliable estimate of the Kolmogorov constant, it does not yield an anomalous exponent for S_2 . Hence, both the frequency and field dependences are bound to be important to capture possible intermittency corrections to K41 exponents. However, more refined approximations including these aspects (such as the SO one implemented for Burgers-KPZ) have not been studied yet, and remain a promising but challenging route to explore in the quest of the computation of intermittency effects from first principles.

In fact, let us emphasise that this program has been recently started in the context of shell models of turbulence, which offer a much simpler setting, yet exhibiting intermittency. For these models, the FRG approach provided for the first time to evidence the associated fixed-point, with intermittency corrections to ζ_2 in very good agreement with values from numerical simulations (Fontaine *et al.* (2022)).

7. Space-time correlations from FRG

This section stresses the second main achievement stemming from FRG methods in turbulence, which is the general expression for the space-time dependence of any correlation function (for any number of points n) of the velocity field in the turbulent stationary state in the limit of large wavenumbers. This expression can be extended to other fields (pressure field, response fields), as well as to correlations of passive scalars transported by a turbulent flow (see Sec. 9). Contrarily to the results presented in Sec. 5 and Sec. 6, this result is not based on an ansatz, it is exact in the limit of infinite wavenumbers.

In the following, we start with a brief overview of what is known on spatio-temporal correlations in turbulence in Sec. 7.1. The principle of the derivation of the FRG results are reviewed in Sec. 7.2, and Sec. 7.3, before providing a simple heuristic explanation of the

large time regime in Sec. 7.4. Thorough comparisons with DNS are reported in Sec. 8 and Sec. 9.

7.1. Overview of space-time correlations in turbulence

One of the earliest insights on the temporal behaviour of correlations was provided by Taylor's celebrated analysis of single particle dispersion in an isotropic turbulent flow (Taylor (1922)). The typical time scale for energy transfers in the turbulent energy cascade can be determined based on Kolmogorov original similarity hypothesis. Assuming a constant energy flux throughout the scales forming the inertial range, one deduces from dimensional analysis that the time for energy transfer from an eddy of size k^{-1} to smaller eddies scales as $\tau \sim (\bar{\epsilon})^{-1/3} k^{-2/3}$, which corresponds to the local eddy turnover time. This scaling is associated with straining, and leads in particular to a frequency spectrum $E(\omega) \sim \omega^{-2}$. However, another mechanism, referred to as sweeping, was identified by Heisenberg (Heisenberg (1948)) and consists in the passive advection of small-scale eddies, without distortion, by the random large-scale eddies, even in the absence of mean flow. This effect introduces a new scale, the root-mean-square velocity U_{rms} , related to the large-scale motion, in the dimensional analysis and yields a typical time scale for sweeping $\tau \sim (U_{\text{rms}} k)^{-1}$. It then follows that the frequency energy spectrum should scale as $E(\omega) \sim \omega^{-5/3}$. The question arises as to which of the two mechanisms dominate the Eulerian correlations, and phenomenological arguments (Tennekes (1975)) suggest that it is the latter, which means that the small-scale eddies are swept faster than they are distorted by the turbulent energy cascade. This conclusion has been largely confirmed by numerical simulations (Orszag & Patterson (1972); Gotoh *et al.* (1993); Kaneda *et al.* (1999); He *et al.* (2004); Favier *et al.* (2010)). In particular, the $\omega^{-5/3}$ frequency spectrum is observed in the Eulerian framework, whereas the ω^{-2} spectrum emerges in the Lagrangian framework, which is devoided of sweeping (Chevillard *et al.* (2005); L  v  que *et al.* (2007)).

Several theoretical attempts were made to calculate the effect of sweeping on the Eulerian spatio-temporal correlations. Kraichnan obtained from a simple model of random advection that the two-point velocity correlations should behave as a Gaussian in the variable kt , where k is the wavenumber and t the time delay (Kraichnan (1964)). In a nutshell, assuming that the velocity field can be decomposed into a large-scale slowly varying component \mathbf{U} and a small-scale fluctuating one \mathbf{u} as $\mathbf{v} \simeq \mathbf{U} + \mathbf{u}$ with $|\mathbf{u}| \ll |\mathbf{U}|$, and assuming that the two components are statistically independent, one arrives at the simplified advection equation $\partial_t \mathbf{u} + \mathbf{U} \cdot \nabla \mathbf{u} = 0$, for scales in the inertial range, *i.e.* neglecting forcing and dissipation. This linear equation can be solved in Fourier space and one obtains $\langle \mathbf{u}(t, \mathbf{k}) \cdot \mathbf{u}(0, -\mathbf{k}) \rangle \propto \exp(-\frac{1}{2} U^2 k^2 t^2)$, which is the anticipated Gaussian, and corroborates the sweeping time scale $\tau \sim (Uk)^{-1}$. However, the previous assumptions cannot be justified for the full NS equation, so it is not clear a priori whether this should be relevant for real turbulent flows.

Correlation functions were later analyzed using Taylor expansion in time in (Kaneda (1993); Kaneda *et al.* (1999)), which yields results compatible with the sweeping time scale k^{-1} for two-point Eulerian correlations, and the straining time scale $k^{-2/3}$ for Lagrangian ones. The random sweeping hypothesis has been used in several approaches, such as the modelling of space-time correlations within the elliptic model (He & Zhang (2006); Zhao & He (2009)) or in models of wavenumber-frequency spectra (Wilczek & Narita (2012)). Beyond phenomenological arguments, more recently, band-pass filtering techniques were applied to the NS equation, and confirmed the dominant contribution of sweeping in the Eulerian correlations (Drivas *et al.* (2017)). Very few works were dedicated to the study of multi-point multi-time correlation functions, and only within the quasi-Lagrangian framework (L'vov *et al.* (1997); Biferale *et al.* (2011)) or within the multifractal approach

(Biferale *et al.* (1999)). We refer to (Wallace (2014)) for a general review on space-time correlations in turbulence.

A closely related problem is the nature of space-time correlations of passive scalar fields transported by a turbulent flow. The scalar field can represent temperature or moisture fluctuations, pollutant or virus concentrations, *etc.* . . . , which are transported by a turbulent flow. The scalar is termed passive when it does not affect the carrier flow. This absence of back-reaction is of course an approximation which only holds at small enough concentration and particle size. Understanding the statistical properties of scalar turbulence plays a crucial role in many domains ranging from natural processes to engineering (see e.g. (Shraiman & Siggia (2000); Falkovich *et al.* (2001); Sreenivasan (2019)) for reviews). The modelling of the scalar spatio-temporal correlations lies at the basis of many approaches in turbulence diffusion problems (Mazzino (1997)). Regarding the relevant time scales, the effect of sweeping for the scalar field was early discussed in (Chen & Kraichnan (1989)), and its importance was later confirmed in several numerical simulations (Yeung & Sawford (2002); O’Gorman & Pullin (2004)) and also experiments of Rayleigh-Bénard convection (He & Tong (2011)).

Of course, one of the major difficulties, which has hindered decisive progress, arises from the non-linear and non-local nature of the hydrodynamical equations. In terms of correlation functions, it implies that the equation for a given n -point correlation function – *i.e.* the correlation of n fields evaluated at n different space-time points – depends on higher-order correlations, and one faces the salient closure problem of turbulence. In order to close this hierarchy, one has to devise some approximation, and many different schemes have been proposed, such as, to mention a few, the Direct Interaction Approximation (DIA) elaborated by Kraichnan (Kraichnan (1964)), approaches based on quasi-normal hypothesis, in particular the eddy damped quasi-normal Markovian (EDQNM) model (Lesieur (2008)), or the local energy transfer (LET) theory (McComb & Yoffe (2017)), we refer to (Zhou (2021)) for a recent review. In this context, field-theoretical and RG approaches offer a systematic framework to study correlation functions, allowing one in principle to devise controlled approximation schemes. Although this program has been largely impeded within the standard perturbative RG framework (see Sec. 2), it turned out to be fruitful within the FRG.

Indeed, the FRG was shown to provide for homogeneous isotropic turbulence the suitable framework to achieve a controlled closure for any n -point Eulerian correlation function, which becomes asymptotically exact in the limit of large wavenumbers. This closure allows one to establish the explicit analytical expression of the spatio-temporal dependence of any generic n -point correlation function in this limit. The main merit of this result is to demonstrate on a rigorous basis, from the NS equations, that the sweeping mechanism indeed dominates Eulerian correlations, and moreover to provide its exact form at large wavenumbers. Thereby, the phenomenological evidence for sweeping is endowed with a very general and systematic expression, extended to any n -point correlation functions. Remarkably, the expression obtained from FRG also carries more information, and predicts in particular a change of behaviour of the Eulerian correlations at large-time delays. In this regime, another time scale emerges, which scales as $\tau \sim D^{-1} k^{-2}$, where $D = U_{\text{rms}}^2 \tau_L$ is a turbulent diffusivity with τ_L the eddy turnover time at the integral scale. The time scale τ can therefore be called a diffusive time scale. The temporal decay of the correlations hence exhibit a crossover from a fast Gaussian decrease at small time delays to a slower exponential one at large time delays. All these results are largely explained and illustrated throughout this section.

7.2. Closure in the large wavenumber limit of the FRG flow equations

The derivation is based on the large wavenumber expansion, which is inspired by the BMW approximation scheme described in Sec. 4.3. Its unique feature for turbulence is that the

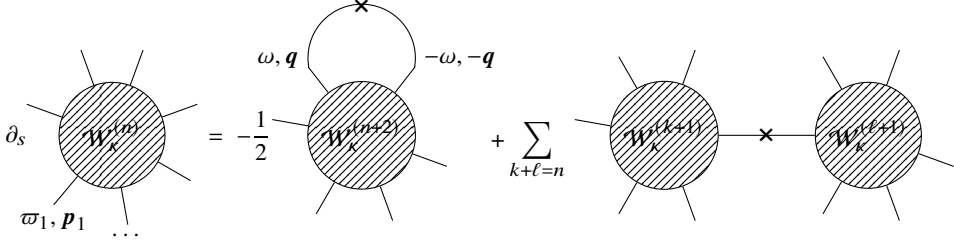


Figure 6: Diagrammatic representation of the flow of an arbitrary n -point generalised correlation function $\mathcal{W}_\kappa^{(n)}$ Eq. (7.1). The crosses represent the derivative of the regulator $\partial_\kappa \mathcal{R}_\kappa$ and the lines the propagator \bar{G}_κ . The correlation $\mathcal{W}_\kappa^{(n)}$ are represented with hatched disks not to be confused with the vertices $\Gamma_\kappa^{(n)}$. The first diagram involves a loop, along which the internal indices are summed over and the internal wavevector q and frequency ω are integrated over.

flow equation for any correlation function can be closed without further approximation than taking the $p_i \rightarrow \infty$ limit, and becomes exact in this limit.

The starting point is the exact flow equation (4.5) for the generating functional \mathcal{W}_κ . A n -point correlation function $\mathcal{W}_\kappa^{(n)}$ is defined according to (3.12) as the n th functional derivative of \mathcal{W}_κ with respect to the corresponding sources $\mathcal{J}_1, \dots, \mathcal{J}_n$. The flow equation for $\mathcal{W}_\kappa^{(n)}$ is thus obtained by taking n functional derivatives of Eq. (4.5), which yields

$$\partial_s \frac{\delta^n \mathcal{W}_\kappa [\mathcal{J}]}{\delta \mathcal{J}_1 \cdots \delta \mathcal{J}_n} = -\frac{1}{2} \partial_s \mathcal{R}_{\kappa, \alpha\beta} \left[\frac{\delta^{n+2} \mathcal{W}_\kappa [\mathcal{J}]}{\delta \mathcal{J}_\alpha \delta \mathcal{J}_\beta \delta \mathcal{J}_1 \cdots \delta \mathcal{J}_n} + \sum_{\substack{(\{a_k\}, \{a_\ell\}) \\ k+\ell=n}} \frac{\delta^{k+1} \mathcal{W}_\kappa [\mathcal{J}]}{\delta \mathcal{J}_\alpha \delta \mathcal{J}_{a_1} \cdots \delta \mathcal{J}_{a_k}} \frac{\delta^{\ell+1} \mathcal{W}_\kappa [\mathcal{J}]}{\delta \mathcal{J}_\beta \delta \mathcal{J}_{a_{k+1}} \cdots \delta \mathcal{J}_{a_{k+\ell}}} \right], \quad (7.1)$$

where $(\{a_k\}, \{a_\ell\})$ indicates all possible bipartitions of the indices $1, \dots, n$. This equation can be represented diagrammatically as in Fig. 6, where the cross stands for $\partial_s \mathcal{R}_\kappa$. It is clear that in the second diagram, the internal line carries a partial sum of external wavevectors $\sum_{i=1}^{k+1} p_i$, which enters the derivative of the regulator. If one considers the large wavenumber limit, defined as the limit where all external wavevectors and all their partial sums are large with respect to the RG scale κ , then this diagram is exponentially suppressed, and can be neglected in this limit.

Let us now consider the first diagram. This diagram involves a loop where the internal wavevector q circulates and is integrated over. Because of the presence of the derivative of the regulator (the cross), q is effectively cut to values $|q| \lesssim \kappa$, and as explained in Sec. 4.3, the limit of large wavenumbers is equivalent in the loop to the limit $q \rightarrow 0$, which we now compute. The wavevector q enters two of the legs of $\mathcal{W}_\kappa^{(n+2)}$. The idea is to apply the $q \rightarrow 0$ expansion on these two legs. Technically, within the FRG framework, approximations are justified and performed on the $\Gamma_\kappa^{(n)}$, not directly on the $\mathcal{W}_\kappa^{(n)}$, because the flow equation of the formers ensures that they remain analytic at any finite scale κ in wavevectors and frequencies (both in the UV and in the IR) thanks to the presence of the regulator. In particular, they can be Taylor expanded. However, any $\mathcal{W}_\kappa^{(n)}$ can be expressed in terms of the $\Gamma_\kappa^{(n)}$, as a sum of tree diagrams whose vertices are the $\Gamma_\kappa^{(k)}$, $k \leq n$, and the edges the propagators. Hence, $\mathcal{W}_\kappa^{(n+2)}$ can be thought of, in its Γ representation, as a functional of the average field Ψ ,

leading to

$$\partial_s \frac{\delta^n \mathcal{W}_\kappa [\mathcal{J}]}{\delta \mathcal{J}_1 \cdots \delta \mathcal{J}_n} = -\frac{1}{2} \partial_s \mathcal{R}_{\kappa, \alpha\beta} \frac{\delta \Psi_\gamma}{\delta \mathcal{J}_\alpha} \frac{\delta \Psi_\delta}{\delta \mathcal{J}_\beta} \frac{\delta^2}{\delta \Psi_\gamma \delta \Psi_\delta} \frac{\delta^n \mathcal{W}_\kappa [\mathcal{J}]}{\delta \mathcal{J}_1 \cdots \delta \mathcal{J}_n}, \quad (7.2)$$

where $\frac{\delta \Psi_\gamma}{\delta \mathcal{J}_\alpha} = \mathcal{W}_{\kappa, \gamma\alpha}^{(2)} \equiv G_{\kappa, \gamma\alpha}$ are simply propagators. The loop wavevector \mathbf{q} then enters either a propagator G_κ or a vertex $\Gamma_\kappa^{(k)}$, which can be evaluated in the limit $\mathbf{q} \rightarrow 0$. At this stage, the symmetries, through the set of associated Ward identities for the $\Gamma_\kappa^{(n)}$, play a crucial role. Indeed, the analysis of Sec. 3.3 has established that any vertex $\Gamma_\kappa^{(n)}$ with one wavevector set to zero can be expressed exactly in a very simple way: if the $\mathbf{q} = 0$ is carried by a velocity field, then it is given in terms of lower-order vertices $\Gamma_\kappa^{(n-1)}$ through the \mathcal{D}_α operator Eq. (3.30), or it vanishes if it is carried by any other fields. This has a stringent consequence, which is that only contributions where Ψ_γ and Ψ_δ are velocity fields survive in Eq. (7.2), yielding

$$\partial_s \mathcal{W}_{\kappa, \alpha_1 \cdots \alpha_n}^{(n)} = -\frac{1}{2} \int_{\omega, \mathbf{q}} \left(\bar{G}_{u_\gamma u_\alpha} \partial_s \mathcal{R}_{\kappa, u_\alpha u_\beta} \bar{G}_{u_\beta u_\delta} \right) (\omega, \mathbf{q}) \frac{\delta}{\delta u_\gamma(-\omega, -\mathbf{q})} \frac{\delta}{\delta u_\delta(\omega, \mathbf{q})} \mathcal{W}_{\kappa, \alpha_1 \cdots \alpha_n}^{(n)}, \quad (7.3)$$

where the α_k 's denote both the field indices and their space components. One can then prove, after some algebra, the following identity

$$\frac{\delta}{\delta u_\gamma(-\omega, -\mathbf{q})} \frac{\delta}{\delta u_\delta(\omega, \mathbf{q})} \mathcal{W}_{\kappa, \alpha_1 \cdots \alpha_n}^{(n)}(\omega_1, \mathbf{p}_1, \cdots) \Big|_{\mathbf{q}=0} = \mathcal{D}_\gamma(-\omega) \mathcal{D}_\delta(\omega) \mathcal{W}_{\kappa, \alpha_1 \cdots \alpha_n}^{(n)}(\omega_1, \mathbf{p}_1, \cdots). \quad (7.4)$$

The proof relies on expressing the $\mathcal{W}_\kappa^{(n)}$ in terms of the $\Gamma_\kappa^{(n)}$ for which the wavenumber expansions are justified and then on using the Ward identities. We refer the interested reader to (Tarpin *et al.* (2018); Tarpin (2018)) for the complete proof. One thus obtains the explicit flow equation

$$\begin{aligned} \partial_s \mathcal{W}_{\kappa, \alpha_1 \cdots \alpha_n}^{(n)}(\cdots, \varpi_i, \mathbf{p}_i, \cdots) &= \frac{1}{2} \int_{\omega, \mathbf{q}} \left(\bar{G}_{u_\gamma u_\alpha} \partial_s \mathcal{R}_{\kappa, u_\alpha u_\beta} \bar{G}_{u_\beta u_\delta} \right) (\omega, \mathbf{q}) \\ &\quad \sum_{k, \ell=1}^n \frac{p_k^\gamma p_\ell^\delta}{\omega^2} \mathcal{W}_{\kappa, \alpha_1 \cdots \alpha_n}^{(n)}(\cdots, \varpi_k + \omega, \mathbf{p}_k, \cdots, \varpi_\ell - \omega, \mathbf{p}_\ell, \cdots) + O(p_{\max}), \end{aligned} \quad (7.5)$$

which constitutes one of the most important results obtained with FRG methods. The flow equation for an arbitrary n -point connected correlation function $\mathcal{W}_\kappa^{(n)}$ (of any fields, velocity, pressure, response fields, ...) is closed in the large wavenumber limit, in the sense that it no longer involves higher-order vertices. Remarkably, it does not depend on the whole hierarchy of $\mathcal{W}_\kappa^{(m)}$ with $m \leq n$, but only on the n -point function for which the flow is expressed and on propagators (*i.e.* two-point functions). Moreover, it is a linear equation in $\mathcal{W}_\kappa^{(n)}$. Once the two-point functions are determined (within some approximation scheme), any n -point correlations can be simply obtained. The term on the r.h.s. is calculated exactly, *i.e.* it is the exact leading term in the large wavenumber expansion. Subleading corrections are at most of order p_{\max} where p_{\max} indicates the largest external wavevector at which the function is evaluated.

This equation can be further simplified, by noting that $\mathcal{W}_\kappa^{(n)}$ in the r.h.s. does not enter the integral over \mathbf{q} , but only the integral over the internal frequency ω . Moreover, $\mathcal{W}_\kappa^{(n)}$ depends

on the latter only through local shifts of the external frequencies. Hence, let us denote by $H_{\kappa,\gamma\delta}$ the term containing the propagators and the regulator

$$H_{\kappa,\gamma\delta}(\omega, \mathbf{q}) = \left(\bar{G}_{u_\gamma u_\alpha} \partial_s \mathcal{R}_{\kappa, u_\alpha u_\beta} \bar{G}_{u_\beta u_\delta} \right) (\omega, \mathbf{q}) . \quad (7.6)$$

One can show that because of incompressibility, the propagators are transverse, hence $H_{\kappa,\gamma\delta}(\omega, \mathbf{q}) = P_{\gamma\delta}^\perp(\mathbf{q}) H_{\kappa,\perp}(\omega, \mathbf{q})$. Finally, by Fourier transforming back in time variables, the shifts in frequency can be transferred to the Fourier exponentials, such that the function $\mathcal{W}_\kappa^{(n)}$ in the mixed time-wavevector coordinates (t_i, \mathbf{p}_i) can be pulled out of the frequency integral also, yielding

$$\begin{aligned} \partial_s \mathcal{W}_{\kappa, \alpha_1 \dots \alpha_n}^{(n)}(\dots, t_i, \mathbf{p}_i, \dots) &= \frac{d-1}{2d} \mathcal{W}_{\kappa, \alpha_1 \dots \alpha_n}^{(n)}(\dots, t_i, \mathbf{p}_i, \dots) \\ &\times \sum_{k, \ell=1}^n \mathbf{p}_k \cdot \mathbf{p}_\ell \int_{\omega, \mathbf{q}} H_{\kappa, \perp}(\omega, \mathbf{q}) \frac{e^{i\omega(t_k - t_\ell)} - e^{i\omega t_k} - e^{-i\omega t_\ell} + 1}{\omega^2} + O(p_{\max}) . \end{aligned} \quad (7.7)$$

Thus, one is left with a linear ordinary differential equation, which can be solved explicitly, as detailed in Sec. 7.3. Again, the detailed proof of this expression can be found in (Tarpin *et al.* (2018); Tarpin (2018)). We discuss in Appendix C the next-to-leading order in the large wavenumber expansion, which has been computed for 2D turbulence in (Tarpin *et al.* (2019)).

7.3. General expression of the time-dependence of n -point correlation functions

Let us now discuss the form of the general solution of the flow equation (7.7) for a generalised correlation function $\mathcal{W}_\kappa^{(n)}$. As emphasised in Sec. 7.2, Eq. (7.7) is very special in many respects: i) it is closed as it depends only on $\mathcal{W}_\kappa^{(n)}$ (besides the propagators) and not on higher-order correlation functions, ii) it is linear in $\mathcal{W}_\kappa^{(n)}$, iii) the leading order in the large p expansion is exact, and iv) it does not decouple, which implies that the large wavenumber limit contains non-trivial information. This information is related to the breaking of standard scale invariance, and reflects the fact that the small-scale properties of turbulence are affected by the large scales.

We have shown in Sec. 6 that the FRG flow for NS equation, in some reasonable approximation, with a physical large-scale forcing, reaches a fixed point. This means that the flow essentially stops when κ crosses the integral scale L^{-1} . However, because of the non-decoupling, the large scale remains imprinted in the solution. It is instructive to uncover the underlying mechanism. At a fixed-point of a RG flow, the system does not depend any longer on the RG scale κ by definition, which leads to scale invariance. The usual way to evidence such a behaviour is to introduce as in Sec. 6 non-dimensionalised quantities, denoted with a hat symbol. Wavevectors are measured in units of κ , e.g. $\hat{\mathbf{p}} = \mathbf{p}/\kappa$, frequencies in units of $\nu_\kappa \kappa^2$, e.g. $\hat{\omega} = \omega/(\nu_\kappa \kappa^2)$. Denoting generically d_n the scaling dimension of a given correlation function $\mathcal{W}_\kappa^{(n)}$, one also defines $\hat{\mathcal{W}}_{\kappa, \alpha_1 \dots \alpha_n}^{(n)}(\dots, \hat{t}_i, \hat{\mathbf{p}}_i, \dots) = \frac{\mathcal{W}_{\kappa, \alpha_1 \dots \alpha_n}^{(n)}}{\kappa^{d_n}}(\dots, \nu_\kappa \kappa^2 t_i, \mathbf{p}_i/\kappa, \dots)$. For a generalised correlation function of m velocity fields and \bar{m} response fields with $m + \bar{m} = n$ in mixed time-wavevector coordinates, one has $d_n = 3(m-1) + (m - \bar{m}/3)$ in $d = 3$. The flow equation for the dimensionless correlation function then writes

$$\left\{ \partial_s - d_n - \hat{\mathbf{p}}_i \cdot \partial_{\hat{\mathbf{p}}_i} + z \hat{t}_i \partial_{\hat{t}_i} \right\} \hat{\mathcal{W}}_{\kappa, \alpha_1 \dots \alpha_n}^{(n)}(\dots, \hat{t}_i, \hat{\mathbf{p}}_i, \dots) = \hat{\mathcal{F}}_{\text{loop}}(\dots, \hat{t}_i, \hat{\mathbf{p}}_i, \dots), \quad (7.8)$$

where $\hat{\mathcal{F}}_{\text{loop}}$ denotes the non-linear part of the flow, corresponding to the contribution of the loop (7.7), expressed in dimensionless quantities.

Scale invariance, as encountered in usual critical phenomena (say at a second order phase transition), emerges if two conditions are fulfilled: existence of a fixed-point, and decoupling. Indeed, as shown in Sec. 5 for the Burgers-KPZ equation, these two conditions yield that the two-point correlation function takes a scaling form (5.2) – which is the hallmark of scale invariance. This derivation can be generalised for any correlation function. Let us assume that the flow reaches a fixed-point, which means $\partial_s \hat{\mathcal{W}}_\kappa^{(n)} = 0$ and that decoupling occurs, which means that the loop contribution of the flow is negligible in the limit of large wavenumber, *i.e.*

$$\frac{\hat{\mathcal{F}}_{\text{loop}}}{\hat{\mathcal{W}}_\kappa^{(n)}} \xrightarrow{\hat{p}_i \rightarrow \infty} 0. \quad (7.9)$$

One can easily show, using some elementary changes of variables, that the general form of the solution to the remaining homogeneous equation is a scaling form

$$\hat{\mathcal{W}}_{*,\alpha_1 \dots \alpha_n}^{(n)}(\dots, \hat{t}_i, \hat{\mathbf{p}}_i, \dots) = \frac{1}{\hat{p}_{\text{tot}}^{d_n}} \hat{w}_{\alpha_1 \dots \alpha_n}^{(n)}\left(\dots, \hat{t}_i \hat{p}_i^z, \frac{\hat{\mathbf{p}}_i}{\hat{p}_i}, \dots\right), \quad (7.10)$$

where $\hat{p}_{\text{tot}} = \sum_{i=1}^{n-1} \hat{p}_i$ and $\hat{w}^{(n)}$ is a universal scaling function which form is not known, and could be determined by explicitly integrating the flow equation.

If there is no decoupling, *i.e.* if the condition (7.9) does not hold, the solution to (7.8) is no longer a scaling form, but is modified by the loop contribution. The explicit expression of this solution can be obtained as an integral expression, which can be simplified in two limits, the limits of small and large time delays, that we study separately in the following.

7.3.1. Small time regime

The limit of small time delays corresponds to the limit where all $\hat{t}_i \rightarrow 0$. In this limit, one can expand the exponential in the second line of (7.7)

$$\int_{\omega, \mathbf{q}} H_{\kappa, \perp}(\omega, \mathbf{q}) \frac{e^{i\omega(t_k - t_\ell)} - e^{i\omega t_k} - e^{-i\omega t_\ell} + 1}{\omega^2} \xrightarrow{t_i \rightarrow 0} I_\kappa t_k t_\ell \quad \text{with} \quad I_\kappa \equiv \int_{\omega, \mathbf{q}} H_{\kappa, \perp}(\omega, \mathbf{q}). \quad (7.11)$$

Note that the explicit expression of H_κ is not needed in the following, one only demands that the frequency integral converges. The flow equation for the dimensionless $\hat{\mathcal{W}}_\kappa^{(n)}$ then simplifies to

$$\left\{ \partial_s - d_n - \hat{\mathbf{p}}_i \cdot \partial_{\hat{\mathbf{p}}_i} + z \hat{t}_i \partial_{\hat{t}_i} \right\} \hat{\mathcal{W}}_{\kappa, \alpha_1 \dots \alpha_n}^{(n)}(\dots, \hat{t}_i, \hat{\mathbf{p}}_i, \dots) = \frac{\hat{I}_\kappa}{3} |\hat{t}_\ell \hat{\mathbf{p}}_\ell|^2 \hat{\mathcal{W}}_{\kappa, \alpha_1 \dots \alpha_n}^{(n)}(\dots, \hat{t}_i, \hat{\mathbf{p}}_i, \dots). \quad (7.12)$$

Since the flow reaches a fixed-point, one can focus on the fixed-point equation as previously ($\partial_s \cdot = 0$). At the fixed-point, $\hat{I}_\kappa \rightarrow \hat{I}_*$ which is just a number. To solve the fixed-point equation, one can introduce a $(n-1) \times (n-1)$ rotation matrix \mathcal{R} in wavevector space such that $\mathcal{R}_{i1} = \frac{\hat{t}_i}{\sqrt{\hat{t}_\ell \hat{t}_\ell}}$ and define new variables $\boldsymbol{\rho}_k$ such that $\mathbf{p}_i = \mathcal{R}_{ij} \boldsymbol{\rho}_j$. This transforms the sum $|\hat{t}_\ell \hat{\mathbf{p}}_\ell|^2$ into $\hat{t}_\ell \hat{t}_\ell |\boldsymbol{\rho}_1|^2$, and allows one to obtain the explicit solution, which reads in physical

units (Tarpin *et al.* (2018))

$$\begin{aligned} \log \left[\bar{\epsilon}^{\frac{\bar{m}-m}{3}} L^{-d_n} \mathcal{W}_{\alpha_1 \dots \alpha_n}^{(m, \bar{m})}(t_1, \mathbf{p}_1, \dots, t_{n-1}, \mathbf{p}_{n-1}) \right] &= -\alpha_0 \bar{\epsilon}^{2/3} L^{2/3} t_\ell t_\ell \rho_1^2 \\ &- d_n \log(\rho_1 L) + w_0^{(m, \bar{m})}{}_{\alpha_1 \dots \alpha_n} \left(\rho_1^{2/3} \bar{\epsilon}^{1/3} t_1, \frac{\rho_1}{\rho_1}, \dots, \rho_1^{2/3} \bar{\epsilon}^{1/3} t_{n-1}, \frac{\rho_{n-1}}{\rho_1} \right) + O(p_{\max} L), \end{aligned} \quad (7.13)$$

where $w_0^{(m, \bar{m})}$ is a universal scaling function, which explicit form is not given by the fixed point equation only, but can be computed numerically by integrating the flow equation in some approximation. The constant $\alpha_0 = \hat{\gamma} \hat{I}_*/2$ is non-universal since it depends on the forcing profile through $\hat{\gamma}$, but it does not depend on the order n of the correlation, nor on the specific fields involved (velocity, response velocity). It is thus the same number for all correlation functions of a given flow.

All the terms in the second line of (7.13) correspond to the K41 scaling form obtained in (7.10). However, these terms are subdominant, that is of the same order as the indicated neglected terms $O(p_{\max} L)$ in the flow equation. Hence, they should be consistently discarded (included in $O(p_{\max} L)$), and were kept here only for the sake of the discussion. As they are of the same order as the neglected terms, it means that they could receive corrections, *i.e.* be modified by these terms. In particular, at equal time, the leading term in the first line of (7.13) vanishes, and one is left with only these subdominant contributions, which are of the form K41 plus possible corrections. In other words, the FRG calculation says nothing at this order about intermittency corrections on the scaling exponents of the structure functions, which are equal-time quantities.

However, at unequal times, the important part of the result is the term in the first line of (7.13), which is the exact leading term at large wavenumber. For this reason, the most meaningful way to write this result is under the form

$$\mathcal{W}_{\alpha_1 \dots \alpha_n}^{(m, \bar{m})}(t_1, \mathbf{p}_1, \dots, t_{n-1}, \mathbf{p}_{n-1}) \propto \exp \left[-\alpha_0 (L/\tau)^2 |t_\ell \mathbf{p}_\ell|^2 + O(p_{\max} L) \right], \quad (7.14)$$

where $\tau = (L^2/\bar{\epsilon}^{1/3})$ is the eddy turnover time at the integral scale, and (L/τ) identifies with U_{rms} , yielding the sweeping time scale $(U_{\text{rms}} p)^{-1}$ expected from phenomenological arguments. The salient feature of this result is that it breaks standard scale invariance, which directly originates in the non-decoupling. As stressed before, if there were decoupling, *i.e.* if the fixed point conformed with a standard critical point, a time variable could only appear through the scaling combination $p^z t$ with $z = 2/3$ in K41 theory. Instead, time enters in (7.14) through the combination pt , which can be interpreted as an effective dynamical exponent $z = 1$. This is a large correction, which can be attributed to the effect of random sweeping. As a consequence, the argument in the exponential explicitly depends on a scale, the integral scale L . This residual dependence in the integral scale of the statistical properties of turbulence in the inertial range is well-known, and crucially distinguishes turbulence from standard critical phenomena.

Let us mention that, interestingly, the non-decoupling also occurs for the passive scalars in the Kraichnan model (see Sec. 9). In this context, the breaking of scale invariance was associated to the existence of zero modes (Falkovich *et al.* (2001)). It would be very interesting to investigate the link between the existence of zero modes and non-decoupling, which could give new insights for the case of NS turbulence.

7.3.2. Large time regime

Let us now consider the large time limit of (7.7), corresponding to $t_i \rightarrow \infty$. One can show that in this limit

$$\int_{\omega, \mathbf{q}} H_{\kappa, \perp}(\omega, \mathbf{q}) \frac{e^{i\omega(t_k - t_\ell)} - e^{i\omega t_k} - e^{-i\omega t_\ell} + 1}{\omega^2} \xrightarrow{t_i \rightarrow \infty} \frac{J_\kappa}{2} (|t_k| + |t_\ell| - |t_\ell - t_k|)$$

with $J_\kappa = \int_{\mathbf{q}} H_{\kappa, \perp}(0, \mathbf{q}),$

(7.15)

and thus the dimensionless flow equation for $\hat{\mathcal{W}}_\kappa^{(n)}$ becomes in this limit

$$\left\{ \partial_s - d_n - \hat{\mathbf{p}}_i \cdot \partial_{\hat{\mathbf{p}}_i} + z \hat{t}_i \partial_{\hat{t}_i} \right\} \hat{\mathcal{W}}_{\kappa, \alpha_1 \dots \alpha_n}^{(n)}(\dots, \hat{t}_i, \hat{\mathbf{p}}_i, \dots) =$$

$$\frac{\hat{J}_\kappa}{6} \sum_{k, \ell} \hat{\mathbf{p}}_k \cdot \hat{\mathbf{p}}_\ell \left(|\hat{t}_k| + |\hat{t}_\ell| - |\hat{t}_\ell - \hat{t}_k| \right) \hat{\mathcal{W}}_{\kappa, \alpha_1 \dots \alpha_n}^{(n)}(\dots, \hat{t}_i, \hat{\mathbf{p}}_i, \dots).$$
(7.16)

This equation can be solved at the fixed-point in an analogous way as for the small time limit, introducing another rotation matrix such that in the new wavevector variables $\varrho_1 = \sum_k \mathbf{p}_k$. Specifying to equal time lags $t_i = t$ for simplicity, the solution reads (Tarpin *et al.* (2018))

$$\log \left(\bar{\epsilon}^{\frac{\bar{m}-m}{3}} L^{-d_n} \mathcal{W}_{\alpha_1 \dots \alpha_n}^{(m, \bar{m})}(t, \mathbf{p}_1, \dots, \mathbf{p}_{n-1}) \right) = -\alpha_\infty \bar{\epsilon}^{1/3} L^{4/3} |t| \varrho_1^2$$

$$- d_n \log(\varrho_1 L) + w_\infty^{(m, \bar{m})}_{\alpha_1 \dots \alpha_n} \left(\varrho_1^{2/3} \bar{\epsilon}^{1/3} t, \frac{\varrho_1}{\varrho_1}, \dots, \frac{\varrho_{n-1}}{\varrho_1} \right) + O(p_{\max} L). \quad (7.17)$$

The non-universal constant $\alpha_\infty = \hat{\gamma} \hat{J}_*/4$ is again the same for any generalised correlation function, irrespective of its order or fields content. Moreover, the same comments apply for the subleading terms in the second line of (7.17): they merely represent K41 scaling, with possible corrections induced by the neglected terms. The main feature of this solution is thus captured by the expression

$$\mathcal{W}_{\alpha_1 \dots \alpha_n}^{(m, \bar{m})}(t_1, \mathbf{p}_1, \dots, t_{n-1}, \mathbf{p}_{n-1}) \propto \exp \left(-\alpha_\infty (L^2/\tau) \left| \sum_{\ell} \mathbf{p}_\ell \right|^2 |t| + O(p_{\max} L) \right). \quad (7.18)$$

At large time delays, the temporal decay of correlation functions is also sensitive to the large scale and thus explicitly breaks scale invariance as in the small time regime. However, the decay drastically slows down, since it crosses over for all wavenumbers from a Gaussian at small time delays to an exponential at large ones. Note that the dependence in the wavenumbers is quadratic in both regime. This large time regime had not been predicted before. However, it was already in germ in early studies of sweeping, as was noted in (Gorbunova *et al.* (2021a)). This allows one to provide a simple physical interpretation of these two regimes, see Sec. 7.4. Let us first summarise for later comparisons the explicit forms of the two-point correlation function of the velocity fields:

$$C_{\alpha\beta}^{(2)}(t, \mathbf{k}) \equiv \text{FT} \left[\left\langle v_\alpha(t_0, \mathbf{r}_0) v_\beta(t_0 + t, \mathbf{r}_0 + \mathbf{r}) \right\rangle \right]$$

$$= C_{\alpha\beta}^{(2)}(0, \mathbf{k}) \begin{cases} \exp \left(-\alpha_0 (L/\tau)^2 t^2 k^2 \right) & t \ll \tau \\ \exp \left(-\alpha_\infty (L^2/\tau) |t| k^2 \right) & t \gg \tau \end{cases} \quad (7.19)$$

and of the three-point correlation function at small time delays $t_1, t_2 \ll \tau$

$$\begin{aligned} C_{\alpha\beta\gamma}^{(3)}(t_1, \mathbf{k}_1, t_2, \mathbf{k}_2) &\equiv \text{FT} \left[\left\langle v_\alpha(t_0 + t_1, \mathbf{r}_0 + \mathbf{r}_1) v_\beta(t_0 + t_2, \mathbf{r}_0 + \mathbf{r}_2) v_\gamma(t_0, \mathbf{r}_0) \right\rangle \right] \\ &= C_{\alpha\beta\gamma}^{(3)}(0, \mathbf{k}_1, 0, \mathbf{k}_2) \exp \left(-\alpha_0 (L/\tau)^2 |\mathbf{k}_1 t_1 + \mathbf{k}_2 t_2|^2 \right). \end{aligned} \quad (7.20)$$

7.4. Intuitive physical interpretation

Let us now provide an heuristic derivation of these results, proposed in (Gorbunova *et al.* (2021a)). The early analysis of Eulerian sweeping effects by Kraichnan (Kraichnan (1964)) was based on the Lagrangian expression for the Eulerian velocity field as

$$u_i(t, \mathbf{r}) = \exp_{\rightarrow} [\boldsymbol{\xi}(t|\mathbf{r}, t_0) \cdot \nabla] u_i(t_0, \mathbf{r}) + \int_{t_0}^t ds \exp_{\rightarrow} [\boldsymbol{\xi}(t|\mathbf{r}, s) \cdot \nabla] [\nu \nabla^2 u_i(s, \mathbf{r}) - \nabla_i p(s, \mathbf{r})]. \quad (7.21)$$

In this equation, $\boldsymbol{\xi}(t|\mathbf{r}, t_0) = \mathbf{X}(t|\mathbf{r}, t_0) - \mathbf{r}$ is the Lagrangian displacement vector, where $\mathbf{X}(t|\mathbf{r}, t_0)$ denotes the position at time t of the Lagrangian fluid particle located at position \mathbf{r} at time t_0 , which satisfies

$$\frac{d}{ds} \mathbf{X}(t|\mathbf{r}, s) = \mathbf{u}(s, \mathbf{X}(t|\mathbf{r}, s)), \quad \mathbf{X}(t|\mathbf{r}, t) = \mathbf{r}. \quad (7.22)$$

One can write using (7.21) the expression of the two-point correlation function. This expression can be simplified under some general assumptions, namely slow variations in space and time of the displacement field, and its statistical independence from the initial velocities at sufficiently long time t . Moreover, since the displacements are dominated by the large scales of the flow, whose statistics are nearly Gaussian (Corrsin (1959, 1962)), one may plausibly further assume a normal distribution for $\boldsymbol{\xi}$, resulting in the following expression

$$C^{(2)}(t, \mathbf{k}) = \exp \left[-\frac{1}{2} \langle |\boldsymbol{\xi}(t|\mathbf{r}, 0)|^2 \rangle k^2 \right] C^{(2)}(0, \mathbf{k}) \left\{ 1 + O(\nu k^2 |t|, k U_{\text{rms}}(k) |t|) \right\}. \quad (7.23)$$

According to these arguments, the two-point velocity correlation undergoes a rapid decay in the time-difference t which arises from an average over rapid oscillations in the phases of Fourier modes due to sweeping, or “convective dephasing” (Kraichnan (1964)).

The connection with the FRG results (7.19) stems from exploiting the results of the classical study by Taylor (Taylor (1922)) on one-particle turbulent dispersion. In this study, the Lagrangian displacement field was shown to exhibit two regimes

$$\langle |\boldsymbol{\xi}(t|\mathbf{r}, 0)|^2 \rangle \sim \begin{cases} U_{\text{rms}}^2 t^2 & |t| \ll \tau \\ 2D|t| & |t| \gg \tau \end{cases} \quad (7.24)$$

where the early-time regime corresponds to ballistic motion with the rms velocity U_{rms} and the long-time regime corresponds to diffusion with a turbulent diffusivity $D \propto U_{\text{rms}}^2 \tau$. Inserting these results in (7.23) then yields the FRG expressions (7.19). This argument can be generalised in principle to multi-point correlation functions, which, under the same kind of assumptions, would also lead to similar expressions as the ones derived from FRG. Of course, the FRG derivation is far more systematic and rigorous than these heuristic arguments, but the latters provide an intuitive physical interpretation of these results.

The FRG results have been tested in extensive DNS, focused on the temporal dependence of two- and three-point correlation functions. We report in Sec. 8 and Sec. 9 the main results.

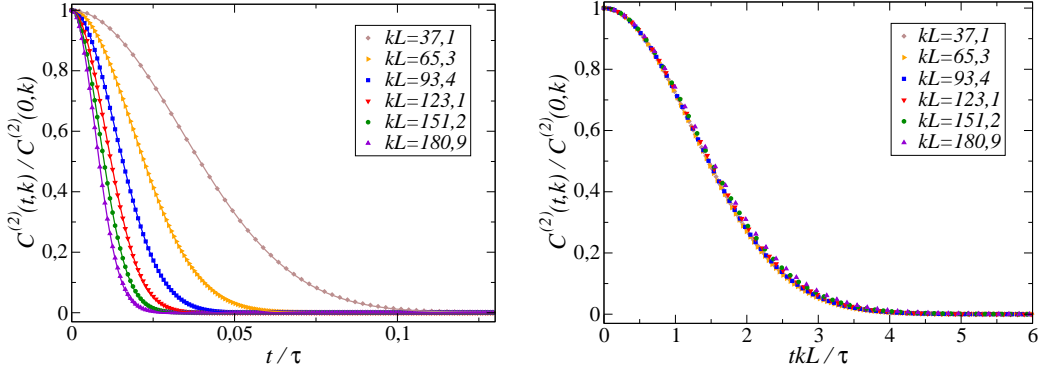


Figure 7: *Left panel*: Time dependence of the normalised two-point correlation function $C^{(2)}(t, k)$ at different wavenumbers k for a simulation at $R_\lambda = 90$. Data from the simulation are represented with symbols, and their Gaussian fits with plain lines. *Right panel*: Same data plotted as a function of kt , which leads to their collapse as expected from the FRG result (7.19).

8. Comparison with Direct Numerical Simulations

Extensive DNS were performed on high-performance computational clusters to quantitatively test the FRG results. The DNS consist of direct numerical integration of the NS equation with a stochastic forcing using standard pseudo-spectral methods and Runge-Kutta scheme for time advancement, with typical spatial resolution conforming the standard criterion $k_{max}\eta \approx 1.5$, and Taylor based Reynolds numbers R_λ from 40 to 250 for corresponding grid sizes from 64^3 to 1024^3 . Details can be found, e.g. in (Gorbunova (2021)). The analysis focused on the two-point and three-point correlation function of the velocity field, which were computed in the stationary state, using averages over spherical shells in wavenumber and over successive time windows, typically

$$C^{(2)}(t, \mathbf{k}) = \frac{1}{N_t} \sum_{j=1}^{N_t} \frac{1}{M_n} \sum_{\mathbf{k} \in S_n} \Re[u_i(t_{0j}, \mathbf{k}) u_i^*(t_{0j} + t, \mathbf{k})], \quad (8.1)$$

where N_t is the number of time windows in the simulation, M_n is the number of modes in the spectral spherical shell S_n , and $k = n\Delta k$, $n \in \mathbb{Z}$.

8.1. Small time regime and sweeping

We first present the result for the two-point correlation function at small time delays, whose theoretical expression is given by Eq. (7.19). The time dependence of $C^{(2)}(t, k)$ is displayed in the left panel of Fig. 7 for a sample of different wavenumbers k . The larger ones exhibit a faster decorrelation as expected. For each k , the normalised curve $C^{(2)}(t, k)/C^{(2)}(0, k)$ is fitted with a two-parameter Gaussian function $f_{\text{Gaus}}(t) = c \exp(-(t/\tau_0)^2)$, which provides a very accurate model for all curves, as illustrated in the figure. Moreover, all curves collapse into a single Gaussian function when plotted as a function of kt , as expected from the theory (7.19). The fine quality of the collapse is shown in the right panel of Fig. 7.

The fitting parameter τ_0 is plotted as a function of kL in the left panel of Fig. 8, which clearly confirms that it is proportional to k^{-1} at large enough k , and not to the K41 time scale $k^{-2/3}$, in plain agreement with the FRG result. Similar results were also obtained in (Sanada & Shanmugasundaram (1992); Favier *et al.* (2010)), where the characteristic decorrelation time is estimated by integrating the correlation function, as well as in the

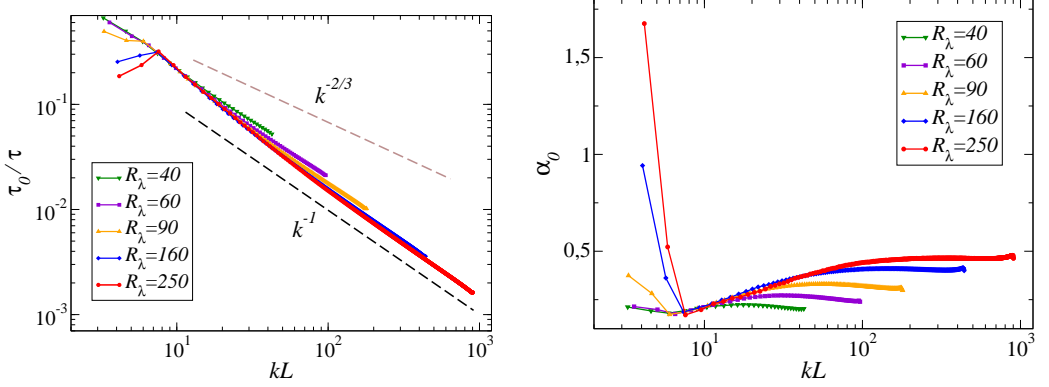


Figure 8: *Left panel*: Decorrelation time τ_0 extracted from the Gaussian fit as a function of the wavenumber for various R_λ . *Right panel*: Non-universal constant α_0 obtained as $\alpha_0 = \tau^2/(\tau_0 k L)^2$. It reaches a plateau at large wavenumber, which extends with increasing R_λ .

work of (Kaneda *et al.* (1999)), where the characteristic time is measured through the second derivative of the correlation function.

The non-universal constant α_0 can be deduced from τ_0 as $\alpha_0 = \tau^2/(\tau_0 k L)^2$. As can be observed in the right panel of Fig. 8, this quantity reaches a plateau, which value corresponds to the theoretical α_0 at large k . The physical origin of the departure from the plateau at intermediate and small wavenumbers can be clearly identified in the simulations as a “contamination” from the forcing (Gorbunova *et al.* (2021a)). Indeed, by analyzing the modal energy transfers, one observes that the plateau is reached when the energy transfer to a mode k is local, *i.e.* mediated by neighbouring modes only through the cascade process. The modes at intermediate and small k also receive energy via direct non-local transfers from the forcing range in the simulations. This means that the large wavenumber limit underlying the FRG derivation corresponds to the modes k in the inertial range with negligible direct energy transfer from the forcing range. Of course, the “large wavenumber” domain extends with the Reynolds number, as visible in Fig. 8. One can also observe that the value of the plateau in the simulations depends on the R_λ . Although only few points are available, they suggest a saturation at high R_λ beyond the values accessible in the DNS. Moreover, although the forcing location and its width are fixed for the different R_λ , its amplitude varies. The theoretical expression for $\alpha_0 = \hat{\gamma} \hat{I}_*/2$ does depend in the precise forcing profile, which could also explain the R_λ dependence. This point was not quantitatively investigated.

8.2. Three-point correlation function

Let us now present the results for the three-point correlation function. The general expression of this correlation (7.20) involves a product of velocities which is not local in \mathbf{k} . This is unpracticable in DNS heavily relying on parallel computation and memory distribution. To overcome this difficulty, one can focus on a particular configuration, which corresponds to an advection-velocity correlation. This correlation is defined as

$$T(t, \mathbf{k}) \equiv \left\langle N_\ell(t_0 + t, \mathbf{k}) u_\ell^*(t_0, \mathbf{k}) \right\rangle \quad (8.2)$$

$$N_\ell(t, \mathbf{k}) = -ik_n P_{\ell m}^\perp(\mathbf{k}) \sum_{\mathbf{k}'} \left\langle u_m(t, \mathbf{k}') u_n(t, \mathbf{k} - \mathbf{k}') \right\rangle,$$

where N is simply the Fourier transform of the advection and pressure term appearing in the NS equation expressed in spectral space

$$\partial_t u_\ell(t, \mathbf{k}) = N_\ell(t, \mathbf{k}) - \nu k^2 u_\ell(t, \mathbf{k}) + f_\ell(t, \mathbf{k}). \quad (8.3)$$

At equal times, $T(0, \mathbf{k})$ is thus the usual energy transfer, and (8.2) represents its time-dependent generalisation. Let us note that $T(t, \mathbf{k})$ is still a statistical moment of order three, although evaluated in a specific configuration involving only two space-time points. It is proportional to a linear combination of three-point correlation function $C^{(3)}$ as

$$T(t, \mathbf{k}) \sim \sum_{\mathbf{k}'} C_{mnl}^{(3)}(t, \mathbf{k}', t, \mathbf{k} - \mathbf{k}') \stackrel{\text{all } |\mathbf{k}| \gg L^{-1}}{\sim} \exp\left(-\alpha_0 (L/\tau)^2 k^2 t^2\right) \quad (8.4)$$

and according to the FRG result, it should behave in the limit where all wavenumbers $|\mathbf{k}|$, $|\mathbf{k}'|$ and $|\mathbf{k} - \mathbf{k}'|$ are large compared to L^{-1} , as the indicated Gaussian in kt .

However, the sum in (8.4) involves all possible wavenumber \mathbf{k}' , and not only large ones. Hence, in order to compare it with the FRG prediction, one needs to perform a scale decomposition, as defined e.g. in Refs. (Frisch (1995); Verma (2019)). Each velocity field $\mathbf{u}(\mathbf{k})$ can be decomposed into a small-scale component $\mathbf{u}^S(\mathbf{k})$ for $|\mathbf{k}| > K_c$ and a large-scale one $\mathbf{u}^L(\mathbf{k})$ for $|\mathbf{k}| \leq K_c$ as $\mathbf{u}(\mathbf{k}) = \mathbf{u}^S(\mathbf{k}) + \mathbf{u}^L(\mathbf{k})$, where K_c is a cutoff wavenumber. This cutoff is chosen such that the direct energy transfers from the forcing range to the modes $|\mathbf{k}| > K_c$ are negligible, which coincides with the regime of validity of the large wavenumber limit of the FRG identified on the basis of the two-point correlation function. This scale decomposition thus leads to terms of the form $T^{XYZ}(t, \mathbf{k}) = -[u_i^X]^*(\mathbf{k}, t_0) \text{FT}[u_j^Y \partial_j u_i^Z](\mathbf{k}, t_0 + t)$ where X, Y, Z stand for S or L . Using the terminology of (Verma (2019)) for instantaneous energy transfers (*i.e.* for $t = 0$), the first superscript of T^{XYZ} is related to the mode receiving energy in a triadic interaction process, the intermediate superscript denotes the mediator mode and the last superscript is related to the giver mode that sends the energy to the receiver mode. The mediator mode does not loose nor receive energy in the interaction, it corresponds to the advecting velocity field, which comes as prefactor of the operator ∇ in the non-linear term of the Navier-Stokes equation.

We are interested in the large wavenumbers \mathbf{k} , which corresponds to short scales in the previous terminology. Thus, fixing $X = S$, the possible contributions for T are given by the following expression:

$$T(t, \mathbf{k}) = [T^{SSS} + T^{SLs} + T^{SSL} + T^{sLL}](t, \mathbf{k}). \quad (8.5)$$

We focus on the term T^{SSS} , which gathers all triadic interactions where the three modes belong to the small scales (all wavenumbers are large). This term constitutes with T^{SLs} the turbulent energy cascade.

We show in Fig. 9 the results for $T^{SSS}(t, \mathbf{k})$ computed from DNS. All the curves for $T(t, \mathbf{k})$ and $T^{SSS}(t, \mathbf{k})$ for the different wavenumbers k are fitted with the function $g_{\text{Gaus}}(t) = c(1 - t/\tau_l) \exp(-(t/\tau_0)^2)$, where c , τ_l and τ_0 are the fit parameters. This function provides a very accurate modellisation of the data both for T and T^{SSS} for all k . However, only the curves T^{SSS} are well approximated by pure Gaussians ($\tau_l \ll \tau_0$), whereas without scale decomposition the curves for T are in general not symmetric and can take negative values (see (Gorbunova *et al.* (2021a)) for details).

The Gaussian form of T^{SSS} is in agreement with the FRG result (8.4). As shown in Fig. 9, all the curves for different wavenumbers collapse onto a single Gaussian when plotted as a function of the variable kt , as expected from Eq. (8.4). Moreover, let us emphasise that the non-universal parameter α_0 in this equation is predicted to be the same as the one for the two-point correlation function in Eq. (7.19). The decorrelation time τ_0 extracted from the fit

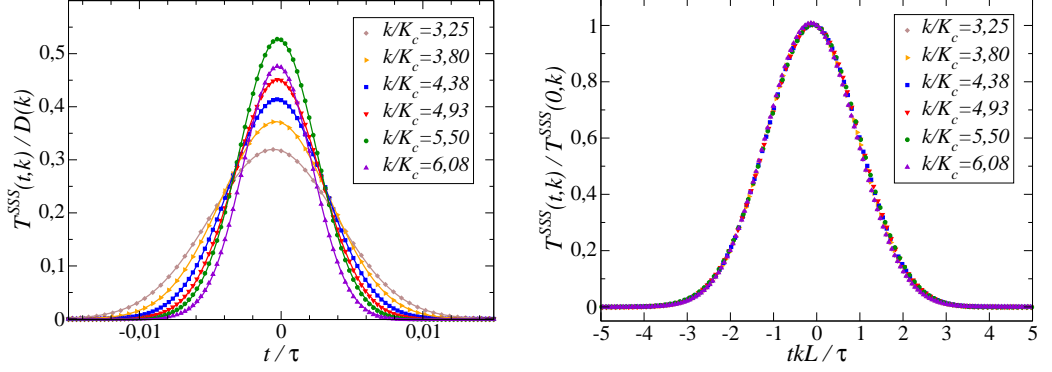


Figure 9: *Left panel:* Advection-velocity spatio-temporal correlation function $T^{SSS}(t, k)$ from DNS at $R_\lambda = 90$, normalised by the dissipation spectrum $\hat{D}(k) = \nu k^2 C^{(2)}(0, k)$. Data from the simulation are represented with symbols, and their Gaussian fits with plain lines. *Right panel:* same curves $T^{SSS}(t, k)$ normalised by $T^{SSS}(0, k)$ and plotted as a function of ktL/τ , which induces their collapse.

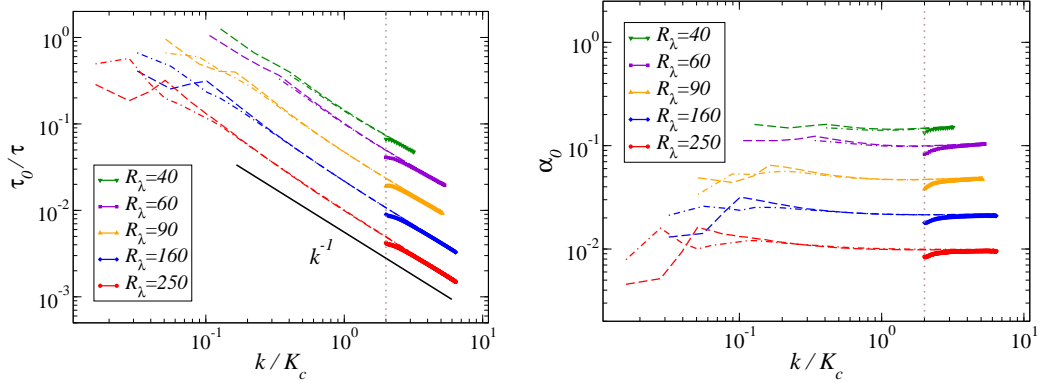


Figure 10: *Left panel:* Decorrelation time τ_0 extracted from the Gaussian fits of the purely small-scale advection-velocity correlation T^{SSS} (plain lines), the two-point correlation function $C^{(2)}$ (dashed lines) and the full advection-velocity correlation T (dashed-dotted lines). *Right panel:* non-universal parameter α_0 obtained as $\alpha_0 = \tau^2/(\tau_0 k L)^2$. The data for the different R_λ in both panels have been shifted vertically for clarity.

with g_{Gaus} is displayed in Fig. 10, together with the value obtained from $C^{(2)}$ and also the one from the full correlation T . They show as expected a k^{-1} dependence. The coefficient α_0 can be obtained as $\alpha_0 = \tau^2/(\tau_0 k L)^2$, and is shown in Fig. 10. At sufficiently large wavenumbers, corresponding to the regime of validity of FRG, the three values coincide with very good precision. At smaller wavenumbers, they are also in good agreement for $C^{(2)}$ and for T , although in this regime τ_l (parameter of the linear part of the fitting function g_{Gaus}) can be large. The detailed analysis of these results can be found in (Gorbunova *et al.* (2021a)).

To summarise this part, the results for the spatio-temporal dependence of the two-point and the specific configuration of the three-point correlation function studied in DNS hence confirm with accuracy the FRG prediction in the small-time regime, including the equality of the non-universal prefactors in the exponentials. This regime corresponds to a fast decorrelation on a time scale $\tau \sim k^{-1}$ related to sweeping. Because of this fast initial decay, the observation in the DNS of the crossover to another slower regime at large-time is very challenging for NS turbulence, as we now briefly discuss.

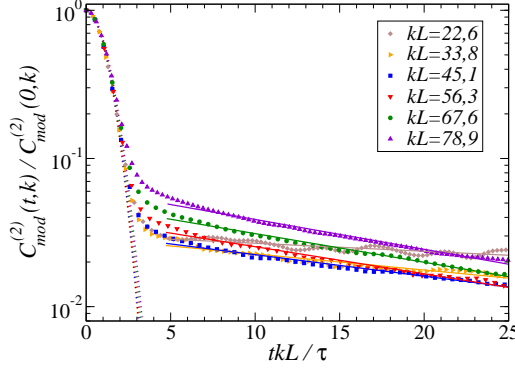


Figure 11: Time dependence of the normalised two-point correlation function of the velocity modulus $C_{mod}^{(2)}(t, k)$ at $R_\lambda = 60$ for different wavenumbers k . The numerical data is represented with dots, the dashed lines correspond to Gaussian fits and the plain lines to exponential fits.

8.3. Large time regime

The initial Gaussian decay of the two-point correlation function leads to a fast decrease of the amplitude of the signal within a short time interval. In all the simulations of NS equation, the correlation function falls to a level comparable with the numerical noise while it is still in the Gaussian regime, which prevents from detecting the crossover to an exponential and resolving the large time regime.

Interestingly, although this crossover could not be accessed for the real part of the correlation function, it was observed for a different quantity, namely the correlation function of the modulus of the velocity, defined as

$$C_{mod}^{(2)}(t, k) = \langle \|\hat{\mathbf{u}}(t_0, \mathbf{k})\| \|\hat{\mathbf{u}}(t_0 + t, \mathbf{k})\| \rangle - \langle \|\hat{\mathbf{u}}(t_0, \mathbf{k})\| \rangle \langle \|\hat{\mathbf{u}}(t_0 + t, \mathbf{k})\| \rangle. \quad (8.6)$$

The result obtained in DNS for this quantity is displayed in Fig. 11, which clearly shows the existence of a Gaussian regime at short time followed by an exponential regime at large time, analogous to the one expected for the real part of the two-point correlation function. Remarkably, very comparable results were obtained in air jet experiments where a similar correlation is measured (Poulain, C. *et al.* (2006)). Of course, $C_{mod}^{(2)}$ is a quite different object from $C^{(2)}$, and there is no theoretical understanding so far of its behaviour, neither from FRG nor from a heuristic argument. Indeed, in the latter argument, the decorrelation stems for a rapid random dephasing of the Fourier modes, while the phases obviously cannot play a role for the decorrelation of the modulus. We mention it here as an interesting puzzle, which deserves further work to be explained.

Although the large time regime appears difficult to access in DNS of NS equation, it can be unraveled in the case of scalar turbulence, which we present in Sec. 9. Prior to this, let us briefly mention another result which concerns the kinetic energy spectrum in the near-dissipation range.

8.4. Kinetic energy spectrum in the near-dissipation range

The expression for the two-point correlation function of the velocity obtained from FRG can also be used to study the kinetic energy spectrum beyond the inertial range, that is beyond the Kolmogorov scale $\eta = \nu^{3/4} \epsilon^{-1/3}$. Based on Kolmogorov hypotheses and dimensional

analysis, the kinetic energy spectrum is expected to endow the universal form

$$E(k) = \bar{\epsilon}^{2/3} k^{-5/3} F(\eta k) \quad (8.7)$$

where $F(x) \rightarrow C_K$ for $x \lesssim 1$ since viscous effects are negligible in the inertial range, and $F(x)$ fastly decays for $x \gtrsim 1$ in the dissipation range. Although F is expected to be universal, its analytical expression is not known. Many empirical expressions of the form $F(x) \sim x^{-\beta} \exp(-\mu x^\gamma)$ with different values for γ ranging from $1/2$ to 2 were proposed (Monin & Yaglom (2007)). We refer to e.g. (Khurshid *et al.* (2018); Gorbunova *et al.* (2020); Buaria & Sreenivasan (2020)) for recent overviews on the various predictions. Despite the absence of consensus on the precise form of $F(x)$, the following general features emerge. There exist two successive ranges:

- the near-dissipation range for $0.2 \lesssim k\eta \lesssim 4$ where the logarithmic derivative of the spectrum is not linear and its curvature clearly indicates $\gamma < 1$,
- the far-dissipation range for $k\eta \gtrsim 4$ where the spectrum is well described by a pure exponential decay, which corresponds to $\gamma = 1$,

irrespective of the value for β . These observations hold for the NS equation in the absence of thermal noise. Of course, at large wavenumbers, the thermal fluctuations become non-negligible and drastically affect the shape of the spectrum, leading to the equilibrium k^2 spectrum reflecting equipartition of energy (Bandak *et al.* (2021); Bell *et al.* (2022); McMullen *et al.* (2022)). This crossover was shown to occur well above the mean-free path, at scales within the dissipation range. Thus, depending on the system actual scales for thermal and turbulent fluctuations, the pure exponential decay associated with far-dissipation range may be unobservable in real turbulence and superseded by the thermal spectrum.

Leaving aside this issue, the form of the spectrum just beyond the inertial range can be deduced from FRG by taking the appropriate $t \rightarrow 0$ limit in the expression for the two-point correlation function at large wavenumbers. If one assumes that the scaling variable $tk^{2/3}$ saturates when t approaches the Kolmogorov time-scale $\tau_K = \sqrt{\nu/\bar{\epsilon}}$ and k reaches L^{-1} , one obtains for the energy spectrum

$$E(k) = \lim_{t \rightarrow 0} 4\pi k^2 C^{(2)}(t, \mathbf{k}) = A\bar{\epsilon}^{2/3} (k\eta)^{-\beta} \exp(-\mu(k\eta)^\gamma) \quad (8.8)$$

with $\gamma = 2/3$ and $\beta = 5/3$. The expression for $C^{(2)}$ is obtained in the large wavenumber expansion and at the fixed-point, thus this behaviour is expected to be valid at wavenumbers large $k \gg L^{-1}$ but still controlled by the fixed-point, which corresponds to the near-dissipation range. Let us emphasise that the result (8.8) does not have the same status as the expression for $C^{(2)}$ (7.19). It clearly relies on an additional assumption, the saturation of the scaling variable, which is reasonable but not rigorous. In particular, if one assumes the existence of different successive scalings, associated with the emergence of quasi-singularities (Dubrulle (2019)), one would obtain a different result. In fact, it would be interesting to investigate whether the distribution of γ displayed in Fig. 12 is compatible with a multi-fractal description.

However, it seems reasonable to assume that the first scaling to dominate close to the inertial range is the Komogorov one, which leads to the stretched exponential (8.8) with the $\gamma = 2/3$ exponent. This prediction has been verified in high-resolution DNS (Canet *et al.* (2017); Gorbunova *et al.* (2020); Buaria & Sreenivasan (2020)). In the simulations, the exponent γ was determined through the local exponent defined as

$$D_3(k) = \frac{d \ln}{d \ln(k\eta)} \left[\frac{d \ln}{d \ln(k\eta)} \left[- \frac{d \ln E(k)}{d \ln(k\eta)} \right] \right] \quad (8.9)$$

Indeed, if $E(k)$ is described by Eq. (8.8) on a certain range of k , one obtains $D_3(k) = \gamma$ on

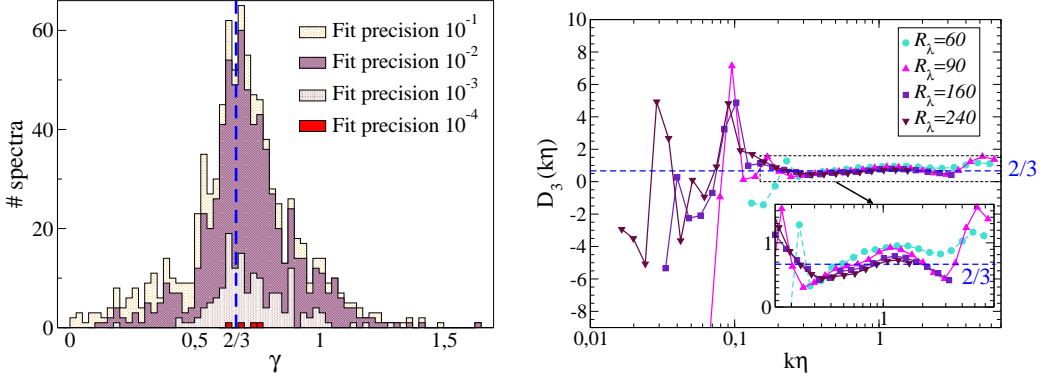


Figure 12: *Left panel:* distribution of the exponent γ of the stretched exponential for over 1600 spectra collected in experimental data from Modane wind tunnel, with different precision criteria for the fit of the spectrum in the dissipation range (see (Gorbunova *et al.* (2020)) for details). *Right panel:* Third logarithmic derivative D_3 of $E(k)$ as a function of the wavenumber from DNS at different Taylor Reynolds number. The spectrum in the near-dissipation range is magnified in the inset. The local exponent approaches the blue dashed line, which indicates the FRG prediction $\gamma = 2/3$, as R_λ increases.

this range (Gorbunova *et al.* (2020)), irrespective of the value for β . In the DNS, significant averaging was used in order to obtain smooth enough data to allow for the numerical evaluation of the three successive derivatives by finite differences.

It has also been observed in experimental data from von Kármán swirling flows (Debye *et al.* (2018)) and from the Modane wind tunnel (Gorbunova *et al.* (2020)). The latter yields the estimate $\gamma \simeq 0.68 \pm 0.19$, which is in very good agreement with the FRG prediction. Two examples of determination of γ are shown on Fig. 12.

9. Time-dependence of correlation functions in passive scalar turbulence

We now consider a passive scalar field $\theta(t, \mathbf{x})$ which dynamics is governed by the advection-diffusion equation (2.4). In this section, we consider three cases for the carrier flow: i) the advecting field $\mathbf{v}(t, \mathbf{x})$ is a turbulent velocity field solution of the incompressible NS equation (2.1), ii) $\mathbf{v}(t, \mathbf{x})$ is a random vector field with a Gaussian distribution characterised by zero mean and covariance

$$\langle v_\alpha(t, \mathbf{x}) v_\beta(t', \mathbf{y}) \rangle = \delta(t - t') D_0 \int_{\mathbf{p}} \frac{e^{i\mathbf{p} \cdot (\mathbf{x} - \mathbf{y})} P_{\alpha\beta}^\perp(\mathbf{p})}{(p^2 + m^2)^{\frac{d}{2} + \frac{\varepsilon}{2}}} \quad (9.1)$$

where $P_{\alpha\beta}^\perp(\mathbf{p})$ is the transverse projector which ensures incompressibility, and iii) the same random vector field with finite time correlations instead of $\delta(t - t')$. The model ii) was proposed by Kraichnan (Kraichnan (1968, 1994)), and has been thoroughly studied (we refer to (Falkovich *et al.* (2001); Antonov (2006)) for reviews). In this model, the parameter $0 < \varepsilon/2 < 1$ corresponds to the Hölder exponent, describing the velocity roughness from very rough for $\varepsilon \rightarrow 0$ to smooth for $\varepsilon \rightarrow 2$, and m acts as an IR cutoff.

The spatio-temporal correlations of the passive scalar in the three models for the carrier flow has been investigated within the FRG formalism in (Pagani & Canet (2021)). We first summarise the main results, and then present comparison with DNS for the three cases.

9.1. FRG results for the correlation functions of passive scalars

9.1.1. Scalar field in Navier-Stokes flow

We start with the model i), *i.e.* a scalar field transported by a NS turbulent flow. We focus on the inertial-convective range, in which the energy spectrum of the scalar decays as $E_\theta(\mathbf{p}) \sim p^{-5/3}$ as established by Obukhov and Corrsin in their seminal works (Obukhov (1949); Corrsin (1951)). As shown in Sec. 3.3, the action for the passive scalar possesses similar extended symmetries as the NS action. As a consequence, the structure of the related Ward identities for the vertices is the same: they all vanish upon setting one wavevector to zero, unless it is carried by a velocity field in which case it can be expressed using the \mathcal{D}_α operator (A.7). Hence, the derivation of Sec. 7.2 can be reproduced identically in the presence of the scalar fields. We refer to (Pagani & Canet (2021)) for details. This yields the general expression for the time-dependence of any n -point generalised correlation function of the scalar in the limit of large wavenumbers.

In this section, we only consider two-point correlation functions, so we drop the superscript ⁽²⁾ on C in the following. The correlation function of the scalar, defined in time-wavevector coordinates as $C_{\theta,NS}(t, \mathbf{p}) \equiv \langle \theta(t, \mathbf{p}) \theta(0, -\mathbf{p}) \rangle$, is given in the FRG formalism by

$$C_{\theta,NS}(t, \mathbf{p}) = \frac{\bar{\epsilon}_\theta \bar{\epsilon}^{-1/3}}{p^{11/3}} \begin{cases} C_0 \exp(-\alpha_0 (L/\tau)^2 p^2 t^2), & t \ll \tau \\ C_\infty \exp(-\alpha_\infty (L^2/\tau) p^2 |t|), & t \gg \tau, \end{cases} \quad (9.2)$$

where $\bar{\epsilon}$ and $\bar{\epsilon}_\theta$ denote the mean energy dissipation rates of the velocity and scalar fields respectively, $\tau \equiv (L^2/\bar{\epsilon})^{-1/3}$ the eddy-turnover time at the energy injection scale, and $C_{0,\infty}$ and $\alpha_{0,\infty}$ are constants. In fact, $\alpha_{0,\infty}$ are the same constants as the ones in the NS velocity correlation function Eq. (7.19). They can be calculated using FRG by integrating the flow equations, for example within the LO approximation presented in Sec. 6, for the forcing profile under consideration (or a reasonable model of it). Hence, the temporal decay of the scalar correlations is determined in the inertial-convective range by the one of the carrier fluid. In particular, these constants depend on the profile of the forcing exerted on the velocity, but not on the one exerted on the scalar field.

9.1.2. Scalar field in white-in-time synthetic velocity flow

Let us now focus on the model ii) proposed by Kraichnan (Kraichnan (1968)), in which the NS velocity field is replaced by a random vector field with white-in-time Gaussian statistics. The remarkable feature of this model is that despite its extreme simplification compared to real scalar turbulence, it still retains its essential features, and in particular universal anomalous scaling exponents of the structure functions. Moreover, it is simple enough to allow for analytical calculation in suitable limits (Chertkov & Falkovich (1996); Chertkov *et al.* (1995); Gawedzki & Kupiainen (1995); Bernard *et al.* (1996, 1998); Adzhemyan *et al.* (1998, 2001); Kupiainen & Muratore-Ginanneschi (2007); Pagani (2015)), see (Falkovich *et al.* (2001); Antonov (2006)) for reviews. The temporal dependence of the scalar correlation function was analyzed in (Mitra & Pandit (2005); Sankar Ray *et al.* (2008)). Within the FRG framework, the large wavenumber expansion also allows in this case for the closure of the flow equations for the scalar correlation functions. Indeed, for Kraichnan model, the action for the velocity field $\mathcal{S}_{NS}[\mathbf{v}, \bar{\mathbf{v}}, p, \bar{p}]$ is simply replaced by

$$S_K[\mathbf{v}] = \int_{\mathbf{x}} \mathbf{v}_\alpha(t, \mathbf{x}) \frac{(-\partial^2 + m^2)^{\frac{d+\epsilon}{2}}}{2D_0} \mathbf{v}_\alpha(t, \mathbf{x}). \quad (9.3)$$

Remarkably, the total action $S_K + S_\theta$ still possesses the same extended symmetries, but for the time-dependent shifts of the response fields (3.31) and (A.4), which reduce to $\bar{\theta}(t, \mathbf{x}) = \bar{\theta}(t, \mathbf{x}) + \bar{\epsilon}(t)$. The resulting Ward identities endow an essentially identical structure, such that

the derivation of the large wavenumber expansion proceeds in the same way. The essential difference arises when computing the loop integral in the second line of Eq. (7.7), in which the velocity propagator in (7.6) is replaced by

$$\bar{G}_{v_\alpha v_\beta}(\omega, \mathbf{q}) = 2D_0 \frac{P_{\alpha\beta}^\perp(\mathbf{q})}{(q^2 + m^2)^{\frac{d+\varepsilon}{2}} + \mathcal{R}_{\kappa, v}(\mathbf{q})}. \quad (9.4)$$

Because of the white-in-time (frequency-independent) nature of the Kraichnan propagator, the loop integral can be computed explicitly for any time delay, and yields a linear dependence in t . This implies that the decay of the scalar correlation is always exponential in time, e.g. for the two-point function

$$C_{\theta, K}(t, \mathbf{p}) = F(p) e^{-2\kappa_{\text{ren}} p^2 |t|}, \quad (9.5)$$

hence there is no Gaussian regime at small times. Moreover, one obtains an explicit expression for the non-universal constant κ_{ren}

$$\kappa_{\text{ren}} = \kappa_\theta + \frac{d-1}{2d} \int_{\mathbf{p}} \frac{D_0}{(p^2 + m^2)^{\frac{d+\varepsilon}{2}}}. \quad (9.6)$$

The second term in the renormalised diffusivity κ_{ren} embodies the effect of fluctuations and can therefore be interpreted as an eddy diffusivity. The prefactor $F(p)$ in (9.5) is given by an integral, which behaves in the inertial range as $F(p) \sim p^{-d-2+\varepsilon}$ while in the weakly non-linear regime (*i.e.* when the convective term is perturbative), it behaves as $F(p) \sim p^{-d-2-\varepsilon}$ (Frisch & Wirth (1996); Pagani & Canet (2021)). For the Kraichnan model, there is no anomalous correction to the second-order structure function (Falkovich *et al.* (2001); Antonov (2006)). The dimensional (analogous to K41) scaling of $F(p)$ is in this case an exact result.

9.1.3. Scalar field in time-correlated synthetic velocity flow

Let us introduce a slight extension of the Kraichnan model, model iii), in which the white-in-time covariance (9.1) of the synthetic velocity field is replaced by one with tunable time-correlations $D_{T_e}(t - t')$, where T_e represents the typical decorrelation time of the synthetic velocity. The pure Kraichnan model is simply recovered in the limit $T_e \rightarrow 0$ where $D_0(t - t') \equiv \delta(t - t')$. The calculation of the scalar correlation functions within the FRG large wavenumber expansion is strictly identical to the pure Kraichnan case, except for the loop integral in Eq. (7.7). Indeed, as soon as some time dependence is introduced in the velocity covariance, hence in the velocity propagator (9.4), one restores the two time regimes. Let us focus for simplicity on the two-point scalar correlation function $C_{\theta, K_{T_e}}(t, \mathbf{p})$. For small time delays $t \ll T_e$, the Fourier exponentials in the loop integral can be expanded and one finds the Gaussian decay in pt , whereas for large time delays $t \gg T_e$, T_e can be replaced by zero in the integral and one recovers the Kraichnan exponential decay in $p^2|t|$.

The great advantage of this model is that the time-scale of the correlation function of the velocity field is adjustable and can be varied independently of the scalar dynamics, in particular in DNS, such that it allows one to access the crossover between the two time regimes, as shown in Sec. 9.4.

9.2. Passive scalars in Navier-Stokes flow

The spatio-temporal behaviour of the correlation function of the scalar transported by NS flow has been studied in DNS in (Gorbunova *et al.* (2021b)), using similar numerical methods as for the NS case. The Schmidt number of the scalar, defined as the ratio of the fluid viscosity

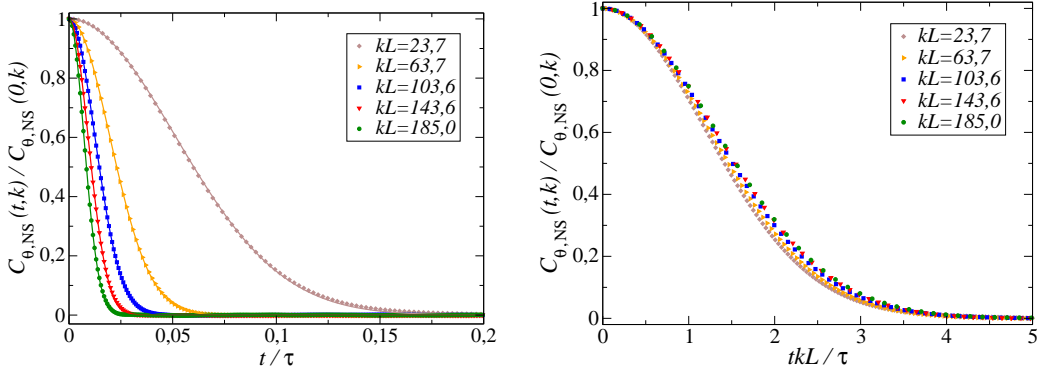


Figure 13: Time dependence of the normalised two-point correlation function $C_{\theta,NS}(t, k)$ of the scalar in the NS flow at different wavenumbers k for $R_\lambda = 90$, as a function of t . (left panel) and of kt (right panel), which results in their collapse. L is the integral length scale, τ is the eddy-turnover time scale at the integral scale.

to the scalar diffusivity $Sc = \nu/\kappa_\theta$ was varied from 0.7 to 36, and the two-point correlations of both the scalar and the velocity fields were recorded during the runs with similar averages as in Eq. (8.1).

The results for $C_{\theta,NS}(t, k)$ are presented in Fig. 13. Each curve for a fixed wavenumber is accurately fitted by a Gaussian $f_{Gaus}(t) = c \exp(-(t/\tau_0)^2)$. Moreover, all curves for different wavenumbers collapse when plotted as a function of the variable kt , as expected from the FRG result (9.2). This behaviour is completely similar to the one of the NS velocity field presented in Fig. 7, as anticipated. The transported scalars behave in the inertial-convective range as the carrier fluid particles.

The decorrelation time τ_0 extracted from the Gaussian fit is displayed in Fig. 14. According to (9.2), it is related to α_0 as $\tau_0/\tau = (\sqrt{\alpha_0}kL)^{-1}$, and it is found to precisely conform to the expected k^{-1} decay. Moreover, beyond this behaviour, the FRG analysis yields that the prefactor α_0 is uniquely fixed by the properties of the carrier fluid, and is therefore equal for the velocity and the transported scalars. The numerical data for α_0 shown in Fig. 14 confirms this result, since the values of α_0 for the velocity correlations and for the scalar correlations are in very close agreement, and almost independent of the scalar properties. Indeed, the variation of Sc from 0.7 to 36 does not lead to significant changes of α_0 . Hence the dynamics of the scalar field is dominated by the random advection and the sweeping effect.

At large time delays, a crossover from the Gaussian in kt to an exponential in k^2t is predicted by the FRG result (9.2). However, the Gaussian decay at small time induces a fast decrease of the correlations, such that the signal approaches zero and becomes oscillatory in the simulations before the crossover can occur. This prevents from its detection, as for the NS flow, which is not surprising since in this inertial-convective range the behaviour of the scalar closely follows the one of the velocity field. It would be very interesting to study other regimes of the scalar in order to find a more favorable situation to observe the large-time regime. Meanwhile, the crossover can be evidenced in the case of synthetic flows, as we now show.

9.3. Passive scalars in the Kraichnan model

The correlation function of the scalar field transported in a white-in-time synthetic velocity field has also been studied in (Gorbunova *et al.* (2021b)). A random vector field, isotropic and divergenceless, conforming to a Gaussian distribution with the prescribed covariance (9.1) is generated. The advection-diffusion equation (2.4) with this synthetic field is then solved

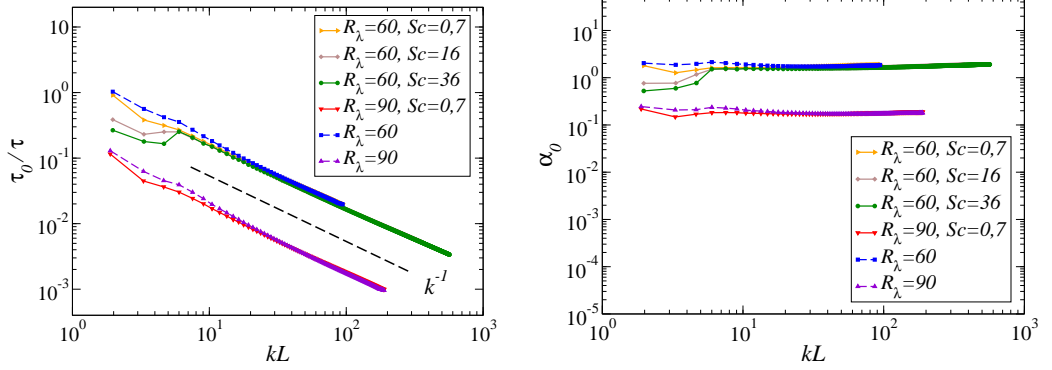


Figure 14: *Left panel*: Decorrelation time τ_0 extracted from the Gaussian fit of the scalar correlations (plain lines) and of the velocity correlations (dashed lines) as a function of the wavenumber for various R_λ and Sc . *Right panel*: non-universal parameter α_0 obtained as $\alpha_0 = \tau^2/(\tau_0 k L)^2$. In both panels, the data for $R_\lambda = 90$ are shifted downward by a factor 10 for visibility.

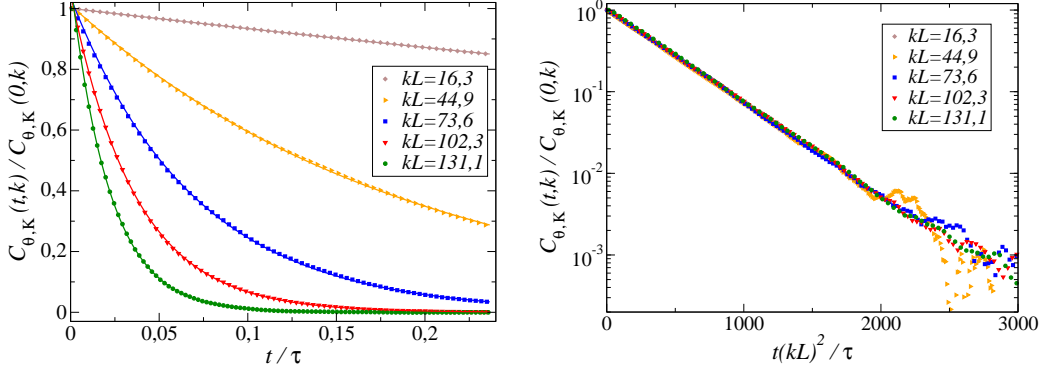


Figure 15: Time dependence of the normalised two-point correlation function of the scalar $C_{\theta,K}(t, k)$ in Kraichnan model at different wavenumbers, as a function of time (*right panel*) and of the variable $k^2 t$ (*left panel*) which leads to their collapse. Data from the numerical simulation, for $\varepsilon = 1$ in this example, are denoted with dots and their exponential fits with continuous lines.

using DNS. The details of the procedure and parameters can be found in (Gorbunova *et al.* (2021b)). In order to achieve a precision test of the FRG result (9.5) and (9.6), 24 different sets of simulations were analyzed, varying the different parameters: Hölder exponent ε , amplitude D_0 of the velocity covariance, and diffusivity κ_θ of the scalar.

For each set, the correlation function of the scalar $C_{\theta,K}(t, k)$ was computed. As illustrated in Fig. 15, it always exhibits an exponential decay in time, perfectly modelled by the fitting function $f_{\text{exp}}(t) = c \exp(-t/\tau_K)$. The decorrelation time τ_K depends on the wavenumber as $\tau_K \sim k^{-2}$, as expected from (9.5), and shown in Fig. 16.

Beyond the global exponential form of the spatio-temporal dependence of the scalar correlation function, the non-universal factor κ_{ren} in the exponential can be computed explicitly for the Kraichnan model within the FRG framework and is given by (9.6). Its value depends on the parameters ε , D_0 characterising the synthetic velocity and κ_θ characterising the scalar. All these parameters have been varied independently in the 24 sets of simulations. For each set, $\kappa_{\text{ren}}^{\text{num}}$ is determined from the numerical data as the plateau value of $\tau_K k^2$,

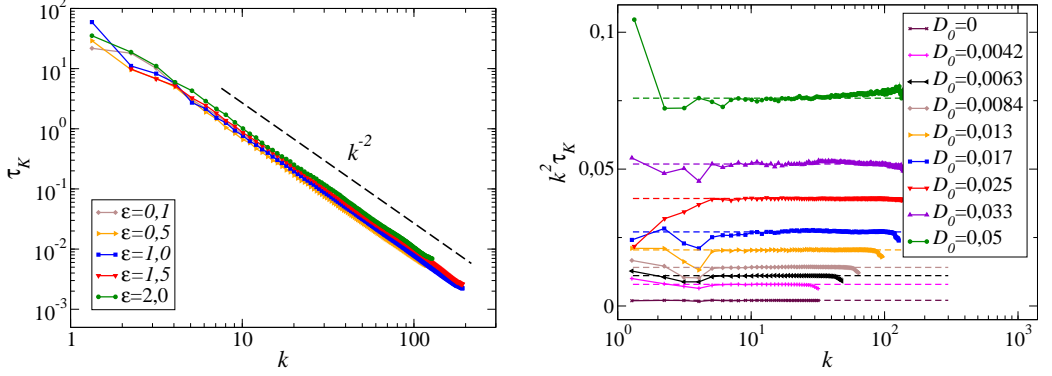


Figure 16: *Left panel*: Decorrelation time τ_K extracted from the exponential fits for different values of the Hölder exponent ε from 0.1 to 2. *Right Panel*: Compensated decorrelation time $k^2 \tau_K$ extracted from the exponential fits, for different values of D_0 and $\varepsilon = 1$. The renormalised diffusivity κ_{ren} for each curve is determined as the fitted value of the plateau represented by dashed lines.

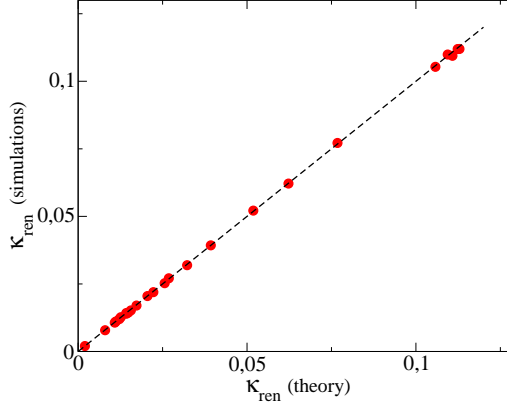


Figure 17: Renormalised scalar diffusivity: κ_{ren} (simulations) is obtained from the plateau values of $k^2 \tau_K$ extracted from the exponential fits of the scalar correlation function; κ_{ren} (theory) is calculated from its theoretical estimate based on Eq. (9.6). The data are gathered from the 24 data sets for which the parameters ε , Sc , D_0 , κ_θ are varied independently (see (Gorbunova *et al.* (2021b)) for detailed parameters).

where τ_K is extracted from the exponential fit, as illustrated in Fig. 16. Besides, the value of $(\kappa_{\text{ren}} - \kappa_\theta)$ depends on the synthetic velocity only and can be computed prior to any simulation as $\kappa_{\text{ren}}^{\text{num}} - \kappa_\theta = A_\varepsilon D_0$ with $A_\varepsilon = \frac{1}{3} \sum_p \frac{D_0}{(p^2 + m^2)^{\frac{3}{2} + \frac{\varepsilon}{2}}}$ following the FRG expression (9.6). The comparison of the two estimations for κ_{ren} is displayed in Fig. 17, which shows a remarkable agreement. Let us emphasise that the numerical data presented spans values of ε up to 1.5, well beyond the perturbative regime $\varepsilon \simeq 0$ (Adzhemyan *et al.* (1998)). This analysis hence provides a thorough confirmation of the FRG theory, including to the precise form of the non-universal prefactor in the exponential.

9.4. Passive scalars in a time-correlated synthetic flow

Let us now turn to the extended Kraichnan model iii), *i.e.* a scalar field advected by a synthetic velocity field with finite time correlations $D_{T_e}(t - t')$. The simplest implementation of these

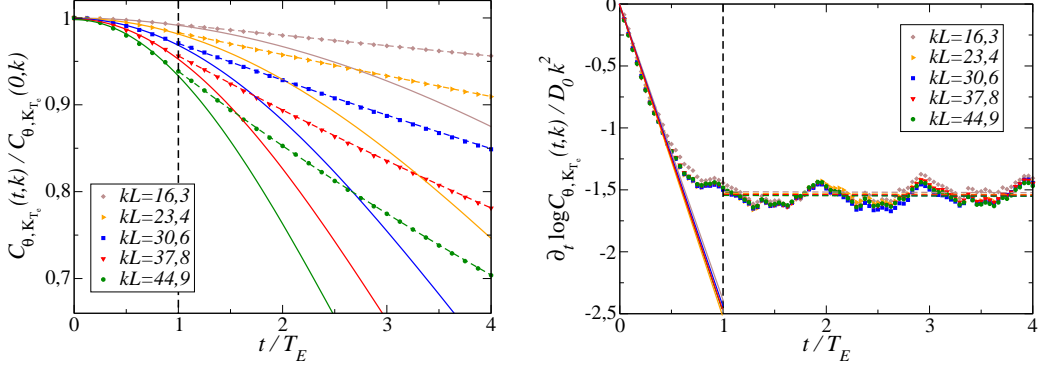


Figure 18: *Left panel:* Time dependence of the normalised two-point correlation function $C_{\theta, K_{T_e}}(t, k)$ at different wavenumbers k . Data from the numerical simulation are denoted with dots, their Gaussian fits calculated for $t \leq T_e$ with continuous lines, their exponential fits calculated for $t \geq T_e$ with dashed lines. *Right panel:* time derivative of the logarithm of the same data (including the fits), divided by $D_0 k^2$.

finite time correlations in the DNS is to define a correlator $D_{T_e}(t) = \frac{1}{T_e} \theta(t - T_e)$ where $\theta(t)$ is the Heavyside step function. Hence, when T_e is negligible compared to the other dynamical time scales of the mixing ($\tau_A \sim \eta_B / U_{\text{rms}}$ for advection, and $\tau_\kappa \sim \eta_B^2 / \kappa_\theta$ for diffusion, with η_B the Batchelor scale, *i.e.* the smallest variation scale of the scalar), the velocity field can be considered as white-in-time (pure Kraichnan model). In contrast, when T_e becomes comparable with the typical decorrelation time of the scalar – say τ_K estimated from the pure Kraichnan model at intermediate wavenumbers – then it realises a correlated synthetic velocity field.

The correlation function of the scalar $C_{\theta, K_{T_e}}(t, k)$, obtained from DNS of model iii), is shown in Fig. 18. At small time delays $t \leq T_e$, the different curves for each wavenumber are well fitted by Gaussian curves, whereas at large time delays, they depart from their Gaussian fits and decay much more slowly. The slower decay is precisely modelled by exponential fits. Hence, the crossover from the small-time Gaussian regime to the large-time exponential one, predicted by FRG, can be observed in this model. It can be further evidenced by computing the time derivative of $\log C_{\theta, K_{T_e}}(t, k)$. According to the FRG results, one should obtain

$$\frac{1}{k^2} \frac{\partial \log C_{\theta, K_{T_e}}(t, k)}{\partial t} = \begin{cases} -2\alpha_0 t & t \ll T_e \\ -\alpha_\infty & t \gg T_e \end{cases}, \quad (9.7)$$

where $\alpha_{0,\infty}$ are the non-universal prefactors depending on the velocity characteristics only. This derivative is displayed in Fig. 18. All the curves collapse when divided by k^2 , and show a linear decay with negative slope at small time, which crosses over to a negative constant at large time, in agreement with (9.7). Note that at higher wavenumbers (not shown), the large-time regime becomes indiscernible as the scalar field decorrelates fast (because of the $\sim k^2$ dependence) down to near-zero noisy values before T_e is reached. This prevents us from resolving the crossover for these wavenumbers. This hints that a similar effect hinders the large-time regime in NS flows.

10. Conclusion and Perspectives

The purpose of this *JFM Perspectives* was to give an overview of what has been achieved using FRG methods in the challenging field of turbulence, and to provide the necessary technical elements for the reader to grasp the basis and the scope of these results. An

important aspect is that the RG is in essence conceived to build effective theories from “first principles”, in the sense that it is a tool to compute statistical properties of a system, by averaging over fluctuations, from its underlying microscopic or fundamental description, that is, in the case of turbulence, from the NS equations, without phenomenological inputs. An essential ingredient in this method is the symmetries, and extended symmetries, which can be fully exploited within the field-theoretical framework through exact Ward identities, that we expounded. So far, the main aspects of turbulence addressed with the FRG methods are the universal statistical properties of stationary, homogeneous and isotropic turbulence. In this context, the main achievements of this approach are twofold.

The first one is the evidence for the existence of a fixed-point of the RG flow, for physical forcing concentrated at large scales, which describes fully developed turbulence. This was not accessible using perturbative RG approaches, because they are restricted to power-law forcing which changes the nature of the turbulence. The very existence of a fixed-point demonstrates two essential properties of turbulence: universality (independence of the precise forcing and dissipation mechanisms) and power-law behaviours. So far, this fixed-point has been studied within a simple approximation of the FRG, called LO (leading-order), which amounts to neglecting all vertices of order $n \geq 3$ but the one present in the NS field theory. Nonetheless, this rather simple approximation allows one to recover the exact result for the third-order structure function, and yields the correct K41 scaling for the energy spectrum and the second-order structure function, with accurate estimates of the Kolmogorov constant. This work calls for further calculations, within improved approximations, in order to determine whether anomalous exponents arise when including higher-order vertices in the FRG ansatz. This is a first route to be explored, possibly coupled with the introduction of composite operators, to achieve this goal. This program has already been started in shell models, which are simplified models of turbulence. It indeed allows to compute intermittency corrections to the exponents of the structure functions (Fontaine *et al.* (2022)).

The second achievement using FRG, which is the most striking one, is the obtainment of the general expression, at large wavenumbers, of the spatio-temporal dependence of any n -point correlation and response function in the turbulent stationary state. The valuable feature of this expression is that it is asymptotically exact in the limit of large wavenumbers. Given the scarcity of rigorous results in 3D turbulence, this point is remarkable and worth highlighting. All the n -point correlation functions are endowed with a common structure for their temporal behaviour, which can be simply summarised, on the example of the two-point function $C(t, \mathbf{p})$ for conciseness, as follows. At small time delays t , $C(t, \mathbf{p})$ exhibits a fast Gaussian decay in the variable pt , while at large time delays, it shows a crossover to a slower exponential decay in the variable $p^2|t|$. The prefactors α_0 entering the Gaussian, and α_∞ entering the exponential, respectively, are non-universal, but are equal for any n -point correlations. Similar expressions have been established in the case of passive scalars transported by turbulent flows, in the three cases where the turbulent velocity field is either the solution of the NS equations, or a synthetic random velocity field (Kraichnan model and its time-correlated extension). For the NS turbulent flow, the behaviour of the scalar follows in the inertial-convective range the one of the velocity field with fully analogous spatio-temporal correlations, including the non-universal prefactors. In the case of the white-in-time Kraichnan model, the temporal decay of the scalar correlations is purely exponential in p^2t , but a Gaussian regime opens up at small time delays when introducing a finite time-correlation in the velocity covariance.

The FRG results can be compared with DNS, which allows one in particular to quantify the precise range of validity of the “large wavenumber limit” which underlies the FRG calculations. Several DNS have been conducted both for NS turbulence and passive scalar turbulence with the different models for the advecting velocity field. They brought a thorough

and accurate confirmation of the FRG predictions in the small-time regime, including high-precision tests in the case of the Kraichnan model. In contrast, the large-time regime has remained elusive in most DNS, due to the steepness of the Gaussian regime, which leads to a fast damping of the correlations to near-zero levels and renders very challenging its numerical detection. The crossover has been evidenced in the time-correlated synthetic velocity field, because in this case, the different time-scales are more easily adjustable in order to reach the large-time exponential decay before the signal gets too low and indiscernible from numerical noise. Although challenging, it would be very interesting to push further the DNS investigations in order to access and study the large-time regime for the NS flow. Another direction which remains unexplored so far is to test in DNS the FRG predictions for 2D turbulence, for which explicit expressions for the spatio-temporal correlations at large wavenumbers are also available (Tarpin *et al.* (2019)).

The temporal behaviour of the n -point correlation functions are obtained within FRG from the leading term in the large wavenumber expansion of the flow equations. Although this leading term is exact at large p , it vanishes at coinciding times $t = 0$, such that it does not carry any information on the structure functions, and in particular on their possible anomalous exponents. Another route in the quest for the intermittency corrections is thus to compute within the large wavenumber expansion, the first non-vanishing term at equal times. Preliminary results were obtained in this direction for 2D turbulence (Tarpin *et al.* (2019)), but it remains to be completed and extended to study 3D turbulence.

The calculation of intermittency corrections within the FRG framework is clearly the next challenge to be addressed and probably the most significant, and recent results (Fontaine *et al.* (2022)) already pave the way for this quest. However, another promising line of research is the use of FRG in turbulence modelling. The FRG is designed by essence to construct a sequence of scale-dependent effective descriptions of a given system from the microscopic scale to the macroscopic one. In particular, if stopped at any chosen scale, the FRG flow provides the effective model at that scale, including the effect of fluctuations on all smaller (distance-)scales (larger wavenumbers). As mentioned in the introduction, computing such effective models from the fundamental equations, e.g. NS equations, via a controlled procedure of integration of fluctuations would be very valuable in many applications. Probably the most relevant one is to improve current models used as a “sub-grid” description – that is model for the non-resolved scales – in many numerical schemes, such as LES, meteorological or climate models. Of course, a long path lies before arriving at competitive results, since one should first extend the FRG framework to describe more realistic situations, such as non-homogeneous, or anisotropic, or non-stationary conditions, the presence of shear, fluxes at the boundaries, etc. . . . Nonetheless, we believe that this path is worth exploring, and should be the subject of future efforts.

Acknowledgements. L.C. would like to sincerely thank all her collaborators involved in the works presented here, whose implication was essential to obtain all these results. She thanks in particular Bertrand Delamotte and Nicolás Wschebor, with whom the FRG approach to turbulence was initiated, and largely developed. She is also grateful to Guillaume Balarac for all the work with DNS, and Gregory Eyink and Vincent Rossetto, who greatly contributed in analysing the data and the results of DNS and experiments. Her special and warm thanks go to the PhD students, Anastasiia Gorbunova and Malo Tarpin, and postdoc Carlo Pagani, whose contributions were absolutely pivotal on FRG or DNS works. L.C. would also like to thank Mickael Bourgoin, Nicolas Mordant, Bérengère Dubrulle and her team for their great help with experimental data.

Funding. This work was supported by the Agence Nationale pour la Recherche (grant ANR-18-CE92-0019 NeqFluids) and by the Institut Universitaire de France.

Declaration of interests. The author reports no conflict of interest.

Appendix A. Additional extended symmetries and Ward identities

A.0.1. Local shift symmetries of the pressure fields

An evident symmetry of the NS action (3.21) is the invariance under a time-dependent shift of the pressure field $\pi(t, \mathbf{x}) \rightarrow \pi(t, \mathbf{x}) + \varepsilon(t)$ since the latter only appears with a gradient. Let us now consider instead an infinitesimal time- and space-dependent shift $\pi(t, \mathbf{x}) \rightarrow \pi(t, \mathbf{x}) + \varepsilon(t, \mathbf{x})$. This field transformation yields a variation of \mathcal{S}_{NS} which is linear in $\bar{\mathbf{v}}$. Since the field transformation is simply a change of variables in the functional integral (3.20), it must leave it unchanged. One deduces to first order in ε the equality

$$0 = \int_{t, \mathbf{x}} \left\langle -\bar{v}_\alpha(t, \mathbf{x}) \partial_\alpha \varepsilon(t, \mathbf{x}) + K(t, \mathbf{x}) \varepsilon(t, \mathbf{x}) \right\rangle, \quad (\text{A } 1)$$

where the first term comes from the variation of the action and the second one from the variation of the source term. Since this equality holds for any arbitrary infinitesimal $\varepsilon(t, \mathbf{x})$, one deduces the following Ward identity

$$\frac{\delta \Gamma}{\delta \langle \pi(t, \mathbf{x}) \rangle} \equiv K(t, \mathbf{x}) = -\frac{1}{\rho} \langle \partial_\alpha \bar{v}_\alpha(t, \mathbf{x}) \rangle = \frac{\delta \mathcal{S}_{\text{NS}}}{\delta \pi(t, \mathbf{x})} \Big|_{\langle \Phi_k \rangle}, \quad (\text{A } 2)$$

where the first equality simply stems from the Legendre conjugate relations (3.15), the second from the relation (A 1), and the third can be deduced from the NS action (3.21). This entails that the dependence of the effective action Γ in the pressure field π remains the same as the one of the original action \mathcal{S}_{NS} , *i.e.* it keeps the same form in terms of the average fields $\frac{1}{\rho} \int_{t, \mathbf{x}} \langle \bar{v} \rangle_\alpha \partial_\alpha \langle \pi \rangle$, or otherwise stated, this term is not renormalised – it is not modified by the fluctuations.

The same analysis can be carried over for the response pressure field, by considering the infinitesimal field transformation $\bar{\pi}(t, \mathbf{x}) \rightarrow \bar{\pi}(t, \mathbf{x}) + \bar{\varepsilon}(t, \mathbf{x})$. This yields the Ward identity

$$\frac{\delta \Gamma}{\delta \langle \bar{\pi}(t, \mathbf{x}) \rangle} \equiv \bar{K}(t, \mathbf{x}) = \langle \partial_\alpha v_\alpha(t, \mathbf{x}) \rangle = \frac{\delta \mathcal{S}_{\text{NS}}}{\delta \bar{\pi}(t, \mathbf{x})} \Big|_{\langle \Phi_k \rangle}, \quad (\text{A } 3)$$

which means that the corresponding term in the effective action is not renormalised either and keeps its original form $\int_{t, \mathbf{x}} \langle \bar{\pi} \rangle \partial_\alpha \langle v_\alpha \rangle$. Hence the effective action remains linear in the pressure and response pressure fields, and there are no mixed pressure-velocity vertices beyond quadratic order, *i.e.* no vertices for $n \geq 3$ with a p or a \bar{p} leg. As a consequence, the pressure fields only enter in the propagator, and the whole pressure sector essentially decouples, as will be manifest in the FRG framework.

Since the pressure fields are not renormalised, we have used throughout the paper the same notation π for both the pressure and the average pressure, and similarly $\bar{\pi}$ for both the response pressure and its average. This is of course not the case for the velocity sector which contains non-trivial fluctuations, and we have used different notations $\mathbf{u} \equiv \langle \mathbf{v} \rangle$ and $\bar{\mathbf{u}} \equiv \langle \bar{\mathbf{v}} \rangle$ for the fields and average fields.

A.0.2. Extended symmetries for the passive scalar fields

Let us now consider the symmetries and extended symmetries of the passive scalar action (3.23). This action possesses two extended symmetries related to time-dependent shifts of the scalar field : $\theta(t, \mathbf{x}) \rightarrow \theta(t, \mathbf{x}) + \varepsilon(t)$ and the joint transformation for the response field

$$\begin{aligned} \bar{\theta}(t, \mathbf{x}) &\rightarrow \bar{\theta}(t, \mathbf{x}) + \bar{\varepsilon}(t) \\ \bar{\pi}(t, \mathbf{x}) &\rightarrow \bar{\pi}(t, \mathbf{x}) + \bar{\varepsilon}(t) \theta(t, \mathbf{x}). \end{aligned} \quad (\text{A } 4)$$

Each of these transformations leads to a variation of the action which is linear in the fields. The corresponding functional Ward identities are straightforward to derive and read respectively

(Pagani & Canet (2021)).

$$\begin{aligned} \int_{\mathbf{x}} \frac{\delta \Gamma}{\delta \theta(t, \mathbf{x})} &= - \int_{\mathbf{x}} \partial_t \bar{\theta}(t, \mathbf{x}) \\ \int_{\mathbf{x}} \frac{\delta \Gamma}{\delta \bar{\theta}(t, \mathbf{x})} &= \int_{\mathbf{x}} \left\{ \partial_t \theta(t, \mathbf{x}) + v_{\beta}(t, \mathbf{x}) \partial_{\beta} \theta(t, \mathbf{x}) \right\}. \end{aligned} \quad (\text{A } 5)$$

These identities imply that the two terms $\int \bar{\theta} \partial_t \theta$ and $\int \bar{\theta} v_{\beta} \partial_{\beta} \theta$ are not renormalised, and they entail that any vertex with one vanishing wavevector carried either by a θ or a $\bar{\theta}$ field vanishes – except for $\Gamma^{\theta \bar{\theta}}$ which keeps its original form given by $\mathcal{S}^{\theta \bar{\theta}} - i.e.$

$$\begin{aligned} \Gamma^{(n_{\nu}, n_{\bar{\nu}}, n_{\theta} \geq 1, n_{\bar{\theta}})}(\dots, \omega_{\theta}, \mathbf{p}_{\theta} = 0, \dots) &= 0 \\ \Gamma^{(n_{\nu}, n_{\bar{\nu}}, n_{\theta}, n_{\bar{\theta}} \geq 1)}(\dots, \omega_{\bar{\theta}}, \mathbf{p}_{\bar{\theta}} = 0, \dots) &= 0 \\ \Gamma^{(0,0,1,1)}(\omega_{\theta}, \mathbf{p}_{\theta} = \mathbf{0}, \omega_{\bar{\theta}}, \mathbf{p}_{\bar{\theta}}) &= i \omega_{\theta} (2\pi)^{d+1} \delta(\omega_{\theta} + \omega_{\bar{\theta}}) \delta^d(\mathbf{p}_{\theta} + \mathbf{p}_{\bar{\theta}}). \end{aligned} \quad (\text{A } 6)$$

These identities are very similar to Eqs. (3.34,3.35) ensuing from the time-gauged shift of the response fields.

Moreover, the time-dependent Galilean symmetry is also an extended symmetry of the total action $\mathcal{S}_{\text{NS}} + \mathcal{S}_{\theta}$. Indeed, the passive scalar and its response field behave as Galilean scalar densities under time-dependent Galilean transformations (3.24), *i.e.* $\delta \theta(t, \mathbf{x}) = \varepsilon_{\beta}(t) \partial_{\beta} \theta(t, \mathbf{x})$ and $\delta \bar{\theta}(t, \mathbf{x}) = \varepsilon_{\beta}(t) \partial_{\beta} \bar{\theta}(t, \mathbf{x})$, which yield a variation of the total action linear in the field. The associated Ward identity constrains the vertices for which one of the velocity has a zero wavenumber,

$$\begin{aligned} \Gamma_{\alpha_1 \dots \alpha_{n_{\nu} + n_{\bar{\nu}} + 1}}^{(n_{\nu} + 1, n_{\bar{\nu}}, n_{\theta}, n_{\bar{\theta}})} \left(\dots, \underbrace{\omega_{\ell}, \mathbf{p}_{\ell} = 0}_{\ell = \text{velocity index}}, \dots \right) &= - \sum_{i=1}^n \frac{p_i^{\alpha_{\ell}}}{\omega_{\ell}} \Gamma_{\alpha_1 \dots \alpha_{n_{\nu} + n_{\bar{\nu}}}}^{(n_{\nu}, n_{\bar{\nu}}, n_{\theta}, n_{\bar{\theta}})} \left(\dots, \underbrace{\omega_i + \omega_{\ell}, \mathbf{p}_i}_{i^{\text{th}} \text{ field}}, \dots \right), \\ &= \mathcal{D}_{\alpha_1}(\omega_{\ell}) \Gamma_{\alpha_1 \dots \alpha_{n_{\nu} + n_{\bar{\nu}}}}^{(n_{\nu}, n_{\bar{\nu}}, n_{\theta}, n_{\bar{\theta}})} \left(\dots, \omega_i, \mathbf{p}_i, \dots \right) \end{aligned} \quad (\text{A } 7)$$

where $\alpha_1 \dots \alpha_{n_{\nu} + n_{\bar{\nu}} + 1}$ are the spatial indices of the velocity (and response velocity) fields, $n = n_{\theta} + n_{\bar{\theta}} + n_{\nu} + n_{\bar{\nu}}$, and \mathcal{D}_{α} is the same operator as in Eq. (3.30).

To summarise, the key point is that the Ward identities for the scalar advected by the NS flow share essentially the same structure as the ones for the NS action. They have a strong implication: when at least one wavevector of any vertex is set to zero, then it vanishes, except if the wavevector is carried by a velocity field, in which case it is controlled by (3.30) or (A 7), *i.e.* given in terms of a linear combination of lower-order vertices through the operator \mathcal{D}_{α} . This constitutes the cornerstone of the large wavenumber closure expounded in Sec. 7.2.

Appendix B. Flow equations in the LO approximation

We report in this Appendix additional details on the derivation of the flow equations for NS, within the LO approximation presented in Sec. 6, for the functions $f_{\kappa, \perp}^{\nu}$ and $f_{\kappa, \perp}^D$, and their explicit expressions. We refer to (Canet *et al.* (2016)) for the full derivation.

From the general form of the effective average action and of the regulator term $\Delta \mathcal{S}_{\kappa}$, one can infer the general structure of the propagator matrix, defined as the inverse of the Hessian of $\Gamma_{\kappa} + \Delta \mathcal{S}_{\kappa}$. It is more conveniently expressed in Fourier space where it is diagonal in wavevector and frequency, such that it is just the inverse of a matrix

$$\bar{G}_{\kappa}(\omega, \mathbf{p}) = \left[\bar{\Gamma}_{\kappa}^{(2)} + \mathcal{R}_{\kappa} \right]^{-1}(\omega, \mathbf{p}). \quad (\text{B } 1)$$

As usual, because of rotational and parity invariance, any generic two-(space)index function (in Fourier space) $F_{\alpha\beta}(\omega, \mathbf{p})$ can be decomposed into a longitudinal and a transverse part as $F_{\alpha\beta}(\omega, \mathbf{p}) = F_{\parallel}(\omega, \mathbf{p})P_{\alpha\beta}^{\parallel}(\mathbf{p}) + F_{\perp}(\omega, \mathbf{p})P_{\alpha\beta}^{\perp}(\mathbf{p})$ where the transverse and longitudinal projectors are defined by

$$P_{\alpha\beta}^{\perp}(\mathbf{p}) = \delta_{\alpha\beta} - \frac{p_{\alpha}p_{\beta}}{p^2}, \quad \text{and} \quad P_{\alpha\beta}^{\parallel}(\mathbf{p}) = \frac{p_{\alpha}p_{\beta}}{p^2}. \quad (\text{B } 2)$$

Inverting the matrix $\left[\bar{\Gamma}_{\kappa}^{(2)} + \mathcal{R}_{\kappa} \right]$, one obtains the general propagator

$$\bar{G}_{\kappa, \alpha\beta}(\omega, \mathbf{p}) = \begin{matrix} u_{\alpha} \\ \bar{u}_{\alpha} \\ \pi \\ \bar{\pi} \end{matrix} \begin{pmatrix} u_{\beta} & \bar{u}_{\beta} & \pi & \bar{\pi} \\ \bar{G}_{\kappa, \alpha\beta}^{uu}(\omega, \mathbf{p}) & \bar{G}_{\kappa, \alpha\beta}^{u\bar{u}}(\omega, \mathbf{p}) & 0 & ip_{\alpha}\bar{G}_{\kappa}^{u\bar{\pi}}(\omega, \mathbf{p}) \\ \bar{G}_{\kappa, \alpha\beta}^{\bar{u}\bar{u}}(-\omega, \mathbf{p}) & 0 & ip_{\alpha}\bar{G}_{\kappa}^{\bar{u}\pi}(\omega, \mathbf{p}) & 0 \\ 0 & -ip_{\beta}\bar{G}_{\kappa}^{\bar{u}\pi}(-\omega, \mathbf{p}) & \bar{G}_{\kappa}^{\pi\pi}(\omega, \mathbf{p}) & \bar{G}_{\kappa}^{\pi\bar{\pi}}(\omega, \mathbf{p}) \\ -ip_{\beta}\bar{G}_{\kappa}^{u\bar{\pi}}(-\omega, \mathbf{p}) & 0 & \bar{G}_{\kappa}^{\pi\bar{\pi}}(-\omega, \mathbf{p}) & 0 \end{pmatrix} \quad (\text{B } 3)$$

with in the pressure sector

$$\bar{G}_{\kappa}^{\pi\pi}(\omega, \mathbf{p}) = -\frac{\rho}{p^2}\bar{\Gamma}_{\kappa, \parallel}^{(0,2)}(\omega, \mathbf{p}) \quad , \quad \bar{G}_{\kappa}^{\pi\bar{\pi}}(\omega, \mathbf{p}) = \frac{\rho}{p^2}\bar{\Gamma}_{\kappa, \parallel}^{(1,1)}(-\omega, \mathbf{p}) \quad , \quad (\text{B } 4)$$

and in the mixed velocity-pressure sector

$$\bar{G}_{\kappa}^{u\bar{\pi}}(\omega, \mathbf{p}) = -\frac{1}{p^2} \quad , \quad \bar{G}_{\kappa}^{\bar{u}\pi}(\omega, \mathbf{p}) = \frac{\rho}{p^2}. \quad (\text{B } 5)$$

Furthermore, the components of the propagator in the velocity sector are purely transverse (that is, all the longitudinal parts vanish), as a consequence of incompressibility, and given by

$$\begin{aligned} \bar{G}_{\kappa, \alpha\beta}^{u\bar{u}}(\omega, \mathbf{q}) &= P_{\alpha\beta}^{\perp}(\mathbf{q}) \frac{1}{\bar{\Gamma}_{\kappa, \perp}^{(1,1)}(-\omega, \mathbf{q}) + R_{\kappa}(\mathbf{q})} \\ \bar{G}_{\kappa, \alpha\beta}^{uu}(\omega, \mathbf{q}) &= -P_{\alpha\beta}^{\perp}(\mathbf{q}) \frac{\bar{\Gamma}_{\kappa, \perp}^{(0,2)}(\omega, \mathbf{q}) - 2N_{\kappa}(\mathbf{q})}{\left| \bar{\Gamma}_{\kappa, \perp}^{(1,1)}(\omega, \mathbf{q}) + R_{\kappa}(\mathbf{q}) \right|^2}. \end{aligned} \quad (\text{B } 6)$$

One can then insert the expression (B 3) into Eq. (5.5), and compute the matrix product and trace to obtain the flow of $\bar{\Gamma}_{\kappa}^{(2)}$. Within the LO approximation, only the vertex $\bar{\Gamma}_{\kappa}^{(2,1)}$ remains and is given by (6.8), such that in Eq. (5.5), one may set $\bar{\Gamma}_{\kappa}^{(4)} = 0$, and only a few elements are non-zero in the matrices $\bar{\Gamma}_{\kappa, \ell}^{(3)}$.

According to the expressions (6.7) for $\bar{\Gamma}_{\kappa, \alpha\beta}^{(0,2)}$ and $\bar{\Gamma}_{\kappa, \alpha\beta}^{(1,1)}$, the flow equations of the transverse functions $f_{\kappa, \perp}^D$ and $f_{\kappa, \perp}^{\nu}$ may be defined as

$$\begin{aligned} \partial_{\kappa} f_{\kappa, \perp}^{\nu}(\mathbf{p}) &= \frac{1}{(d-1)} P_{\alpha\beta}^{\perp}(\mathbf{p}) \partial_{\kappa} \Gamma_{\kappa, \alpha\beta}^{(1,1)}(\nu=0, \mathbf{p}) \\ \partial_{\kappa} f_{\kappa, \perp}^D(\mathbf{p}) &= -\frac{1}{2(d-1)} P_{\alpha\beta}^{\perp}(\mathbf{p}) \partial_{\kappa} \Gamma_{\kappa, \alpha\beta}^{(0,2)}(\nu=0, \mathbf{p}). \end{aligned} \quad (\text{B } 7)$$

After some calculations (Canet *et al.* (2016)), one deduces the following flow equations

$$\begin{aligned} \partial_s f_{\kappa,\perp}^\nu(\mathbf{p}) = & \frac{1}{(d-1)} \int_{\mathbf{q}} \left\{ \frac{\partial_s R_\kappa(\mathbf{q}) \tilde{f}_\perp^D(\mathbf{p} + \mathbf{q})}{\tilde{f}_\perp^\nu(\mathbf{p} + \mathbf{q}) (\tilde{f}_\perp^\nu(\mathbf{q}) + \tilde{f}_\perp^\nu(\mathbf{p} + \mathbf{q}))^2} \right. \\ & \times \left[\left(-\mathbf{p}^2 + \frac{(\mathbf{p} \cdot (\mathbf{p} + \mathbf{q}))^2}{(\mathbf{p} + \mathbf{q})^2} \right) (d-1) - 2\mathbf{p} \cdot \mathbf{q} \left(1 - \frac{(\mathbf{p} \cdot \mathbf{q})^2}{\mathbf{q}^2 \mathbf{p}^2} \right) \right] \\ & + \frac{1}{\tilde{f}_\perp^\nu(\mathbf{q}) (\tilde{f}_\perp^\nu(\mathbf{q}) + \tilde{f}_\perp^\nu(\mathbf{p} + \mathbf{q}))} \left[\partial_s R_\kappa(\mathbf{q}) \frac{\tilde{f}_\perp^D(\mathbf{q}) (2\tilde{f}_\perp^\nu(\mathbf{q}) + \tilde{f}_\perp^\nu(\mathbf{p} + \mathbf{q}))}{\tilde{f}_\perp^\nu(\mathbf{q}) (\tilde{f}_\perp^\nu(\mathbf{q}) + \tilde{f}_\perp^\nu(\mathbf{p} + \mathbf{q}))} - \partial_s N_\kappa(\mathbf{q}) \right] \\ & \times \left[\left(-\mathbf{p}^2 + \frac{(\mathbf{p} \cdot \mathbf{q})^2}{\mathbf{q}^2} \right) (d-1) + 2 \frac{\mathbf{p} \cdot (\mathbf{p} + \mathbf{q})}{(\mathbf{q} + \mathbf{p})^2} \left(\mathbf{q}^2 - \frac{(\mathbf{p} \cdot \mathbf{q})^2}{\mathbf{p}^2} \right) \right] \left. \right\} \quad (\text{B } 8) \end{aligned}$$

$$\begin{aligned} \partial_s f_{\kappa,\perp}^D(\mathbf{p}) = & -\frac{1}{2(d-1)} \int_{\mathbf{q}} \left\{ \frac{2\tilde{f}_\perp^D(\mathbf{q} + \mathbf{p})}{\tilde{f}_\perp^\nu(\mathbf{p} + \mathbf{q}) \tilde{f}_\perp^\nu(\mathbf{q}) (\tilde{f}_\perp^\nu(\mathbf{q}) + \tilde{f}_\perp^\nu(\mathbf{p} + \mathbf{q}))} \right. \\ & \times \left[\partial_s R_\kappa(\mathbf{q}) \frac{\tilde{f}_\perp^D(\mathbf{q}) (2\tilde{f}_\perp^\nu(\mathbf{q}) + \tilde{f}_\perp^\nu(\mathbf{p} + \mathbf{q}))}{\tilde{f}_\perp^\nu(\mathbf{q}) (\tilde{f}_\perp^\nu(\mathbf{q}) + \tilde{f}_\perp^\nu(\mathbf{p} + \mathbf{q}))} - \partial_s N_\kappa(\mathbf{q}) \right] \\ & \times \left[2 \frac{1}{\mathbf{q}^2 (\mathbf{p} + \mathbf{q})^2} \left(\mathbf{q}^2 - \frac{(\mathbf{p} \cdot \mathbf{q})^2}{\mathbf{p}^2} \right) \left(\mathbf{p}^2 \mathbf{p} \cdot \mathbf{q} + 2(\mathbf{p} \cdot \mathbf{q})^2 - \mathbf{p}^2 \mathbf{q}^2 \right) \right. \\ & \left. \left. + \left(2\mathbf{p}^2 - \frac{(\mathbf{p} \cdot (\mathbf{p} + \mathbf{q}))^2}{(\mathbf{p} + \mathbf{q})^2} - \frac{(\mathbf{p} \cdot \mathbf{q})^2}{\mathbf{q}^2} \right) (d-1) \right] \right\} \quad (\text{B } 9) \end{aligned}$$

where $\partial_s \equiv \kappa \partial_\kappa$, $\tilde{f}_\perp^\nu(\mathbf{p}) \equiv f_{\kappa,\perp}^\nu(\mathbf{p}) + R_\kappa(\mathbf{q})$ and $\tilde{f}_\perp^D(\mathbf{p}) \equiv f_{\kappa,\perp}^D(\mathbf{p}) + N_\kappa(\mathbf{q})$. Note that a typo has been corrected in the last line of Eq. (B 9) compared to (Canet *et al.* (2016)).

Appendix C. Next-to-leading order term in 2D Navier-Stokes equation

The large wavenumber expansion underlying the derivation of Eq. (7.7) is inspired by the BMW approximation scheme. This scheme can be in principle improved order by order. There are two possible strategies to achieve this. The first one is to increase the order at which the closure using the BMW expansion is performed. Let us consider for instance the flow equation for the two-point function $\Gamma_\kappa^{(2)}$. At leading order, the three- and four-point vertices entering this equation are expanded around $\mathbf{q} = 0$. At the next-to-leading order, one keeps the full vertices in the flow equation for $\Gamma_\kappa^{(2)}$, and perform the $\mathbf{q} = 0$ expansion for the higher-order vertices entering the flow equations of $\Gamma_\kappa^{(3)}$ and $\Gamma_\kappa^{(4)}$, and so on. An alternative way to improve the BMW approximation scheme is to include higher-order terms in the Taylor expansion of the vertices for a given order n , e.g.

$$\begin{aligned} \Gamma_\kappa^{(n)}(\omega, \mathbf{q}, \varpi_1, \mathbf{p}_1, \dots) & \stackrel{q \approx 0}{\simeq} \Gamma_\kappa^{(n)}(\omega, 0, \varpi_1, \mathbf{p}_1, \dots) + \frac{\partial}{\partial \mathbf{q}} \Gamma_\kappa^{(n)}(\omega, \mathbf{q}, \varpi_1, \mathbf{p}_1, \dots) \Big|_{\mathbf{q}=0} \\ & + \frac{1}{2} \frac{\partial^2}{\partial \mathbf{q}^2} \Gamma_\kappa^{(n)}(\omega, \mathbf{q}, \varpi_1, \mathbf{p}_1, \dots) \Big|_{\mathbf{q}=0}. \quad (\text{C } 1) \end{aligned}$$

This second strategy has been implemented to study 2D turbulence in (Tarpin *et al.* (2019)). The reason for focusing on 2D rather than 3D turbulence is that the 2D NS action possesses additional symmetries, which can be used to control exactly the derivatives of vertices at $\mathbf{q} = 0$.

In 2D, the incompressibility constraint allows one to express the velocity field as the curl

of a pseudo-scalar field $\psi(t, \mathbf{x})$ called the stream function: $v_\alpha = \varepsilon_{\alpha\beta} \partial_\beta \psi$. Formulating the action in term of the stream function allows one to simply integrate out the pressure fields, yielding

$$S_\psi[\psi, \bar{\psi}] = \int_{t, \mathbf{x}} \partial_\alpha \bar{\psi} \left[\partial_t \partial_\alpha \psi - \nu \nabla^2 \partial_\alpha \psi + \varepsilon_{\beta\gamma} \partial_\gamma \psi \partial_\beta \partial_\alpha \psi \right] - \int_{t, \mathbf{x}, \mathbf{x}'} \partial_\alpha \bar{\psi}(t, \mathbf{x}) N \left(\frac{|\mathbf{x} - \mathbf{x}'|}{L} \right) \partial'_\alpha \bar{\psi}(t, \mathbf{x}') \}. \quad (\text{C } 2)$$

This action possesses all the extended symmetries discussed in Sec. 3.3. In particular, the Galilean transformation reads in this formulation

$$\delta\psi = \varepsilon_{\alpha\beta} x_\alpha \dot{\eta}_\beta(t) + \eta_\alpha(t) \partial_\alpha \psi, \quad \delta\bar{\psi} = \eta_\alpha(t) \partial_\alpha \bar{\psi}, \quad (\text{C } 3)$$

and the time-gauged shift of the response fields now simply amounts to the transformation

$$\delta\psi = 0, \quad \delta\bar{\psi} = x_\alpha \bar{\eta}_\alpha(t), \quad (\text{C } 4)$$

where $\eta, \bar{\eta}$ are the time-dependent parameters of the transformations. Note that these transformations are linear in x . Thus, in Fourier space, this leads to Ward identity constraining the first derivative of a vertex at one vanishing wavevector. If the zero wavevector is carried by a response stream, one deduces from (C 4) the following Ward identity

$$\frac{\partial}{\partial q_{m+1}^\alpha} \Gamma_\kappa^{(m,n)}(\dots, \varpi_{m+1}, \mathbf{q}_{m+1}, \dots) \Big|_{\mathbf{q}_{m+1}=0} = 0. \quad (\text{C } 5)$$

which is equivalent to Eq. (3.33) in terms of the velocity. Similarly, if the zero wavevector is carried by a stream field, the time-gauged Galilean transformation (C 3) yields a Ward identity, equivalent to Eq. (3.33), which exactly fixes the ∂_q derivative of this vertex in the stream formulation.

One can study the action (C 2) within the FRG formalism. It is clear that the same closure can be achieved in the limit of large wavenumber. In the stream formulation, the zeroth order in the large wavenumber expansion is trivial. This just reflects the fact that the stream and response stream functions are defined up to a constant function of time, and the functional integral does not fix this gauge invariance, such that the zeroth order carries no information. One thus has to consider the next term (first \mathbf{q} derivative) in the Taylor expansion of the vertices, which are precisely the ones fixed by the Ward identities. One thus obtains the exact same result as (7.7) expressed in term of the stream function. One can derive from it in a similar way the expression of the time dependence for generic n -point correlation functions in 2D turbulence. Note that they bare a different form than in 3D, due to the different scaling exponents (in particular z). Contrary to the 3D case, this result has not been tested yet in direct numerical simulations.

As in 3D, the leading order term in the limit of large wavenumber vanishes at equal times, such than one is left with power laws in wavenumbers with exponents stemming from standard scale invariance (Kraichnan-Leith scaling). However, additional extended symmetries were unveiled for the 2D action, which can be exploited to compute the next-to-leading order term (given by the second line of Eq. (C 1)). At equal times, *i.e.* integrated over all external

frequencies, this term writes

$$\begin{aligned} \partial_s \int_{\varpi_\ell} \mathcal{W}_\kappa^{(n)} \Big|_{\text{next-to-leading}} &= -\frac{1}{2} \int_{\omega_1, \mathbf{q}_1, \omega_2, \mathbf{q}_2} H_{\kappa, \gamma \delta}(-\omega_1, -\mathbf{q}_1, -\omega_2, -\mathbf{q}_2) \\ &\times \int_{\varpi_\ell} \left[\frac{q_a^\mu q_b^\nu q_c^\rho q_d^\sigma}{4!} \frac{\partial^2}{\partial q_a^\mu \partial q_b^\nu \partial q_c^\rho \partial q_d^\sigma} \frac{\delta}{\delta u_\gamma(\omega_1, \mathbf{q}_1)} \frac{\delta}{\delta u_\delta(\omega_2, \mathbf{q}_2)} \mathcal{W}_\kappa^{(n)} \right] \Big|_{\mathbf{q}_1=\mathbf{q}_2=0} \end{aligned} \quad (\text{C } 6)$$

where a, b, c, d take values in $\{1, 2\}$, and we have not used explicitly translational invariance so that the \mathbf{q} derivatives can be expressed unambiguously. One can show that the only non-vanishing contributions are the ones with two q_1 and two q_2 . The contributions with four q_1 vanish when evaluated at $\mathbf{q}_2 = 0$ because of the extended symmetry, while the ones with three q_1 and one q_2 are proportional to a \mathcal{D}_μ operator and vanish when integrated over frequencies. To go further requires to control second derivatives of vertices. This can partially be achieved in 2D because the field theory (C 2) exhibits two additional extended symmetries, which correspond to transformations quadratic in x , and thus yield Ward identities for the second \mathbf{q} derivative of vertices in Fourier space.

The first new symmetry is a quadratic in x shift of the response fields, following

$$\delta\psi = 0, \quad \delta\bar{\psi} = \frac{x^2}{2} \bar{\eta}(t). \quad (\text{C } 7)$$

One deduces the following Ward identity for second derivatives of a vertex function evaluated at a vanishing wavenumber carried by a response field

$$\frac{\partial^2}{(\partial q_{\bar{\ell}}^\alpha)^2} \Gamma_\kappa^{(m,n)}(\cdots, \omega_{\bar{\ell}}, \mathbf{q}_{\bar{\ell}}, \cdots) \Big|_{\mathbf{q}_{\bar{\ell}}=0} = 0, \quad (\text{C } 8)$$

where $\bar{\ell}$ is a response field index. Remarkably, the transformation (C 7), which reads in the velocity formulation

$$\delta\bar{\nabla}_\alpha = \varepsilon_{\alpha\beta\gamma} x_\beta \eta_\gamma(t), \quad \delta\bar{\pi} = v_\alpha \varepsilon_{\alpha\beta\gamma} x_\beta \eta_\gamma(t), \quad (\text{C } 9)$$

is also an extended symmetry of the 3D NS equation, but it has not been exploited yet.

In analogy with the extended Galilean transformation, which can be interpreted as a time-dependent generalisation of space translations, one can write the time-dependent extension of space rotations, which reads in the stream formulation

$$\delta\psi = -\dot{\eta}(t) \frac{x^2}{2} + \eta(t) \varepsilon_{\alpha\beta\gamma} x_\beta \partial_\alpha \psi, \quad \delta\bar{\psi} = \eta(t) \varepsilon_{\alpha\beta\gamma} x_\beta \partial_\alpha \bar{\psi}. \quad (\text{C } 10)$$

This transformation leads to a new extended symmetry of the 2D action, while it is not an extended symmetry of the 3D one. It is interesting to notice that time-dependent rotations are also an extended symmetry of the action corresponding to the Kraichnan model in any spatial dimension. As this transformation is also quadratic in x , it leads as well to a Ward identity for the second \mathbf{q} derivative of a vertex in Fourier space, this time when the \mathbf{q} wavevector is carried by the field itself

$$\frac{\partial^2}{(\partial q^\alpha)^2} \Gamma_\kappa^{(m+1,n)}(\omega, \mathbf{q}, \omega_1, \mathbf{q}_1, \cdots) \Big|_{\mathbf{q}=0} = \mathcal{R}(\omega) \Gamma_\kappa^{(m,n)}(\omega_1, \mathbf{q}_1, \cdots), \quad (\text{C } 11)$$

where $\mathcal{R}(\omega)$ is an operator achieving finite shifts by ω of the external frequencies of the function on which it acts, similarly to $\mathcal{D}_\alpha(\omega)$ in (3.30), at the difference that it also involves a derivative with respect to external wavevectors (see (Tarpin *et al.* (2019)) for details).

Using translation and rotation invariance of $H_{\kappa,\gamma,\delta}$ in (C 6), one can show that there are only two remaining contributions of the form $\frac{\partial^4}{\partial q_1^\mu \partial q_1^\mu \partial q_2^\gamma \partial q_2^\gamma}$ and $\frac{\partial^4}{\partial q_1^\mu \partial q_1^\gamma \partial q_2^\mu \partial q_2^\gamma}$. The first type of contributions are controlled by the Ward identities (C 8) and (C 11). Hence, either they are zero or they are proportional to a \mathcal{R} operator, and thus vanish when integrated over frequencies. However, the second type of contributions, the crossed derivatives, are not controlled by these identities. One can argue that they are nevertheless suppressed by a combinatorial factor. One thus arrives at the conclusion that most of the sub-leading terms in the large wavenumber expansion are exactly controlled by symmetries and vanish, while the remaining terms, which are not controlled by the symmetries, appear small based on combinatorics. This suggests that corrections to standard Kraichnan-Leith scaling of equal-time quantities in the large wavenumber regime, *i.e.* for the direct cascade, should be small, although it can only be argued at this stage.

REFERENCES

- ADZHEMYAN, L.Ts., ANTONOV, N.V. & KIM, T. L. 1994 Composite operators, operator expansion, and galilean invariance in the theory of fully developed turbulence. Infrared corrections to Kolmogorov scaling. *Theor. Math. Phys.* **100**, 1086.
- ADZHEMYAN, L. Ts., ANTONOV, N. V., BARINOV, V. A., KABRITS, YU. S. & VASIL'EV, A. N. 2001 Anomalous exponents to order ε^3 in the rapid-change model of passive scalar advection. *Phys. Rev. E* **63**, 025303.
- ADZHEMYAN, L. Ts., ANTONOV, N. V. & VASIL'EV, A. N. 1998 Renormalization group, operator product expansion, and anomalous scaling in a model of advected passive scalar. *Phys. Rev. E* **58**, 1823–1835.
- ADZHEMYAN, L. Ts., ANTONOV, N. V. & VASIL'EV, A. N. 1999 *The Field Theoretic Renormalization Group in Fully Developed Turbulence*. London: Gordon and Breach.
- ANTONOV, N. V. 2006 Renormalization group, operator product expansion and anomalous scaling in models of turbulent advection. *J. Phys. A: Math. Gen.* **39** (25), 7825–7865.
- ANTONOV, N. V., BORISENOK, S. V. & GIRINA, V. I. 1996 Renormalisation Group approach in the theory of fully developed turbulence. Composite operators of canonical dimension 8. *Theor. Math. Phys.* **106**, 75.
- BALOG, IVAN, CHATÉ, HUGUES, DELAMOTTE, BERTRAND, MAROHNÍČ, MAROJE & WSCHBOR, NICOLÁS 2019 Convergence of nonperturbative approximations to the renormalization group. *Phys. Rev. Lett.* **123**, 240604.
- BANDAK, DMYTRO, EYINK, GREGORY L., MAILYBAEV, ALEXEI & GOLDENFELD, NIGEL 2021 Thermal noise competes with turbulent fluctuations below millimeter scales.
- BARBI, DIRK & MÜNSTER, GERNOT 2013 Renormalisation group analysis of turbulent hydrodynamics. *Physics Research International* **2013**, 872796.
- BEC, JÉRÉMIE & KHANIN, KONSTANTIN 2007 Burgers turbulence. *Physics Reports* **447** (1), 1–66.
- BELL, JOHN B., NONAKA, ANDREW, GARCIA, ALEJANDRO L. & EYINK, GREGORY 2022 Thermal fluctuations in the dissipation range of homogeneous isotropic turbulence. *Journal of Fluid Mechanics* **939**, A12.
- BENITEZ, FEDERICO, MÉNDEZ-GALAIN, RAMÓN & WSCHBOR, NICOLÁS 2008 Calculations on the two-point function of the $o(n)$ model. *Phys. Rev. B* **77** (2), 024431.
- BERGES, JURGEN, TETRADIS, NIKOLAOS & WETTERICH, CHRISTOF 2002 Non-perturbative Renormalization flow in quantum field theory and statistical physics. *Phys. Rep.* **363** (4-6), 223 – 386, arXiv: [hep-ph/0005122](https://arxiv.org/abs/hep-ph/0005122).
- BERNARD, DENIS, GAWEDZKI, K. & KUPIAINEN, A. 1996 Anomalous scaling in the N point functions of passive scalar. *Phys. Rev. E* **54**, 2564, arXiv: [chao-dyn/9601018](https://arxiv.org/abs/chao-dyn/9601018).
- BERNARD, DENIS, GAWEDZKI, K. & KUPIAINEN, A. 1998 Slow Modes in Passive Advection. *Journal of Statistical Physics* **90**, 519, arXiv: [cond-mat/9706035](https://arxiv.org/abs/cond-mat/9706035).
- BIFERALE, L., BOFFETTA, G., CELANI, A. & TOSCHI, F. 1999 Multi-time, multi-scale correlation functions in turbulence and in turbulent models. *Physica D: Nonlinear Phenomena* **127** (3), 187–197.
- BIFERALE, LUCA, CALZAVARINI, ENRICO & TOSCHI, FEDERICO 2011 Multi-time multi-scale correlation functions in hydrodynamic turbulence. *Physics of Fluids* **23** (8), 085107.

- BLAIZOT, JEAN-PAUL, MÉNDEZ-GALAIN, RAMÓN & WSCHEBOR, NICOLÁS 2006 A new method to solve the non-perturbative Renormalization Group equations. *Phys. Lett. B* **632** (4), 571 – 578.
- BLAIZOT, J.-P., MÉNDEZ-GALAIN, R. & WSCHEBOR, N. 2007 Non-perturbative Renormalization Group calculation of the scalar self-energy. *Eur. Phys. J. B* **58**, 297–309.
- BUARIA, DHAWAL & SREENIVASAN, KATEPALLI R. 2020 Dissipation range of the energy spectrum in high reynolds number turbulence. *Phys. Rev. Fluids* **5**, 092601.
- BUCKMASTER, TRISTAN & VICOL, VLAD 2019 Nonuniqueness of weak solutions to the Navier-Stokes equation. *Annals of Mathematics* **189** (1), 101 – 144.
- BURGERS, J.M. 1948 A mathematical model illustrating the theory of turbulence. *Advances in Applied Mechanics*, vol. 1, pp. 171–199. Elsevier.
- CALLAN, CURTIS G. 1970 Broken scale invariance in scalar field theory. *Phys. Rev. D* **2**, 1541–1547.
- CANET, LÉONIE 2005 Strong-coupling fixed point of the Kardar-Parisi-Zhang equation. *arXiv:cond-mat/0509541*, arXiv: [arXiv:cond-mat/0509541](https://arxiv.org/abs/cond-mat/0509541).
- CANET, LÉONIE, CHATÉ, HUGUES & DELAMOTTE, BERTRAND 2011a General framework of the non-perturbative Renormalization Group for non-equilibrium steady states. *J. Phys. A* **44** (49), 495001.
- CANET, LÉONIE, CHATÉ, HUGUES, DELAMOTTE, BERTRAND & WSCHEBOR, NICOLÁS 2010 Nonperturbative renormalization group for the Kardar-Parisi-Zhang equation. *Phys. Rev. Lett.* **104** (15), 150601.
- CANET, LÉONIE, CHATÉ, HUGUES, DELAMOTTE, BERTRAND & WSCHEBOR, NICOLÁS 2011b Nonperturbative Renormalization Group for the Kardar-Parisi-Zhang equation: General framework and first applications. *Phys. Rev. E* **84**, 061128.
- CANET, LÉONIE, DELAMOTTE, BERTRAND & WSCHEBOR, NICOLÁS 2015 Fully developed isotropic turbulence: Symmetries and exact identities. *Phys. Rev. E* **91**, 053004.
- CANET, LÉONIE, DELAMOTTE, BERTRAND & WSCHEBOR, NICOLÁS 2016 Fully developed isotropic turbulence: Nonperturbative renormalization group formalism and fixed-point solution. *Phys. Rev. E* **93**, 063101.
- CANET, LÉONIE, ROSSETTO, VINCENT, WSCHEBOR, NICOLÁS & BALARAC, GUILLAUME 2017 Spatiotemporal velocity-velocity correlation function in fully developed turbulence. *Phys. Rev. E* **95**, 023107.
- CHEN, SHIYI & KRAICHNAN, ROBERT H. 1989 Sweeping decorrelation in isotropic turbulence. *Physics of Fluids A* **1** (12), 2019–2024.
- CHEKHOV, M. & FALKOVICH, G. 1996 Anomalous scaling exponents of a white-adveced passive scalar. *Phys. Rev. Lett.* **76**, 2706–2709.
- CHEKHOV, M., FALKOVICH, G., KOLOKOLOV, I. & LEBEDEV, V. 1995 Normal and anomalous scaling of the fourth-order correlation function of a randomly advected passive scalar. *Phys. Rev. E* **52**, 4924–4941.
- CHEVILLARD, L., ROUX, S. G., LÉVÊQUE, E., MORDANT, N., PINTON, J.-F. & ARNÉODO, A. 2005 Intermittency of velocity time increments in turbulence. *Phys. Rev. Lett.* **95**, 064501.
- CORRSIN, STANLEY 1951 On the Spectrum of Isotropic Temperature Fluctuations in an Isotropic Turbulence. *J. Appl. Phys.* **22** (4), 469–473.
- CORRSIN, S 1959 Progress report on some turbulent diffusion research. *Advances in Geophysics* **6**, 161–164.
- CORRSIN, S. 1962 Theories of turbulent dispersion. In *Mécanique de la Turbulence* (ed. A. Favre), *Colloques Internationaux du CNRS* 108, pp. 27–52. Paris: Éditions du Centre National de la Recherche Scientifique, proceedings of the International Colloquium on Turbulence at the University of Aix-Marseille, 28 August-2 September, 1961.
- CORWIN, IVAN 2012 The Kardar-Parisi-Zhang equation and universality classes. *Random Matrices* **01** (01), 1130001.
- DANNEVIK, WILLIAM P., YAKHOT, VICTOR & ORSZAG, STEVEN A. 1987 Analytical theories of turbulence and the ϵ expansion. *The Physics of Fluids* **30** (7), 2021–2029.
- DE POLSI, GONZALO, BALOG, IVAN, TISSIER, MATTHIEU & WSCHEBOR, NICOLÁS 2020 Precision calculation of critical exponents in the $o(n)$ universality classes with the nonperturbative renormalization group. *Phys. Rev. E* **101**, 042113.
- DE POLSI, GONZALO, HERNÁNDEZ-CHIFFLET, GUZMÁN & WSCHEBOR, NICOLÁS 2021 Precision calculation of universal amplitude ratios in $o(n)$ universality classes: Derivative expansion results at order $O(\partial^4)$. *Phys. Rev. E* **104**, 064101.
- DE POLSI, GONZALO, HERNÁNDEZ-CHIFFLET, GUZMÁN & WSCHEBOR, NICOLÁS 2022 The regulator dependence in the functional renormalization group: a quantitative explanation. *to appear Phys. Rev. E* p. [arXiv:2204.09170](https://arxiv.org/abs/2204.09170).
- DEBUE, PAUL, KUZAY, DENIS, SAW, EWE-WEI, DAVIAUD, FRANÇOIS, DUBRULLE, BÉRENGÈRE, CANET, LÉONIE, ROSSETTO, VINCENT & WSCHEBOR, NICOLÁS 2018 Experimental test of the crossover between the inertial and the dissipative range in a turbulent swirling flow. *Phys. Rev. Fluids* **3**, 024602.

- DEDOMINICIS, C. & MARTIN, P. C. 1979 Energy spectra of certain randomly-stirred fluids. *Phys. Rev. A* **19**, 419–422.
- DELAMOTTE, BERTRAND 2012 An Introduction to the nonperturbative renormalization group. *Lect. Notes Phys.* **852**, 49–132.
- DELIGIANNIS, K., FONTAINE, K., SQUIZZATO, D., RICHARD, M., RAVETS, S., BLOCH, J., MINGUZZI, A. & CANET, L. 2022 Kardar-parisi-zhang universality in discrete two-dimensional driven-dissipative exciton polariton condensates. *arXiv:2207.03886*, arXiv: [arXiv:2207.03886](https://arxiv.org/abs/2207.03886).
- DE DOMINICIS, C. 1976 Techniques de renormalisation de la théorie des champs et dynamique des phénomènes critiques. *J. Phys. (Paris) Colloq.* **37** (C1), 247–253.
- DRIVAS, THEODORE D., JOHNSON, PERRY L., LALESCU, CRISTIAN C. & WILCZEK, MICHAEL 2017 Large-scale sweeping of small-scale eddies in turbulence: A filtering approach. *Phys. Rev. Fluids* **2**, 104603.
- DUBRULLE, BÉRENGÈRE 2019 Beyond kolmogorov cascades. *Journal of Fluid Mechanics* **867**, P1.
- DUCLUT, CHARLIE & DELAMOTTE, BERTRAND 2017 Frequency regulators for the nonperturbative renormalization group: A general study and the model a as a benchmark. *Phys. Rev. E* **95**, 012107.
- DUPUIS, N., CANET, L., EICHORN, A., METZNER, W., PAWLOWSKI, J.M., TISSIER, M. & WSCHEBOR, N. 2021 The nonperturbative functional renormalization group and its applications. *Physics Reports* **910**, 1–114, the nonperturbative functional renormalization group and its applications.
- ELLWANGER, U. 1994 Flow equations and BRS invariance for Yang-Mills theories. *Phys. Lett. B* **335**, 364.
- EYINK, GREGORY & GOLDENFELD, NIGEL 1994 Analogies between scaling in turbulence, field theory, and critical phenomena. *Phys. Rev. E* **50**, 4679–4683.
- EYINK, GREGORY L. 1994 The renormalization group method in statistical hydrodynamics. *Physics of Fluids* **6** (9), 3063–3078.
- FALKOVICH, G., FOUXON, I. & OZ, Y. 2010 New relations for correlation functions in Navier–Stokes turbulence. *J. Fluid Mech.* **644**, 465–472.
- FALKOVICH, G., GAWĘDZKI, K. & VERGASSOLA, M. 2001 Particles and fields in fluid turbulence. *Rev. Mod. Phys.* **73** (4), 913–975.
- FAVIER, B., GODEFERD, F. S. & CAMBON, C. 2010 On space and time correlations of isotropic and rotating turbulence. *Physics of Fluids* **22** (1), 015101.
- FEDORENKO, ANDREI A., DOUSSAL, PIERRE LE & WIESE, KAY JÖRG 2013 Functional Renormalization Group approach to decaying turbulence. *J. Stat. Mech.: Theor. and Exp.* **2013** (04), P04014.
- FONTAINE, C., TARPIN, M., BOUCHET, F. & CANET, L. 2022 Functional renormalisation group approach to shell models of turbulence. *arXiv:2208.00225*, arXiv: [arXiv:2208.00225](https://arxiv.org/abs/2208.00225).
- FORSTER, DIETER, NELSON, DAVID R. & STEPHEN, MICHAEL J. 1977 Large-distance and long-time properties of a randomly stirred fluid. *Phys. Rev. A* **16** (2), 732–749.
- FOURNIER, J. D. & FRISCH, U. 1983 Remarks on the renormalization group in statistical fluid dynamics. *Phys. Rev. A* **28**, 1000–1002.
- FREY, ERWIN & TÄUBER, UWE CLAUS 1994 Two-loop Renormalization-Group analysis of the Burgers–Kardar–Parisi–Zhang equation. *Phys. Rev. E* **50** (2), 1024–1045.
- FRISCH, U. 1995 *Turbulence: the legacy of A. N. Kolmogorov*. Cambridge: Cambridge University Press.
- FRISCH, U & WIRTH, A 1996 Inertial-diffusive range for a passive scalar advected by a white-in-time velocity field. *Europhysics Letters (EPL)* **35** (9), 683–688.
- GAWĘDZKI, KRZYSZTOF & KUPIAINEN, ANTTI 1995 Anomalous Scaling of the Passive Scalar. *Phys. Rev. Lett.* **75**, 3834–3837, arXiv: [chao-dyn/9506010](https://arxiv.org/abs/chao-dyn/9506010).
- GORBUNOVA, ANASTASIIA 2021 Fonctions de corrélation en turbulence : simulations numériques et comparaison avec l’analyse par le groupe de renormalisation fonctionnel. PhD thesis, thèse de doctorat dirigée par Rossetto-Giaccherino, Vincent Balarac, Guillaume et Canet, Léonie Physique théorique Université Grenoble Alpes 2021.
- GORBUNOVA, ANASTASIIA, BALARAC, GUILLAUME, BOURGOIN, MICKAËL, CANET, LÉONIE, MORDANT, NICOLAS & ROSSETTO, VINCENT 2020 Analysis of the dissipative range of the energy spectrum in grid turbulence and in direct numerical simulations. *Phys. Rev. Fluids* **5**, 044604.
- GORBUNOVA, A., BALARAC, G., CANET, L., EYINK, G. & ROSSETTO, V. 2021a Spatio-temporal correlations in three-dimensional homogeneous and isotropic turbulence. *Physics of Fluids* **33** (4), 045114.
- GORBUNOVA, ANASTASIIA, PAGANI, CARLO, BALARAC, GUILLAUME, CANET, LÉONIE & ROSSETTO, VINCENT 2021b Eulerian spatiotemporal correlations in passive scalar turbulence. *Phys. Rev. Fluids* **6**, 124606.
- GOTOH, TOSHIYUKI, ROGALLO, ROBERT S., HERRING, JACKSON R. & KRAICHNAN, ROBERT H. 1993 Lagrangian velocity correlations in homogeneous isotropic turbulence. *Physics of Fluids A* **5** (11), 2846–2864.
- HALPIN-HEALY, TIMOTHY 2013a Erratum: Extremal paths, the stochastic heat equation, and the three-

- dimensional Kardar-Parisi-Zhang universality class [Phys. Rev. E **88** (2013), 042118]. *Phys. Rev. E* **88**, 069903.
- HALPIN-HEALY, TIMOTHY 2013*b* Extremal paths, the stochastic heat equation, and the three-dimensional Kardar-Parisi-Zhang universality class. *Phys. Rev. E* **88**, 042118.
- HALPIN-HEALY, TIMOTHY & ZHANG, YI-CHENG 1995 Kinetic roughening phenomena, stochastic growth, directed polymers and all that. Aspects of multidisciplinary statistical mechanics. *Phys. Rep.* **254** (4–6), 215 – 414.
- HAYOT, F. & JAYAPRAKASH, C. 1996 Multifractality in the stochastic Burgers equation. *Phys. Rev. E* **54**, 4681–4684.
- HE, GUO-WEI, WANG, MENG & LELE, SANJIVA K. 2004 On the computation of space-time correlations by large-eddy simulation. *Physics of Fluids* **16** (11), 3859–3867.
- HE, GUO-WEI & ZHANG, JIN-BAI 2006 Elliptic model for space-time correlations in turbulent shear flows. *Phys. Rev. E* **73**, 055303.
- HE, XIAOZHOU & TONG, PENDER 2011 Kraichnan’s random sweeping hypothesis in homogeneous turbulent convection. *Phys. Rev. E* **83**, 037302.
- HEISENBERG, W. 1948 Zur statistischen theorie der turbulenz. *Zeitschrift für Physik* **124** (7), 628–657.
- JANSSEN, HANS-KARL 1976 On a lagrangean for classical field dynamics and Renormalization Group calculations of dynamical critical properties. *Z. Phys. B* **23**, 377–380.
- JANSSEN, H. K., TÄUBER, U. C. & FREY, E. 1999 Exact results for the KPZ equation with spacially correlated noise. *Eur. Phys. J. B* **9**, 491.
- KANEDA, YUKIO 1993 Lagrangian and Eulerian time correlations in turbulence. *Physics of Fluids A: Fluid Dynamics* **5** (11), 2835–2845.
- KANEDA, YUKIO, ISHIHARA, TAKASHI & GOTOH, KOJI 1999 Taylor expansions in powers of time of lagrangian and eulerian two-point two-time velocity correlations in turbulence. *Physics of Fluids* **11** (8), 2154–2166.
- KARDAR, MEHRAN, PARISI, GIORGIO & ZHANG, YI-CHENG 1986 Dynamic scaling of growing interfaces. *Phys. Rev. Lett.* **56** (9), 889–892.
- VON KÁRMÁN, THEODORE & HOWARTH, LESLIE 1938 On the statistical theory of isotropic turbulence. *Proc. R. Soc. Lond. A* **164** (917), 192–215.
- KHURSHID, SUALEH, DONZIS, DIEGO A. & SREENIVASAN, K. R. 2018 Energy spectrum in the dissipation range. *Phys. Rev. Fluids* **3**, 082601.
- KLOSS, THOMAS, CANET, LÉONIE, DELAMOTTE, BERTRAND & WSCHBOR, NICOLÁS 2014*a* Kardar-Parisi-Zhang equation with spatially correlated noise: A unified picture from nonperturbative Renormalization Group. *Phys. Rev. E* **89**, 022108.
- KLOSS, THOMAS, CANET, LÉONIE & WSCHBOR, NICOLÁS 2012 Nonperturbative Renormalization Group for the stationary Kardar-Parisi-Zhang equation: Scaling functions and amplitude ratios in 1+1, 2+1, and 3+1 dimensions. *Phys. Rev. E* **86**, 051124.
- KLOSS, THOMAS, CANET, LÉONIE & WSCHBOR, NICOLÁS 2014*b* Strong-coupling phases of the anisotropic Kardar-Parisi-Zhang equation. *Phys. Rev. E* **90**, 062133.
- KOPIETZ, PETER, BARTOSCH, LORENZ & SCHÜTZ, FLORIAN 2010 *Introduction to the Functional Renormalization Group, Lecture Notes in Physics*, vol. 798. Berlin: Springer.
- KRAICHNAN, R. H. 1964 Kolmogorov’s hypotheses and eulerian turbulence theory. *Physics of Fluids* **7** (11), 1723.
- KRAICHNAN, ROBERT H. 1965 Lagrangian-history closure approximation for turbulence. *The Physics of Fluids* **8** (4), 575–598.
- KRAICHNAN, ROBERT H. 1968 Small-Scale Structure of a Scalar Field Convected by Turbulence. *Phys. Fluids* **11** (5), 945.
- KRAICHNAN, ROBERT H. 1994 Anomalous scaling of a randomly advected passive scalar. *Phys. Rev. Lett.* **72**, 1016–1019.
- KRUG, JOACHIM 1997 Origins of scale invariance in growth processes. *Adv. Phys.* **46** (2), 139 – 282.
- KUPIAINEN, A. & MURATORE-GINANNESCHI, P. 2007 Scaling, renormalization and statistical conservation laws in the Kraichnan model of turbulent advection. *J. Statist. Phys.* **126**, 669, arXiv: [nlin/0603031](https://arxiv.org/abs/nlin/0603031).
- LESIEUR, M. 2008 *Turbulence in Fluids*, 4th edn. Springer.
- LÉVÊQUE, E., CHEVILLARD, L., PINTON, J.-F., ROUX, S., ARNÉODO, A. & MORDANT, N. 2007 Lagrangian intermittencies in dynamic and static turbulent velocity fields from direct numerical simulations. *Journal of Turbulence* **8**, N3.

- L'VOV, VICTOR & PROCACCIA, ITAMAR 1995 Exact resummations in the theory of hydrodynamic turbulence. i. the ball of locality and normal scaling. *Phys. Rev. E* **52**, 3840–3857.
- L'VOV, VICTOR S., PODIVILOV, EVGENII & PROCACCIA, ITAMAR 1997 Temporal multiscaling in hydrodynamic turbulence. *Phys. Rev. E* **55**, 7030–7035.
- MARTIN, P. C., SIGGIA, E. D. & ROSE, H. A. 1973 Statistical dynamics of classical systems. *Phys. Rev. A* **8**, 423–437.
- MAZZINO, A. 1997 Effective correlation times in turbulent scalar transport. *Phys. Rev. E* **56**, 5500–5510.
- MCCOMB, W. D. & YOFFE, S. R. 2017 A formal derivation of the local energy transfer (LET) theory of homogeneous turbulence*. *Journal of Physics A: Mathematical and Theoretical* **50** (37), 375501.
- McMULLEN, RYAN M., KRYGIER, MICHAEL C., TORCZYNSKI, JOHN R. & GALLIS, MICHAEL A. 2022 Navier-stokes equations do not describe the smallest scales of turbulence in gases. *Phys. Rev. Lett.* **128**, 114501.
- MEDINA, ERNESTO, HWA, TERENCE, KARDAR, MEHRAN & ZHANG, YI-CHENG 1989 Burgers equation with correlated noise: Renormalization-Group analysis and applications to directed polymers and interface growth. *Phys. Rev. A* **39** (6), 3053–3075.
- MEJÍA-MONASTERIO, CARLOS & MURATORE-GINANNESCHI, PAOLO 2012 Nonperturbative Renormalization Group study of the stochastic Navier-Stokes equation. *Phys. Rev. E* **86**, 016315.
- MITRA, DHRUBADITYA & PANDIT, RAHUL 2005 Dynamics of Passive-Scalar Turbulence. *Phys. Rev. Lett.* **95** (14), 144501.
- MONIN, A. S. & YAGLOM, A. M. 2007 *Statistical Fluid Mechanics: Mechanics of turbulence*. Cambridge, Massachusetts and London, England: MIT Press.
- MORRIS, T. R. 1994 The exact Renormalisation Group and approximate solutions. *Int. J. Mod. Phys. A* **9**, 2411.
- NELKIN, MARK 1974 Turbulence, critical fluctuations, and intermittency. *Phys. Rev. A* **9**, 388–395.
- NELKIN, MARK & TABOR, M. 1990 Time correlations and random sweeping in isotropic turbulence. *Phys. Fluids A* **2** (1), 81–83.
- OBUKHOV, A M 1949 Structure of Temperature Field in Turbulent Flow. *Izv. Geogr. Geophys.* **13** (1), 58–69.
- O'GORMAN, P. A. & PULLIN, D. I. 2004 On modal time correlations of turbulent velocity and scalar fields. *J. of Turbulence* **5**, N35.
- ORSZAG, STEVEN A. & PATTERSON, G. S. 1972 Numerical simulation of three-dimensional homogeneous isotropic turbulence. *Phys. Rev. Lett.* **28**, 76–79.
- PAGANI, C. 2015 Functional Renormalization Group approach to the Kraichnan model. *Phys. Rev. E* **92** (3), 033016, [Addendum: *Phys. Rev. E* **97**, 4, 049902(2018)], arXiv: 1505.01293.
- PAGANI, CARLO & CANET, LÉONIE 2021 Spatio-temporal correlation functions in scalar turbulence from functional renormalization group. *Physics of Fluids* **33** (6), 065109.
- PAGNANI, ANDREA & PARISI, GIORGIO 2015 Numerical estimate of the kardar-parisi-zhang universality class in (2+1) dimensions. *Phys. Rev. E* **92**, 010101.
- POLCHINSKI, JOSEPH 1984 Renormalization and effective lagrangians. *Nuclear Physics B* **231** (2), 269 – 295.
- POULAIN, C., MAZELLIER, N., CHEVILLARD, L., GAGNE, Y. & BAUDET, C. 2006 Dynamics of spatial fourier modes in turbulence - sweeping effect, long-time correlations and temporal intermittency. *Eur. Phys. J. B* **53** (2), 219–224.
- PRÄHOFER, MICHAEL & SPOHN, HERBERT 2000 Universal distributions for growth processes in 1 + 1 dimensions and random matrices. *Phys. Rev. Lett.* **84**, 4882–4885.
- PRÄHOFER, MICHAEL & SPOHN, HERBERT 2004 Exact scaling functions for one-dimensional stationary KPZ growth. *J. Stat. Phys.* **115** (1-2), 255–279.
- SANADA, T. & SHANMUGASUNDARAM, V. 1992 Random sweeping effect in isotropic numerical turbulence. *Physics of Fluids A: Fluid Dynamics* **4** (6), 1245–1250.
- SANKAR RAY, SAMRIDDIH, MITRA, DHRUBADITYA & PANDIT, RAHUL 2008 The universality of dynamic multiscaling in homogeneous, isotropic Navier–Stokes and passive-scalar turbulence. *New J. Phys.* **10** (3), 033003.
- SHRAIMAN, BORIS I. & SIGGIA, ERIC D. 2000 Scalar turbulence. *Nature* **405** (6787), 639–646.
- SMITH, LESLIE M. & WOODRUFF, STEPHEN L. 1998 Renormalization-group analysis of turbulence. *Annual Review of Fluid Mechanics* **30** (1), 275–310.
- SQUIZZATO, DAVIDE & CANET, LÉONIE 2019 Kardar-parisi-zhang equation with temporally correlated noise: A nonperturbative renormalization group approach. *Phys. Rev. E* **100**, 062143.
- SREENIVASAN, KATEPALLI R. 1995 On the universality of the kolmogorov constant. *Physics of Fluids* **7** (11), 2778–2784.

- SREENIVASAN, KATEPALLI R. 2019 Turbulent mixing: A perspective. *PNAS* **116** (37), 18175–18183.
- SYMANZIK, K. 1970 Small distance behaviour in field theory and power counting. *Communications in Mathematical Physics* **18**.
- TAKEUCHI, KAZUMASA A. 2018 An appetizer to modern developments on the kardar–parisi–zhang universality class. *Physica A: Statistical Mechanics and its Applications* **504**, 77 – 105, lecture Notes of the 14th International Summer School on Fundamental Problems in Statistical Physics.
- TARPIN, MALO 2018 Non-perturbative renormalisation group approach to some out of equilibrium systems : diffusive epidemic process and fully developped turbulence. PhD thesis, thèse de doctorat dirigée par Canet, Léonie Physique théorique Université Grenoble Alpes (ComUE) 2018.
- TARPIN, MALO, CANET, LÉONIE, PAGANI, CARLO & WSCHEBOR, NICOLÁS 2019 Stationary, isotropic and homogeneous two-dimensional turbulence: a first non-perturbative renormalization group approach. *Journal of Physics A: Mathematical and Theoretical* **52** (8), 085501.
- TARPIN, MALO, CANET, LÉONIE & WSCHEBOR, NICOLÁS 2018 Breaking of scale invariance in the time dependence of correlation functions in isotropic and homogeneous turbulence. *Physics of Fluids* **30** (5), 055102.
- TAYLOR, GEOFFREY I 1922 Diffusion by continuous movements. *Proceedings of the London Mathematical Society* **2** (1), 196–212.
- TENNEKES, H. 1975 Eulerian and lagrangian time microscales in isotropic turbulence. *J. Fluid Mech.* **67**, 561–567.
- TOMASSINI, PAOLO 1997 An exact renormalization group analysis of 3d well developed turbulence. *Physics Letters B* **411** (1), 117 – 126.
- VERMA, MAHENDRA K. 2019 *Energy Transfers in Fluid Flows: Multiscale and Spectral Perspectives*. Cambridge University Press.
- WALLACE, JAMES M. 2014 Space-time correlations in turbulent flow: A review. *Theoretical and Applied Mechanics Letters* **4** (2), 022003.
- WETTERICH, CHRISTOF 1993 Exact evolution equation for the effective potential. *Phys. Lett. B* **301** (1), 90 – 94.
- WIESE, KAY JÖRG 1998 On the perturbation expansion of the KPZ equation. *J. Stat. Phys.* **93** (1-2), 143–154.
- WILCZEK, M. & NARITA, Y. 2012 Wave-number–frequency spectrum for turbulence from a random sweeping hypothesis with mean flow. *Phys. Rev. E* **86**, 066308.
- WILSON, K. G. & KOGUT, J. 1974 The Renormalization Group and the ϵ -expansion. *Phys. Rep. C* **12**, 75.
- YAGLOM, A. M. 1949 Über die lokale Struktur des Temperaturfeldes in einer turbulenten Strömung. *Dokl. Akad. Nauk SSSR, n. Ser.* **69**, 743–746.
- YAKHOT, VICTOR & ORSZAG, STEVEN A. 1986 Renormalization-group analysis of turbulence. *Phys. Rev. Lett.* **57**, 1722–1724.
- YAKHOT, VICTOR, ORSZAG, STEVEN A. & SHE, ZHEN-SU 1989 Space-time correlations in turbulence: Kinematical versus dynamical effects. *Physics of Fluids A* **1** (2), 184–186.
- YEUNG, P. K. & SAWFORD, BRIAN L. 2002 Random-sweeping hypothesis for passive scalars in isotropic turbulence. *J. Fluid Mech.* **459**, 129–138.
- ZHAO, XIN & HE, GUO-WEI 2009 Space-time correlations of fluctuating velocities in turbulent shear flows. *Phys. Rev. E* **79**, 046316.
- ZHOU, YE 2010 Renormalization Group theory for fluid and plasma turbulence. *Phys. Rep.* **488** (1), 1 – 49.
- ZHOU, YE 2021 Turbulence theories and statistical closure approaches. *Physics Reports* **935**, 1–117, turbulence theories and statistical closure approaches.
- ZINN-JUSTIN, JEAN 2002 *Quantum Field Theory and Critical Phenomena*, 4th edn. Oxford: Oxford University Press.